Engineering Considerations on Thermoelectric Power in Electrochemical Systems(Dissertation_全文)

AUTHOR(S):

Kamata, Masahiro

Engineering Considerations
on
Thermoelectric Power in Electrochemical Systems

A Thesis Presented

by

Masahiro Kamata

to

Faculty of Engineering,

Kyoto University

in partial fulfillment of the requirements for the degree of

Doctor of Engineering.

Engineering Considerations
on
Thermoelectric Power in Electrochemical Systems

A Thesis Presented

by

Masahiro Kamata

to

Faculty of Engineering,

Kyoto University

in partial fulfillment of the requirements for the degree of

Doctor of Engineering.

PREFACE

The study presented here has been carried out under the supervision of Associate Professor Yasuhiko Ito, Department of Nuclear Engineering, Kyoto University.

The author would like to express his sincere thanks to Associate Professor Yasuhiko Ito for his kind guidance, valuable suggestions and continuous encouragement throughout this study. The author is also greatly indebted to Professor Jun Oishi, Department of Nuclear Engineering, Kyoto University, for his kind guidance and stimulating discussions throughout the course of this study.

Grateful acknowledgment is made to Mr.Mikio Inoue for his patient cooperation in this experiment. Mr.Shunji Horikawa's instruction in an early stage of this work was also very helpful.

In addition, the author wishes to thank Dr.Hirotake Moriyama, Mr.Kimikazu Moritani and Mrs.Keiko Ema for their kind encouragement.

Masahiro Kamata

Department of Nuclear Engineering
Faculty of Engineering
Kyoto University
Sakyo-ku, Kyoto 606, Japan

CONTENTS

INTRODUCTION

Significance of thermoelectric power in engineering

Thermoelectric power has two significant meanings in the field of engineering. One is grounded on the fact that the thermoelectric power can be one of the driving forces of the mass transfer phenomena in nonisothermal systems, and the other is that the Peltier heat of single electrode reactions can be determined from the value of thermoelectric power. The relation between thermoelectric power and Peltier heat is to be discussed in detail later. (cf. Chapter4)

The former is very important in studying corrosion of a system where the temperature gradient exists and so is the latter in designing or analyzing the energy balance of electrochemical reactors.

The purpose of this study is to show these engineering significances and at the same time, to investigate thermoelectric power of various systems theoretically and experimentally. Especially, the author believes that the experimental technique of thermoelectric power measurement has been established through this study.

1.MASS TRANSFER PHENOMENA

Many kinds of heat transfer material have been or are

planned to be used in nuclear reactors for power generation. Some of them are water, CO_2 gas, Na liquid metal and molten salt[1].

In any case, since a large amount of heat has to be removed from a core of a reactor, there exists a temperature gradient in a heat transfer system and this condition sometimes gives serious effect to the compatibility of structural material and heat transfer material.

In case of FBR(Fast Breeder Reactor), the structural material is stainless steel and the heat transfer material is liquid sodium metal. Since the solubility of some constituents of stainless steel gets larger as the temperature rises, they dissolve into the liquid sodium near the core of a reactor, where the temperature is high, and in turn precipitate on the stainless steel in the heat exchanger, where the temperature is lower[2].

The same kind of phenomenon is observed in a gas cooled reactor. The mechanism of this phenomenon is reported to be caused by the temperature dependence of the equilibrium constant of the reaction shown below[3].

$$C + CO_2 = 2CO \qquad (1)$$

On the other hand, this phenomenon can occur in molten salt systems, too, eg. heat transfer loop of MSBR (Molten-Salt Breeder Reactor)[4], and three different mechanisms are considered to cause this phenomenon in these systems.

One of them is grounded on the temperature dependence of the solubility of the oxide on the surface of structural material, and the other one is on temperature dependence of the equilibrium

constant of the disproportionation reactions, such as

$$M^{2+} + M = 2M^{+}. \quad [5] \qquad (2)$$

Thus, the former is similar to the mechanism in FBR and the latter is to that in the gas cooled reactor.

The third mechanism is considered to be electrochemical one. That is, this sort of phenomenon can also be caused by the thermoelectric power in a system. In order to prove the possibility of the third mechanism and to make its mechanism clear, an experiment has been conducted as described below[6].

The experimental cell is shown in Fig.I. The inside of the pyrex holder is filled with argon to minimize any side effects. LiCl-KCl eutectic melt was used as a solvent and appropriate amount (0.05 mol/Kg-salt) of $NiCl_2$ was added as a solute. To obtain a certain temperature gradient in a cell, the upper part of the holder was covered with glass wool and the lower part was cooled by air.

Figure II shows two different types of testing pieces. Each testing piece is constructed of two small nickel plates (7*25mm), and these plates are electrically connected in one type and electrically insulated in the other. During the experiment this testing piece was immersed into the melt as shown in Fig.I, where one of the nickel plates was exposed to the high temperature melt(450℃) and the other was exposed to the low temperature one (400℃).

After 100 hours of immersion, these pieces were compared

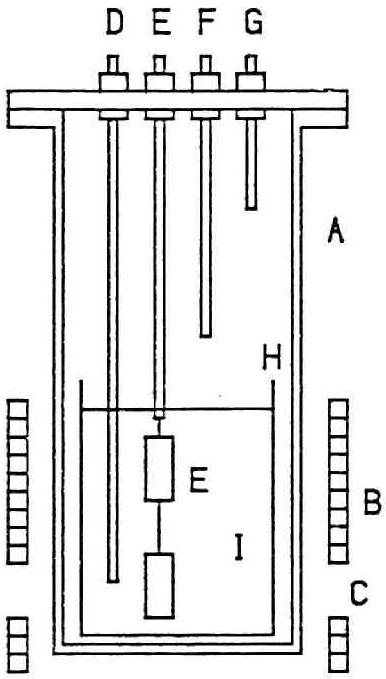

A: pyrex holder
B: heater
C: cooling window
D: thermocouple
E: nickel plate
F: Ar inlet
G: Ar outlet
H: quartz cell
I : LiCl -KCl - $NiCl_2$

Fig. I Experimental apparatus

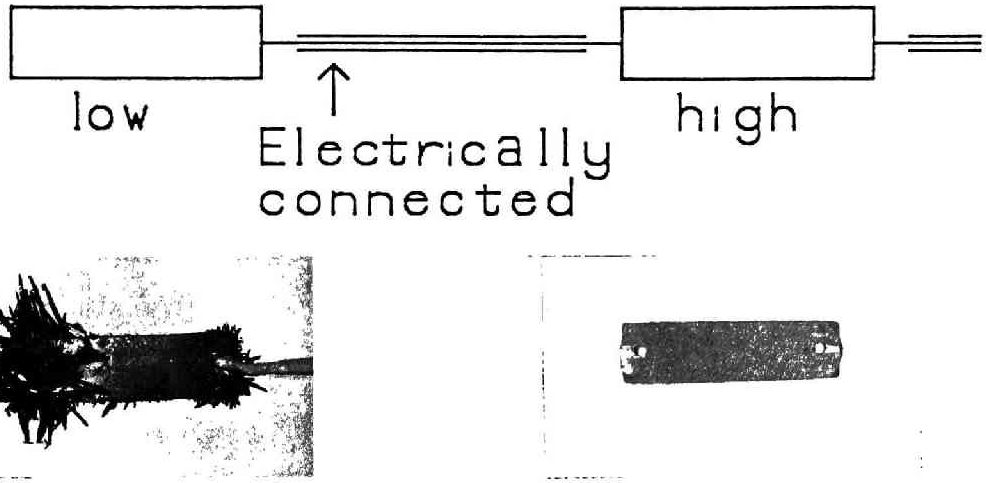

(1)

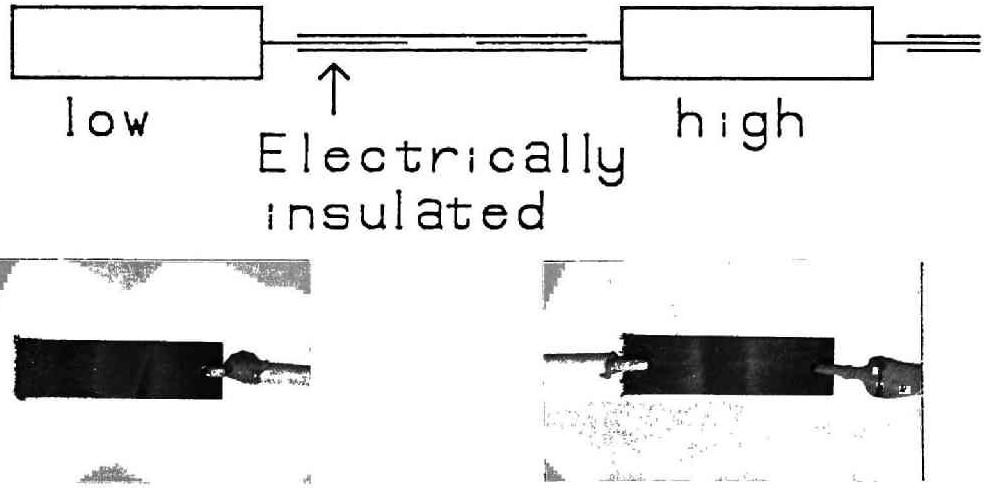

(2)

Fig. II Testing pieces

with each other.

Figure II shows photographs of the nickel plates after 100 hours of immersion. The difference is obvious, and was confirmed by weighing the gain and loss of each plate. In case of the testing pieces with electrical connection, the increase in weight at the lower temperature side plate was 0.51g, while the decrease at the higher temperature side plate was 0.44g. On the other hand, in case of the testing pieces with no electrical connection, the weight change was less than 0.01g in both the lower temperature side plate and the higher one.

These results indicate that the mass transfer by electrochemical mechanism can occur in molten salt systems under some condition. The mechanism was confirmed from the fact that the electric insulation between the two nickel plates prevented this phenomenon.

2.PELTIER HEAT

It is very important to understand temperature distribution in electrolytic cells quantitatively for designing their structure or establishing their electrolytic conditions.

For example, if Joule heat or the other kinds of heat evolved from electrode reaction is not estimated properly, the temperature of various materials such as electrodes, electrolyte or membranes, rises and in some case it leads to the destruction of the cell[7]. Conversely, if insufficient heat is supplied to the electrode region, where the reaction is endothermic, the

temperature may fall, thus increases the voltage required for the electrolysis. Besides, in molten salt systems, even freezing of the electrolyte in a cell might occur under extreme conditions.

For such reasons, the quantitative evaluation of single electrode heat is very important from the engineering viewpoint. Especially it is indispensable for the optimization of electrolytic condition. But so far little attention has been paid to the single electrode heat in spite of its importance and most attention has been paid to the total enthalpy change in the electrolysis reactions, instead.

In this study, the relation between thermoelectric power and Peltier heat has been theoretically derived and empirically proved. So the author believes that this sort of study will certainly contribute to the energy analysis of many types of electrochemical reactors of aqueous and molten salt systems, such as water electrolyzers, brine electrolyzers and fuel cells.

REFERENCES

[1] Reactor handbook 2nd ed. 1, Interscience(1960)

[2] K.Furukawa, Zairyo Gakkai-si, 9,141(1972)

[3] A.R.Anderson et al,: 1st International Conference of Peaceful Uses of Atomic Energy in Geneva, Paper A/CONF(1955) 15/p.303

[4] "Molten Salt Breeder Reactor" Atomic Energy Society of Japan (1981)

[5] T.Oki, Proceedings of the Joint International Symposium on Molten Salts, p765, Electrochem.Soc(1987)

[6] Y.Ito, M.Kamata, S.Horikawa and J.Oishi, DENKIKAGAKU 53, P375(1985)

[7] Y.Ito, H.Kaiya, S.Yoshizawa, S.K.Ratkje and T.Førland, J.electrochem.Soc. 131, 2504(1984)

PART 1. THERMOELECTRIC POWER

CHAPTER 1. Thermodynamic description of thermoelectric power

The thermoelectric power can be thermodynamically described by use of irreversible thermodynamics. Here, the thermoelectric power in a nonisothermal but isobaric system is to be treated and that in nonisothermal and nonisobaric system is presented in Chapter 3.

According to Førland and Ratkje[1], the entropy production θ per unit time and unit volume can be written as :

$$T\cdot\theta = -\nabla \ln T\cdot J_q - \sum_{i=1}^{k} \nabla \mu_{Ti}\cdot J_i - \nabla \phi^{obs}\cdot I \qquad (I\text{-}1)$$

J_q is the flux of heat, J_i is the flux of the component i, I is electric current density and $\nabla \phi^{obs}$ stands for the differential emf that is observable by using a pair of identical electrodes. k independent components in the system can be divided into two groups: the components i=n+1～k which belong to the electrode and those i=1～n involved in the electrolyte phase. Using the independent fluxes, eqn.(I-1) can be rewritten as:

$$T\cdot\theta = -\nabla \ln T\cdot J_q - \sum_{i=1}^{n} \nabla \mu_{Ti}\cdot J_i - \nabla \phi\cdot I \qquad (I\text{-}2)$$

,where

$$\nabla \phi = \nabla \phi^{obs} + \sum_{i=n+1}^{k} Z_i\cdot \nabla \mu_{Ti} \qquad (I\text{-}3)$$

(Z_i stands for complete coupling coefficient between mass flux of component i (i=n+1～k) and current density)

From eqn.(I-2), the fluxes of heat, mass, and charge are

expressed as follows by using their conjugate forces.

$$J_q = -Y_{qq}\nabla \ln T - \Sigma Y_{qi}\nabla \mu_{Ti} - Y_{qQ}\nabla \phi \qquad (I-4)$$

$$J_i = -Y_{iq}\nabla \ln T - \Sigma Y_{ii}\nabla \mu_{Ti} - Y_{iQ}\nabla \phi \qquad (I-5)$$

$$I = -Y_{Qq}\nabla \ln T - \Sigma Y_{Qi}\nabla \mu_{Ti} - Y_{QQ}\nabla \phi \qquad (I-6)$$

The gradient of chemical potential $\nabla \mu_{Ti}$ is expressed as eqn.(I-7) by using the chemical potential gradient $\nabla \mu_i$.

$$\nabla \mu_{Ti} = \nabla \mu_i - (\delta \mu_i / \delta T)\nabla T \qquad (I-7)$$

This eqn.(I-7) represents that the second terms in the rights of eqns.(I-4),(I-5) and (I-6) are equal to zero under the condition of no pressure gradient and no concentration gradient. The latter is achieved when there exists convection in a system or when the system is far from Soret equilibrium.

When $\nabla \mu_{Ti}$ is equal to zero, the relation;

$$\nabla \phi = \nabla \phi^{obs} \qquad (I-8)$$

is obtained from eqn.(I-3). By substituting eqn.(I-8) and $\nabla \mu_{Ti}=0$ in eqns.(I-4),(I-5) and (I-6), they can be simplified as follows.

$$J_q = -Y_{qq}\nabla \ln T - Y_{qQ}\nabla \phi^{obs} \qquad (I-9)$$

$$J_i = -Y_{iq}\nabla \ln T - Y_{iQ}\nabla \phi^{obs} \qquad (I-10)$$

$$I = -Y_{Qq}\nabla \ln T - Y_{QQ}\nabla \phi^{obs} \qquad (I-11)$$

When the condition I=0 during thermoelectric power measurment

is taken into account, the next equation is obtained from eqn.(I-11)

$$\nabla \phi^{obs} = -(Y_{Qq}/Y_{QQ})\nabla \ln T \qquad (I-12)$$

From this equation, thermoelectric power ε_T is expressed as;

$$\varepsilon_T = (\delta \phi^{obs}/\delta T) = -(Y_{Qq}/Y_{QQ})(1/T) \qquad (I-13)$$

(It is noted that ε_T stands for initial thermoelectric power, where the system is far from Soret equilibrium.)

Next, physical meaning of the coefficient Y_{Qq}/Y_{QQ} in eqn.(I-13) will be discussed.

The fluxes of heat, mass and charge are expressed as eqns.(I-9),(I-10) and (I-11) under the condition $\Delta P=0$ and $\Delta C=0$. By eliminating $\nabla \phi^{obs}$ from eqns.(I-9) and (I-11), eqn.(I-14) is obtained.

$$J_q = -(Y_{qq}-Y_{qQ}\frac{Y_{Qq}}{Y_{QQ}})\nabla \ln T + \frac{Y_{qQ}}{Y_{QQ}} I \qquad (I-14)$$

The coefficient Y_{qQ}/Y_{QQ} of the second term on the right of eqn.(I-14) represents the heat that is transferred with unit charge.

The entropy absorbed from the external heat reservoir by the reversible transfer of unit charge is called Peltier entropy, which is usually symbolized as S'(Q). Using this entropy S'(Q) and the temperature of the electrode region T, the heat absorbed from the external heat reservoir under the condition described

above, is expressed as $T \cdot S'(Q)$, so the coefficient of the second term of eqn.(I-14) is expressed as:

$$Y_{qQ}/Y_{QQ} = T \cdot S'(Q)/F \qquad \text{(I-15)}$$

Taking into account the Onsager reciprocal relation[2][3]:

$$Y_{qQ} = Y_{Qq} \qquad \text{(I-16)}$$

,eqn.(I-13) is rewritten as

$$\varepsilon_T = (\delta \phi^{obs}/\delta T) = -S'(Q)/F \qquad \text{(I-17)}$$

Peltier entropy $S'(Q)$ is the sum of the transported entropy $\overset{=}{S}$ and the entropy change Δs as shown in eqn.(I-18).

$$S'(Q) = \overset{=}{S} + \Delta s \qquad \text{(I-18)}$$

The former is the entropy that flows out from the electrode region into the electrolyte with the reversible transfer of unit charge and the latter is the change of the entropy in the electrode region under the same condition. The entropy change Δs is written as follows by use of the concentration of the oxidized and/or reduced species involved in the electrode reaction:

$$\Delta s = \Delta s^{\circ} - \frac{R}{n} \ln \frac{[OX]}{[Red]}. \qquad \text{(I-19)}$$

Consequently the concentration dependence of thermoelectric

power is expressed as:

$$\varepsilon_T = (\delta \phi^{obs} / \delta T)$$

$$= [-(\bar{\bar{S}} + \Delta s^\circ) + \frac{2.303R}{n} \log \frac{[Ox]}{[Red]}]/F \quad (I\text{-}20)$$

This equation has been experimentally confirmed in various kinds of systems and some of them are to be presented in the following chapters.

CHAPTER 2. Thermoelectric power measurement in various molten salt systems

Thermoelectric power measurement has been carried out in several kinds of molten salt systems. Obtained data from these experiments are very important not only in engineering but also from a viewpoint of thermodynamical considerations on thermoelectric power.

The description of thermoelectric power derived in previous chapter will be confirmed by using these empirical data and it will be discussed how the thermoelectric power is effected by electrode material composition and its phase state.

Besides, the evaluation of transported entropy in LiCl-KCl systems is also to be presented here.

2-1 The relation between thermoelectric power and valence number of electrode reactants.

2-1-1 Experimental

Here, the thermoelectric powers measured in ;

(T)Ag/LiCl-KCl+AgCl /Ag(T+dT),

(T)Ni/LiCl-KCl+$NiCl_2$/Ni(T+dT),

(T)Pb/LiCl-KCl+$PbCl_2$/Pb(T+dT),

(T)Al/LiCl-KCl+$AlCl_3$/Al(T+dT),

and (T)Li/LiCl-KCl/Li(T+dT)

are to be discussed. (The first system was investigated by Y.Ito, et al[4].) The experimental cell used in the first 4

systems is shown in Fig.I-1. Commercial LiCl and KCl (Reagent Grade, Wako Chemicals Co.Ltd.) were mixed and the eutectic mixture was vacuum dried at the temperature of 200℃ for more than 48 hours. It was melted in the H-type cell shown in Fig.I-1 under argon atmosphere.

After preparing the eutectic LiCl-KCl solvent, the appropriate amount of solute ion (AgCl, $NiCl_2$, $PbCl_2$, or $AlCl_3$) was added, and in case of Pb/Pb(Ⅱ) system, water as impurity in melt was expelled by supplying HCl gas into the melt.

On the other hand, in case of Al/Al(Ⅲ) system, a special pyrex tube whose tail was narrowed (cf.Fig.I-2) was used to dissolve $AlCl_3$ into melt, and the concentration of $AlCl_3$ in melt was measured by sampling small amount of salt and measuring it with ICP(Inductively coupled plasma-optical emission analytical spectrometry) method.

The structure of the Pb electrode was shown in Fig.I-3. Though the extra thermoelectric power between Pb and Ni lead wire is included in measured thermoelectric power when this type of electrode is used, this extra value was estimated from other experiments and corrected.

Since the other electrodes were solid state, they were used as a wire.

The temperature difference was established between the left part of the cell and the right part by using 2 separated heaters. After setting the temperature gradient in this way, the electric potential difference between 2 electrodes was measured with a digital multimeter and recorded.

As for Li/Li(I) system, the apparatus shown in Fig.I-4 is a

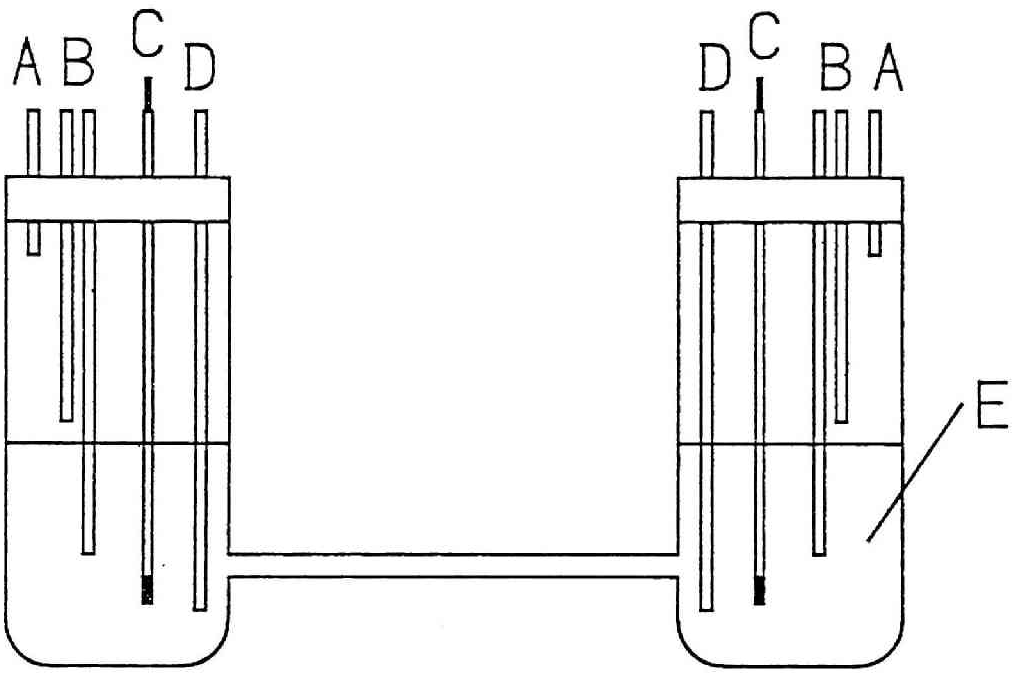

A:gas outlet
B:gas inlet
C:electrode
D:thermocouple
E:LiCl-KCl eutectic salt

Fig.I-1 Experimental apparatus

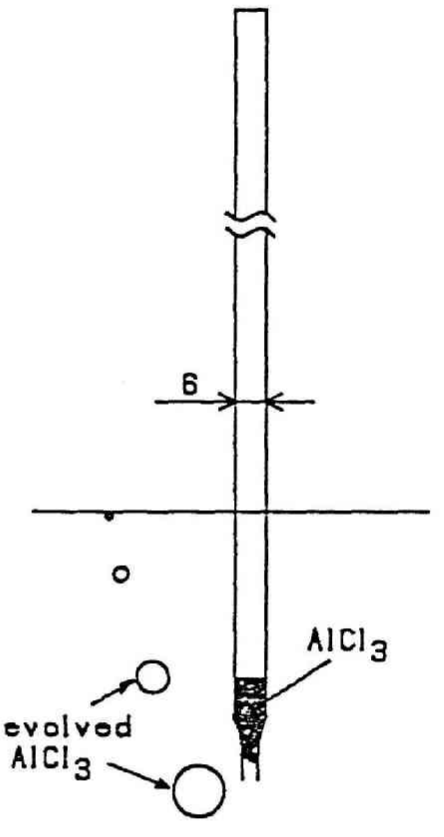

Fig.1-2

Pyrex tube to dissolve $AlCl_3$

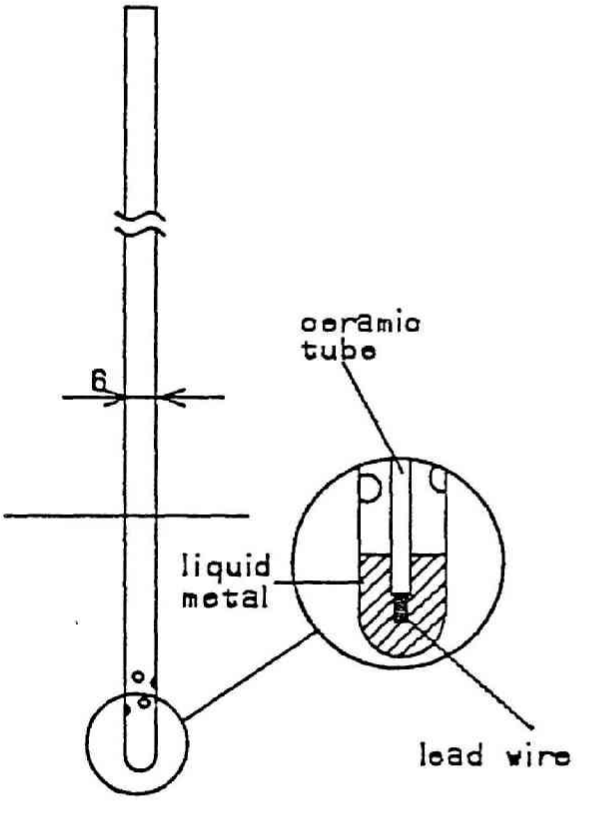

Fig.1-3

Perforated pyrex tube for liquid metal electrode

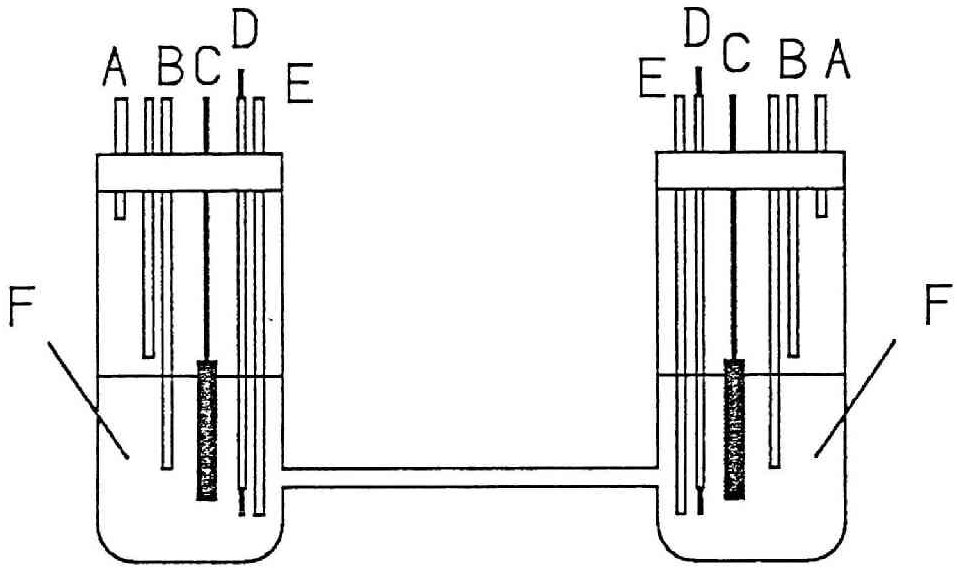

A:gas outlet
B:gas inlet
C:counter electrode
D:working electrode
E:thermocouple
F:LiCl - KCl eutectic salt

Fig.I-4 Experimental apparatus

little different from the previous one. This apparatus has a pair of carbon counter electrodes that were used to electrodeposit lithium metal on nickel wire.

2-1-2 Results and discussion

First, the relations between temperature difference and electromotive force in systems of Ag/Ag(I), Ni/Ni(II) and Li/Li(I) are presented in Fig.I-5,I-6 and I-7, respectively.

Every result of each system shows a good linearity between ΔT and emf. Since the emf on the vertical axis is the value measured on reference to low temperature electrode, it means that the electric potential of high temperature electrode is always more negative than that of the low temperature one except the case of Li/Li(I) system, and this tendency was observed in other systems, too.

In case of Li/Li(I) system, observed thermoelectric power shown in Fig.I-7 includes the thermoelectric power ε' between lithium metal and nickel lead. Since ε' is estimated as -0.0641mV/K at 500℃ from the published data[5], the net thermoelectric power of Li/Li(I) system is expressed as;

$$\varepsilon_T = (\delta \phi^{obs}/\delta T) - \varepsilon' \qquad \text{(I-21)}$$
$$= 0.0947 \times 10^{-3} \quad V/K$$

Though the similar relations were obtained when concentration of the solute ion was changed, the slope (electric potential difference per unit temperature difference) was different. The

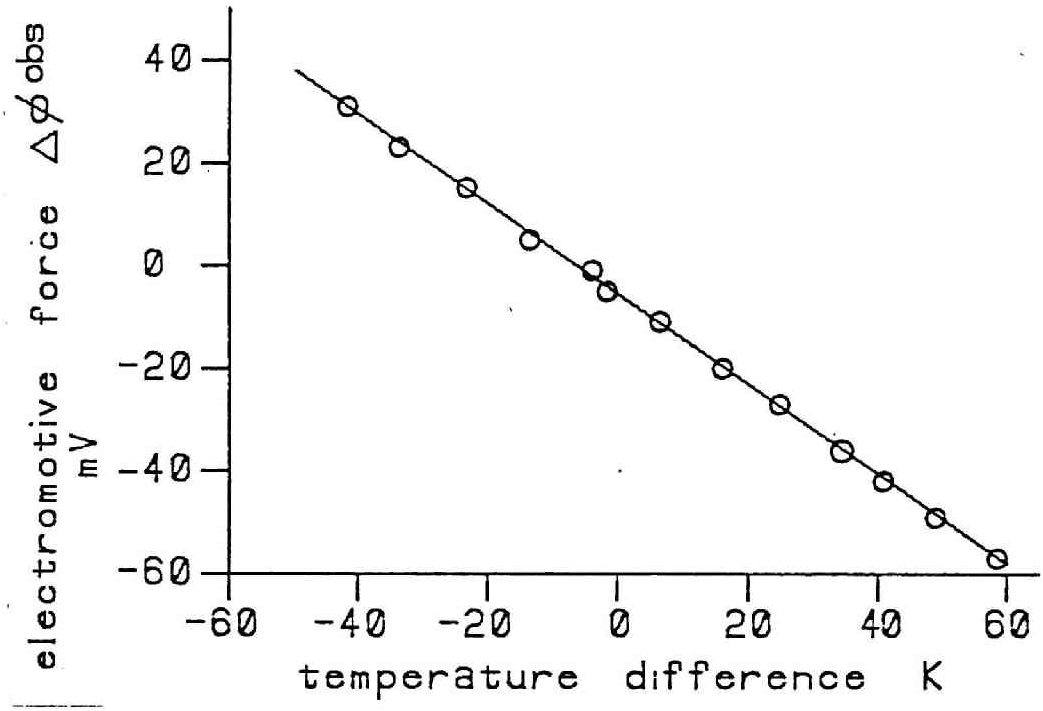

Fig.I-5 Relation between temperature difference and electromotive force (Ag/AgCl system)

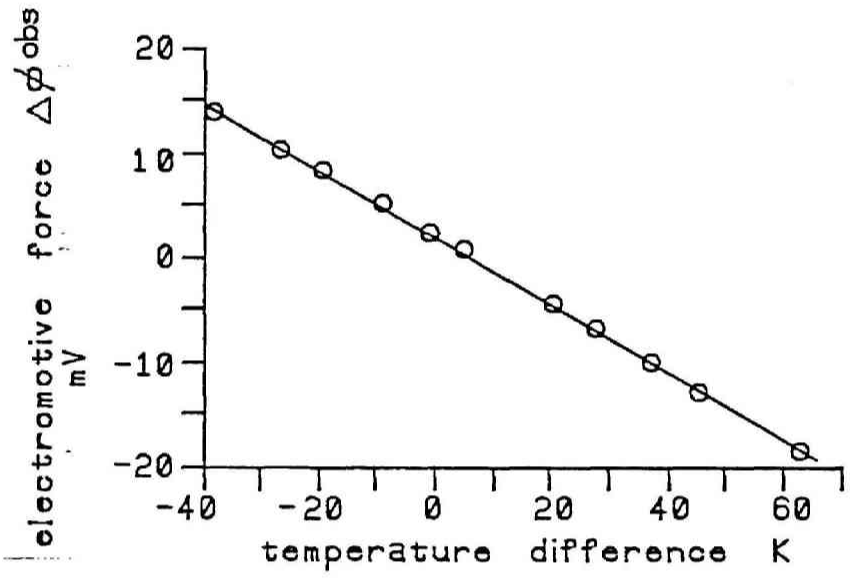

Fig.I-6 Relation between temperature difference and electromotive force ($Ni/NiCl_2$ system)

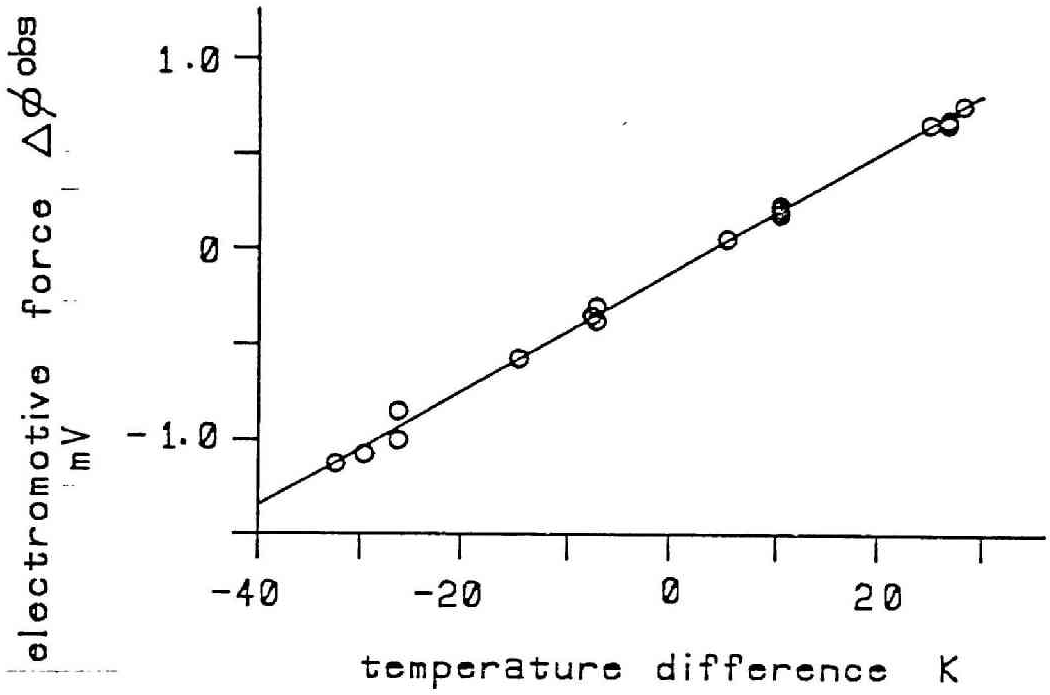

Fig.I-7 Relation between temperature difference and electromotive force (Li/LiCl system)

concentration dependence of this slope, i.e. thermoelectric power, was shown in Fig.I-8,9,10 and 11, and expressed as follows with respect to each system mentioned above.

$$\mathrm{Ag/Ag(I)}: \varepsilon = \underset{(\pm 0.015)}{-0.271} + \underset{(\pm 0.032)}{0.203}\cdot\log[\mathrm{Ag(I)}] \quad [\times 10^{-3}\ \mathrm{V/K}]$$

$$\mathrm{Ni/Ni(II)}: \varepsilon = \underset{(\pm 0.032)}{-0.094} + \underset{(\pm 0.015)}{0.1022}\cdot\log[\mathrm{Ni(II)}] \quad [\times 10^{-3}\ \mathrm{V/K}]$$

$$\mathrm{Pb/Pb(II)}: \varepsilon = \underset{(\pm 0.087)}{+\ 0.0081} + \underset{(\pm 0.018)}{0.0921}\cdot\log[\mathrm{Pb(II)}] \quad [\times 10^{-3}\ \mathrm{V/K}]$$

$$\mathrm{Al/Al(III)}: \varepsilon = \underset{(\pm 0.0051)}{-\ 0.0039} + \underset{(\pm 0.021)}{0.075}\cdot\log[\mathrm{Al(III)}] \quad [\times 10^{-3}\ \mathrm{V/K}]$$

In all systems, there exists a good linearity between the logarithm of the mole fraction of solute ion in melt and the thermoelectric power.

As seen from those figures and equations, when the solute ion is monovalent, the slope is very close to 2.303R/F, and when it is divalent the slope is close to 2.303R/2F. As for the Al/Al(III) system, the slope gets near to 2.303R/3F, though the deviation is large.

This tendency in concentration dependence of thermoelectric power is in very good accordance with theoretically derived eqn.(I-20) mentioned in Chapter1.

On the other hand, in case of Al/Al(III) system, the slope in Fig.I-11 is not in good accordance with 2.303R/3F. One of the reasons for this phenomenon might be the disproportionation reaction on Al/Al(III) electrode. The other reason is that the concentration of $AlCl_3$ in a melt was not stable due to its high vapour pressure and changed between after and before the emf measurement.

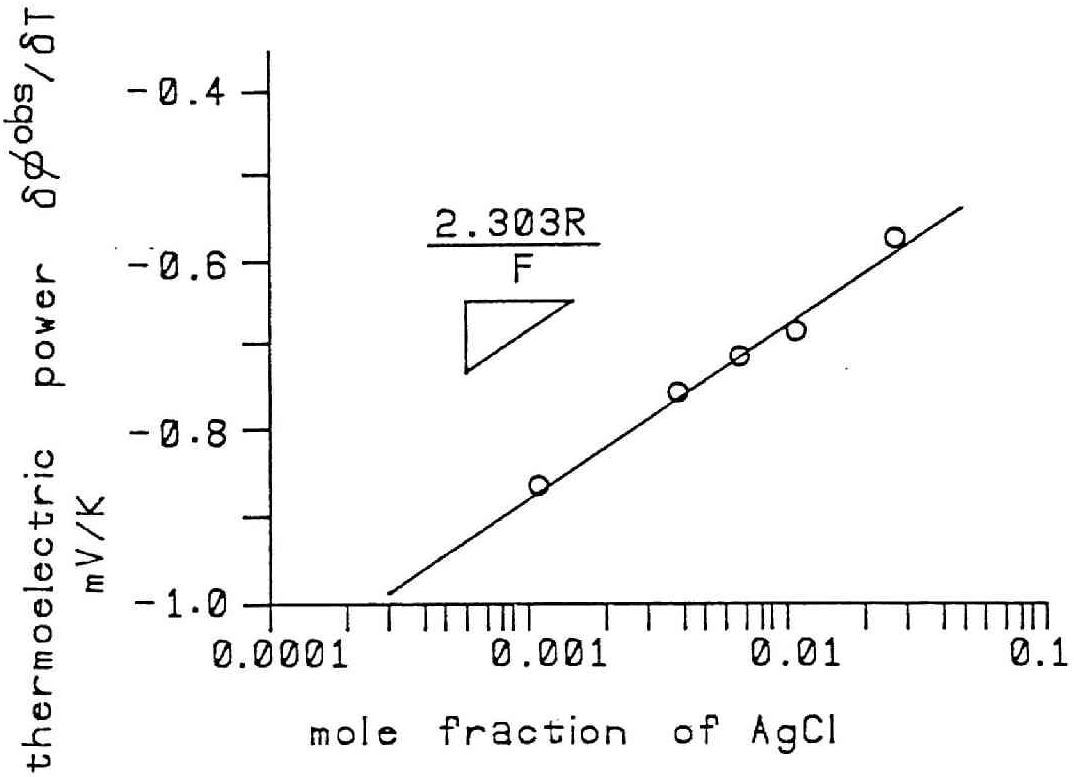

Fig.I-8 Concentration dependence of thermoelectric power (Ag/AgCl system)

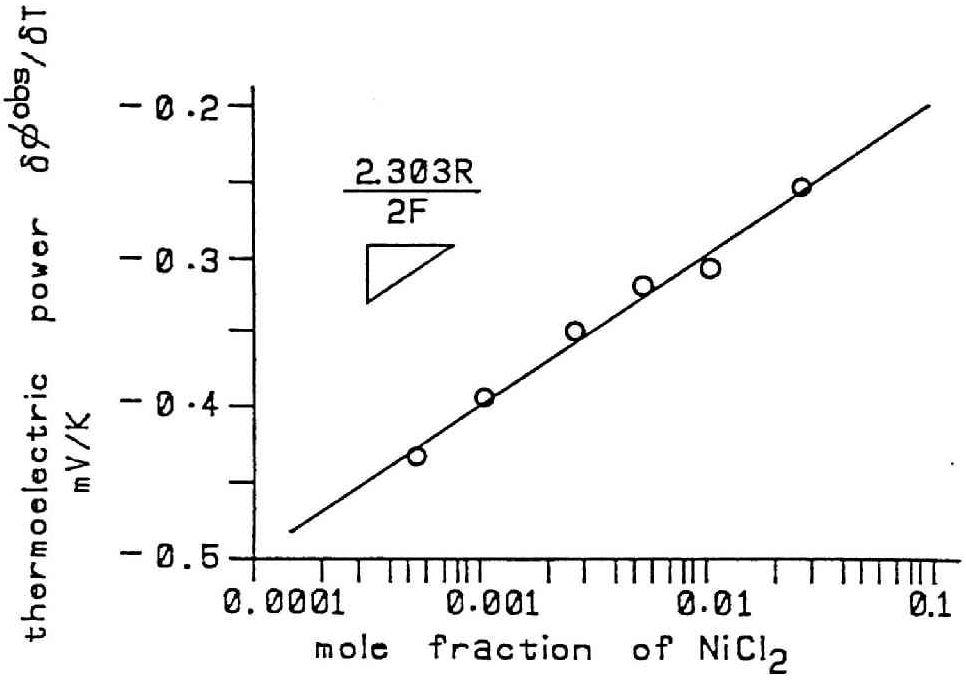

Fig.I-9 Concentration dependence of thermoelectric power ($Ni/NiCl_2$ system)

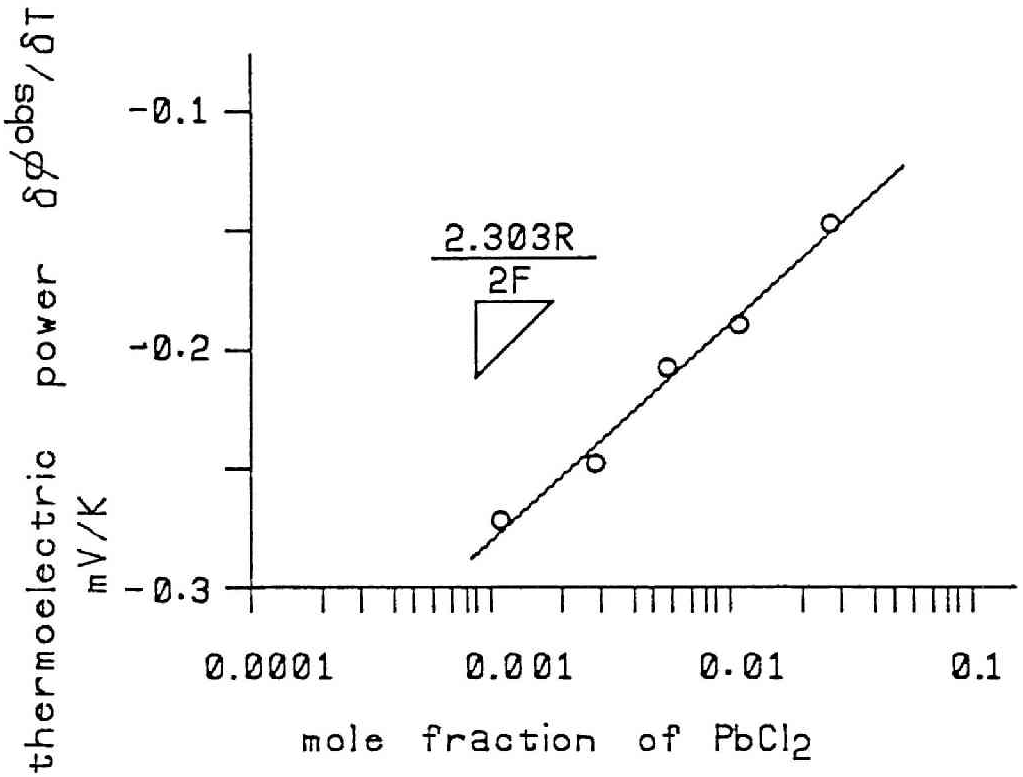

Fig.I-10 Concentration dependence of thermoelectric power ($Pb/PbCl_2$ system)

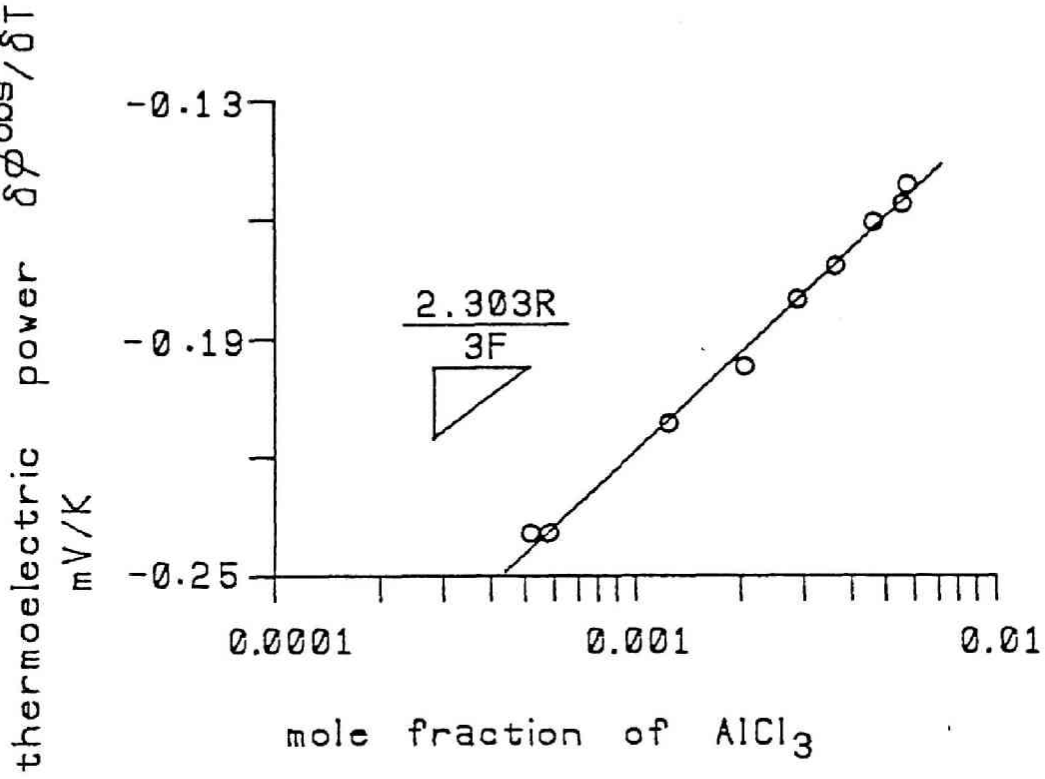

Fig.I-11 Concentration dependence of thermoelectric power ($Al/AlCl_3$ system)

2-2 The effect of composition and phase change of electrode material on thermoelectric power

Though many works including the author's have been presented concerning the theoretical and/or experimental study of thermoelectric power, almost no report exists that uses alloy in a single or coexisting phase as an electrode.

But, since construction material of heat transfer loop is made from metal alloys in most cases[6] and electrodes of electrochemical reactors are not necessarily pure metal[7], thermoelectric power measurement with an alloy electrode is very important in studying mass transfer in such a loop or analyzing energy balance of reactors with alloy electrodes.

From such an engineering viewpoint, the author has studied on various aspects of thermoelectric power, especially how the thermoelectric power is effected by the composition or phase change of the electrode material.

2-2-1 Experimental

In this work, LiCl-KCl was used as a melt and the tin-lithium alloy of various compositions was used as an electrode.

In order to confirm the appropriateness of the experimental method adopted by the author, the same kind of experiment was carried out at first in Zn/Zn(Ⅱ) electrode systems.

The experimental apparatus is shown in Fig.I-12. Inside of the cell was kept argon atmosphere, and the temperature

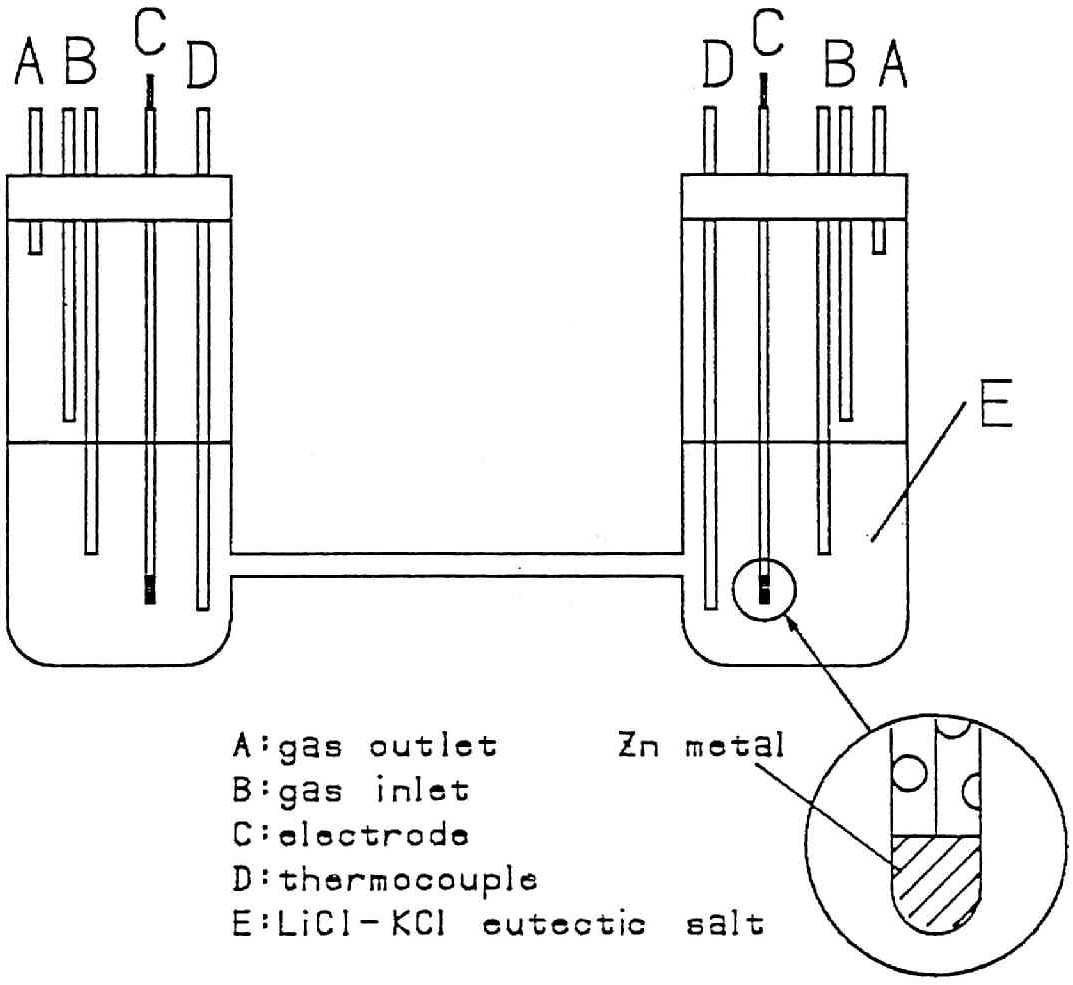

Fig.I-12 Experimental apparatus

fference was established between the left part of the cell and ıe right part by using two separated heaters. After setting a ;rtain temperature difference, electric potential difference ;tween two electrodes was measured. The structure of the .ectrode is illustrated in detail underneath the same figure.

LiCl-KCl eutectic melt was used as a solvent and appropriate nount of $ZnCl_2$ was added as a solute. The mixture of LiCl and :l had been vacuum dried for more than 48 hours, and ıermoelectric power measurement was carried out both over and ıder the melting point of zinc metal.

In case of tin-lithium alloy electrode systems, experiments ave been conducted as in the followings. As shown in ig.I-13[8], when the lithium concentration is less than 40%, ıis alloy keeps single liquid phase between 400 and 500℃. As or more concentrated alloy, solid-liquid coexisting zone exists ı the same temperature range. When the lithium concentration in lloy is larger than 50%, the alloy is composed of two solid ıases under the temperature of 470℃.

Thus, the experimental research concerning this alloy lectrode is composed of three parts. The first part is the tudy on single liquid phase electrode and the second is that on iquid-solid coexisting electrode and the last is that on olid-solid coexisting electrode.

Since the temperature of this system is much higher than that f Zn/Zn(Ⅱ) system, a different type of experimental cell as ıown in Fig.I-14 was used.

The cylindrical cell was made of quartz glass and the

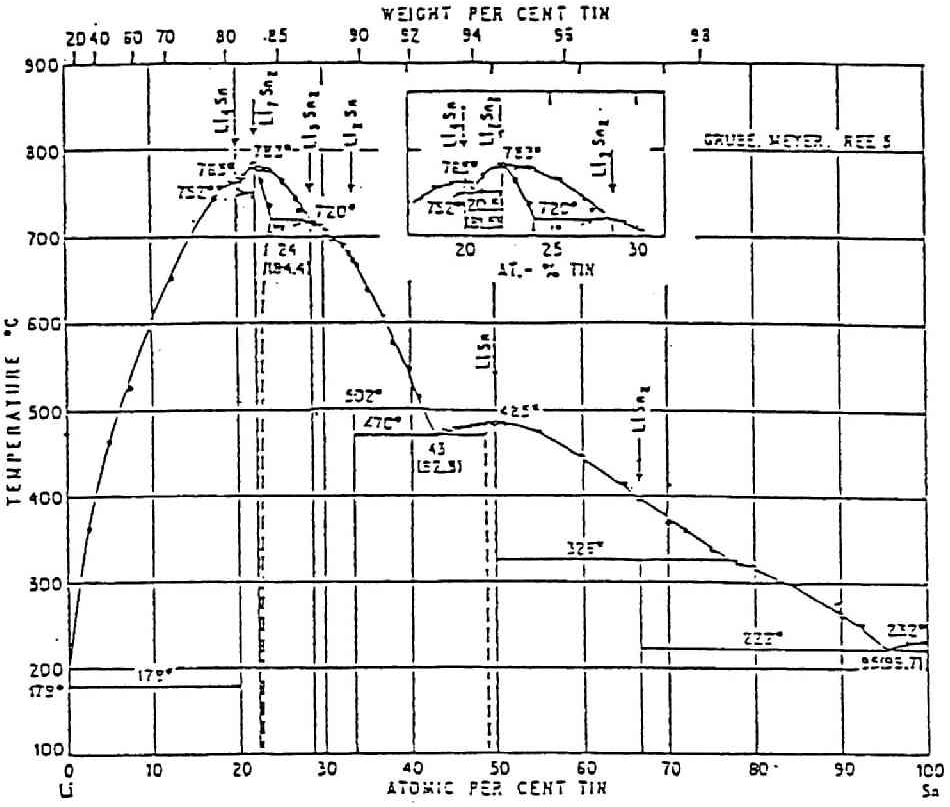

Fig. I - 13
Phase diagram of Li-Sn [8]

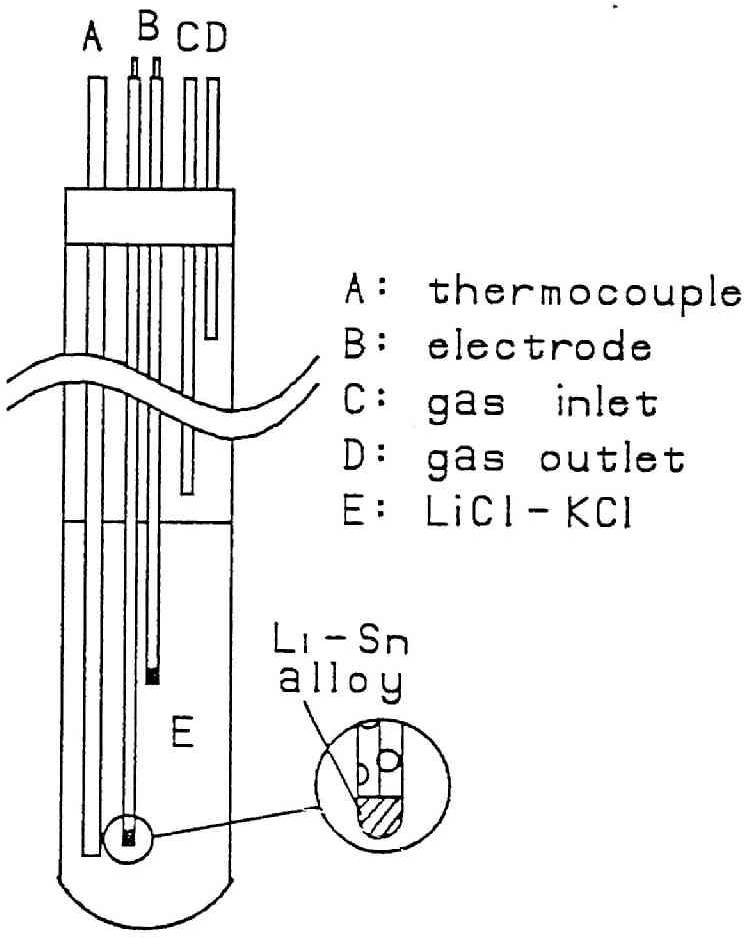

Fig.I-14 Experimental apparatus

vertical temperature difference was established by air cooling the bottom part of the cell. The temperature of the electrode was controlled by changing its elevation in a cell, and the temperature distribution in a cell was measured with chromel-alumel thermocouples before and after the experiments.

Lithium-tin alloy was prepared in the other apparatus and put into the pyrex glass tube with a molybdenum lead wire as illustrated in the circle of Fig.I-14.

On the other hand, the activity coefficients of lithium in liquid alloy were measured with an apparatus shown in Fig.I-15. These data are indispensable because thermoelectric power cannot be analyzed without them.

The principle of measuring the activity coefficients was very simple. By measuring the potential differences between alloy electrodes and the pure lithium electrode and by analyzing them with Nernst's equation, activity coefficients of lithium in liquid alloy can be obtained.

This experiment was repeated as changing the temperature of the system, because their temperature dependence was also needed.

The condition of purification of salt and atmosphere in a cell was the same as that of the previous experiment.

2-2-2 Results and discussion.

1)Zn/Zn(Ⅱ) electrode system

The result obtained from Zn/Zn(Ⅱ) electrode system is presented in Fig.I-16(A). The vertical axis of this figure presents the electromotive force between two electrodes, and the

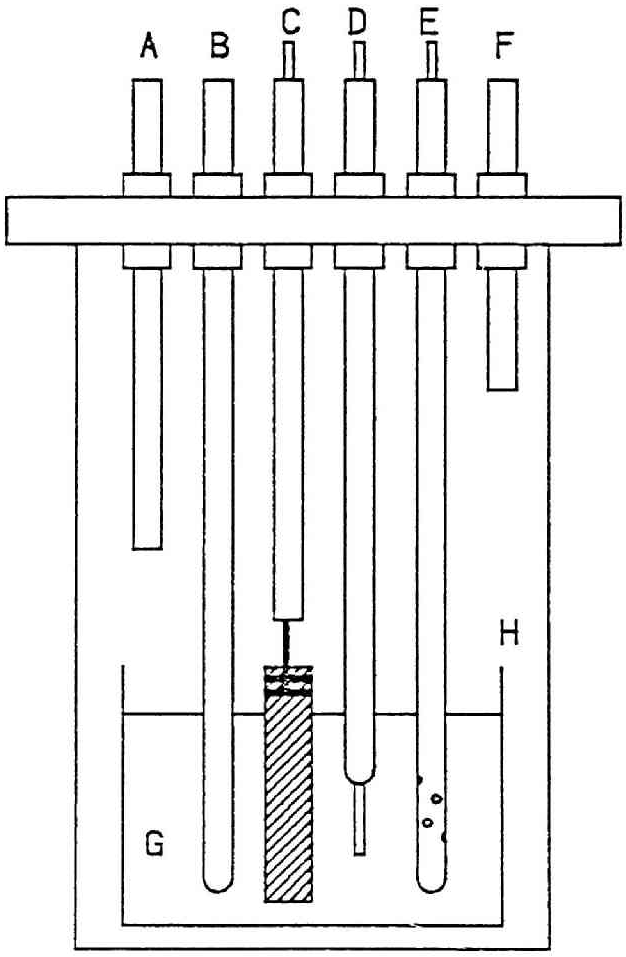

A: Ar inlet
B: thermocouple
C: counter electrode
D: Li/Li(I) electrode
E: Li-Sn electrode
F: Ar outlet
G: LiCl-KCl
H: quartz cell

Fig.I-15 Experimental apparatus

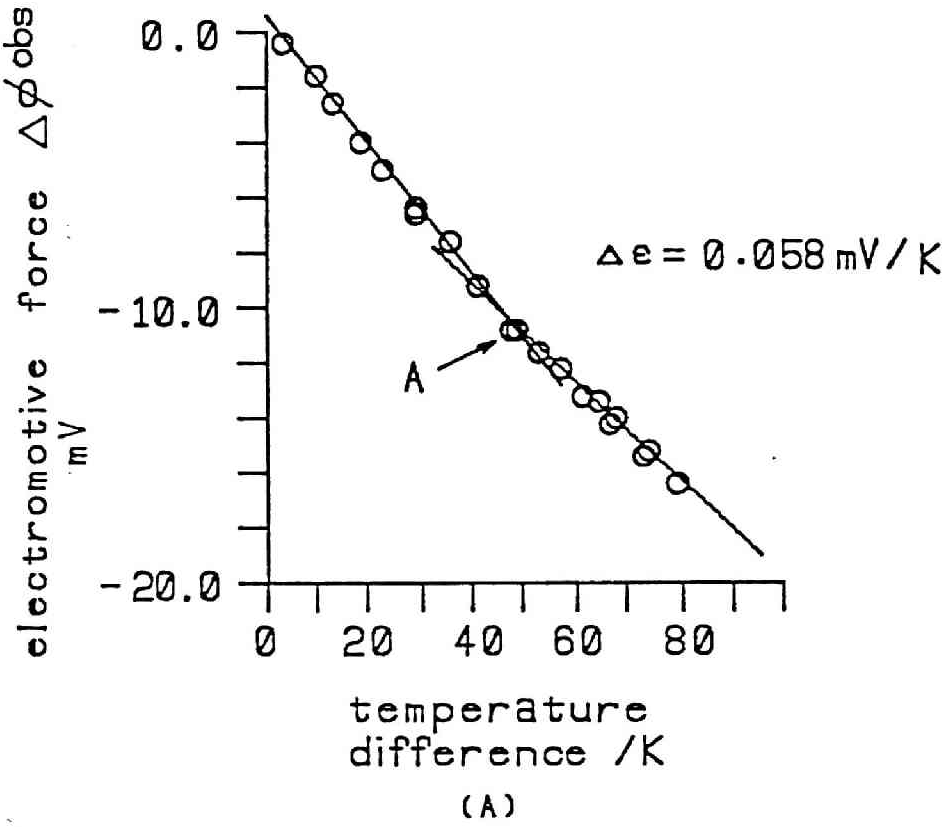

Fig. I-16

(A) Relation between temperature difference and electromotive force

(B) Relation between temperature and thermoelectric power

($Zn/ZnCl_2$ system)

horizontal axis shows the temperature difference between them.

Since the temperature of low temperature electrode was about 370℃ and melting point of zinc is 420℃, the change of slope at point "A" is considered to be caused by the phase change of zinc metal.

In Fig.I-16(B), the change of thermoelectric power mentioned above is expressed more clearly, where the vertical axis presents $\delta \phi^{oba} / \delta T$ and the horizontal axis presents temperature of the system.

According to eqn.(I-20), the thermoelectric power is expressed as the sum of transported entropy and entropy change in the electrode region. Since the former can not be affected by the phase change of electrode, it must be considered how the latter is effected by it.

As seen in Fig.I-17, the molar change of each component in the electrode region under the transfer of unit charge is expressed as;

Zn	:	$-(1/2)$	mol
Zn^{2+}	:	$(1/2)(1-t_{Zn2+})$	mol
Li^{+}	:	$-t_{Li+}$	mol
K^{+}	:	$-t_{K+}$	mol
Cl^{-}	:	t_{Cl-}	mol

,where t_i stands for the transport number of component i.

The entropy change in the electrode region can be obtained as a sum of the products of these values presented above and the

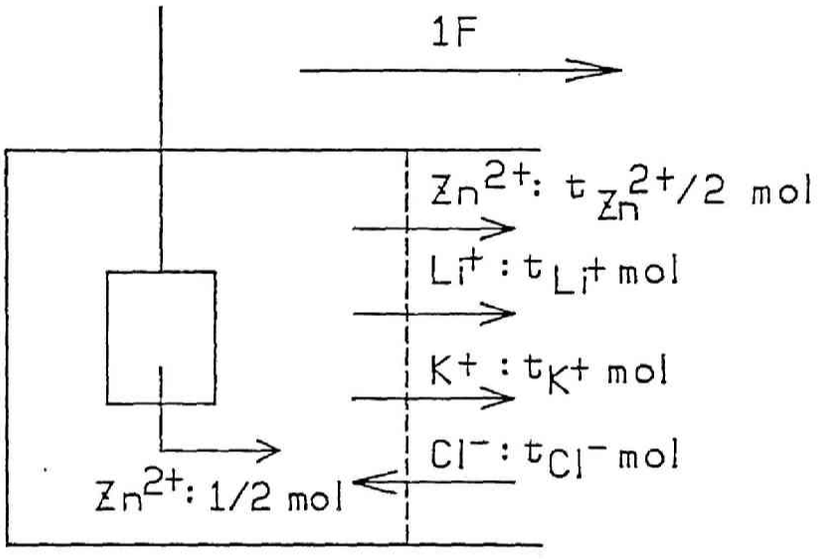

Fig.I-17 Mass balance in anode region

partial molar entropy of each component, therefore it can be expressed as follows.

In case zinc is liquid;

$$\Delta S_{liquid} = -(1/2) S_{Zn(liquid)} + (1-t_{Zn^{2+}})/2 \cdot S_{Zn^{2+}} - t_{K^+} S_{K^+} - t_{Li^+} S_{Li^+} + t_{Cl^-} S_{Cl^-} \quad (I-22)$$

In case zinc is solid;

$$\Delta S_{solid} = -(1/2) S_{Zn(solid)} + (1-t_{Zn^{2+}})/2 \cdot S_{Zn^{2+}} - t_{K^+} S_{K^+} - t_{Li^+} S_{Li^+} + t_{Cl^-} S_{Cl^-} \quad (I-23)$$

Here, $S_{Zn(liquid)}$ and $S_{Zn(solid)}$ stand for the molar entropy of pure zinc metal in liquid and solid phases, respectively.

Therefore the difference of thermoelectric power due to the phase change of zinc metal is expressed as follows.

$$\Delta \varepsilon = (\Delta S_{solid} - \Delta S_{liquid})/F = (1/2) \cdot (S_{Zn(solid)} - S_{Zn(liquid)})/F \quad (I-24)$$

Since the fusion entropy of zinc is 2*0.055mV/K[8], $\Delta \varepsilon$ must be equal to 0.055mV/K. On the other hand, the change of the slope in Fig.I-16(A) is 0.058 ± 0.013mV/K, so it can be concluded that both values are equal within experimental errors and our experimental method is reliable enough.

2)Sn-Li electrode system (single liquid phase)

Next the experimental result where the electrode was in single liquid phase is to be discussed. The relation between the

temperature difference and the electromotive force is shown in Fig.I-18. Though a good linearity is observed between them just as the case of zinc electrode systems, the slope of the line, or thermoelectric power, changes according as the lithium concentration in the alloy. The concentration dependence of thermoelectric power is shown in Fig.I-19.

One of the interesting points is that the thermoelectric power decreases as the lithium concentration increases and the sign of the thermoelectric power changes at the point "A". This means that the electrodeposition of lithium metal in tin-lithium alloy is endothermic when lithium concentration of the electrode is lower than 30% and exothermic when it is higher than that.

Since a rigorous explanation between thermoelectric power and single electrode heat is presented in Chapter4, only a brief and conceptual explanation is to be described here concerning the reason why the negative sign of thermoelectric power corresponds to the exothermic reaction.

When the reaction;

$$Li^{+} + e^{-} \rightarrow Li$$

is exothermic, the equilibrium shifts to the left as the temperature rises. It means that the electrode at high temperature presents more negative potential than a low temperature one.

On the other hand, in case of discussing how the thermoelectric power is effected by a phase change of an electrode, its effect on the entropy change of the electrode region; Δs must be considered because such a phase change of the

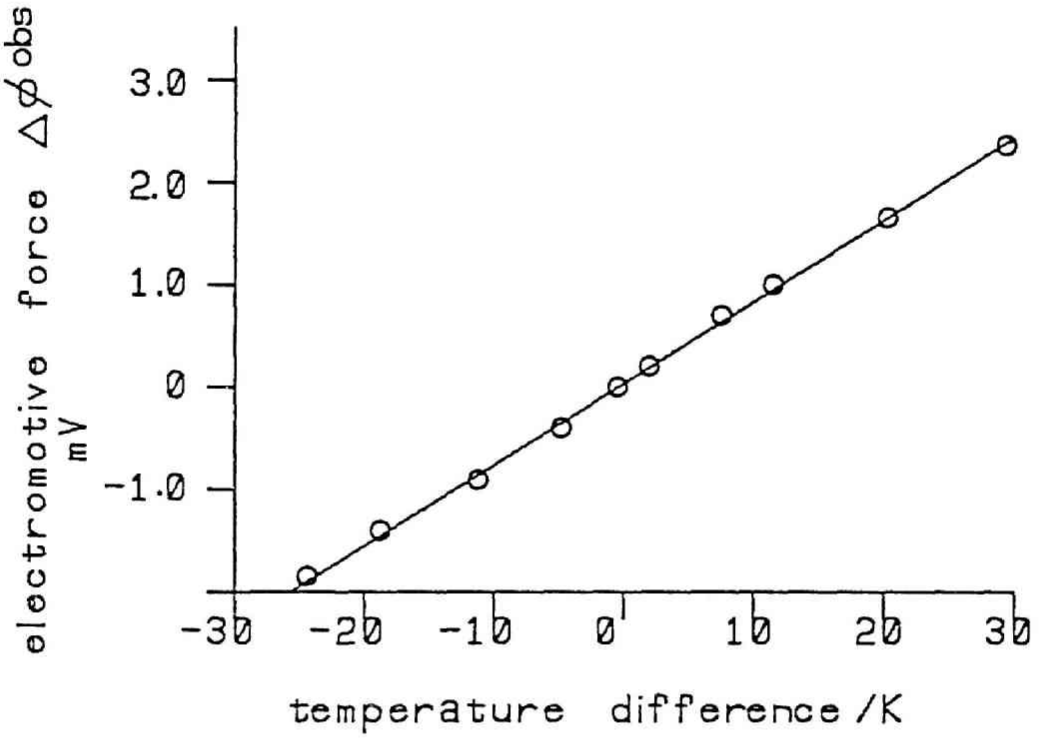

Fig.I-18 Relation between temperature difference and electromotive force (Sn-Li alloy in single liquid alloy)

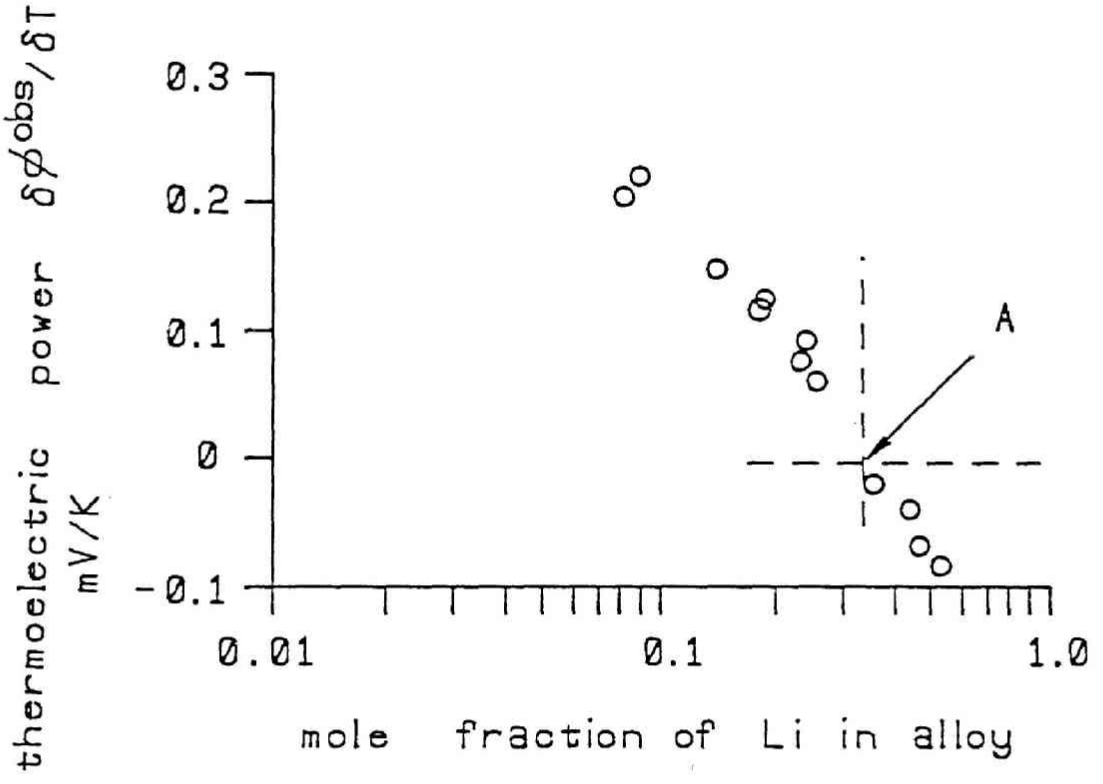

Fig.I-19 Concentration dependence of thermoelectric power

electrode metal causes no effect on the entropy of a salt phase in the system.

This Δs can be expressed as the next eqn.(I-25) just like the case of Zn/Zn(Ⅱ) system.

$$\Delta s = -s_{Li} + (1-t_{Li+})s_{Li+} - t_{K+}s_{K+} + t_{Cl-}s_{Cl-} \qquad (1-25)$$

Here, all terms on the right except the first one are regarded constant with respect to the composition of the alloy. Therefore eqn.(I-25) can be rewritten as ;

$$\Delta s = \text{const.} - s^{\circ}_{Li} + 2.303R \cdot \log [Li] - s^{*}_{Li} \qquad (I-26)$$

,where s^{*}_{Li} stands for the excess partial molar entropy of lithium in alloy.

According to eqn.(I-26), if $\varepsilon - s^{*}/F$ is plotted against the logarithm of Li mole fraction in the alloy, a good linearity whose slope is 2.303R/F must be obtained.

The excess partial molar entropy of lithium in the liquid alloy can be calculated from the activity coefficients of lithium in alloy by use of next equation.

$$s^{*} = - R\ln\gamma - RT(\delta \ln\gamma / \delta T) \qquad (I-27)$$

The measured activity coefficients of Li in alloy are shown in TableI-1. According to these data, $RT(\delta \ln\gamma / \delta T)$ can be regarded as constant whose value is 0.762 ± 0.02mV/K, and s^{*} in

Table.I-1 Activity coefficient of Li in Li-Sn alloy

temperature	50.8Li%	24.99Li%	9.17Li%	6.00Li%
482.6 ℃	8.2123e-04	3.8718e-04	1.5413e-04	1.1930e-04
487.5	8.5428e-04	4.0875e-04	1.6188e-04	1.2575e-04
493.7	9.1498e-04	4.4228e-04	1.7418e-04	1.3543e-04
500.0	9.8136e-04	4.7386e-04	1.8495e-04	1.4503e-04
506.97	1.0709e-03	5.1718e-04	2.0011e-04	1.5763e-04
511.7	1.1271e-03	5.4545e-04	2.0840e-04	1.6493e-04

eqn.(I-27) can be approximately expressed as;

$$s^{*}_{Li}/F = 0.653X_{Li}^{2}-0.738X_{Li}+0.406 \quad [\times 10^{-3}\ V/K] \qquad (I-28)$$

, where X_{Li} represents the mole fraction of lithium in alloy. Then the relation between $\varepsilon - s^{*}/F$ and the logarithm of lithium mole fraction were obtained as shown in Fig.I-20. A good linearity is observed between them and the slope of the line accords with 2.303R/F as expected.

On the other hand, the activity coefficient of lithium; γ is equal to 1 at the point where lithium mole fraction is equal to 1, therefore s_{Li}^{*} must be zero there. This means if the line in Fig.I-20 is extrapolated to the point of $X_{Li}=1$, the vertical value of that point must be in coincidence with the thermoelectric power of pure lithium electrode systems.

Since the observed thermoelectric power includes the thermoelectric power between liquid alloy and molybdenum lead wire, the extrapolated value of thermoelectric power in Fig.I-20 must be the sum of thermoelectric powers of pure lithium electrode and that between liquid lithium and molybdenum lead in a more rigorous sense. As obtained in the previous section, the former is 0.095mV/K, and from the published data[5], the latter is estimated as -0.029mV/K.

The result is that the extrapolated value was 0.047 ± 0.024mV/K and the sum of 2 thermoelectric powers is 0.095-0.029=0.066mV/K. Though the coincidence is not perfect, it can be concluded that both values are equal within experimental

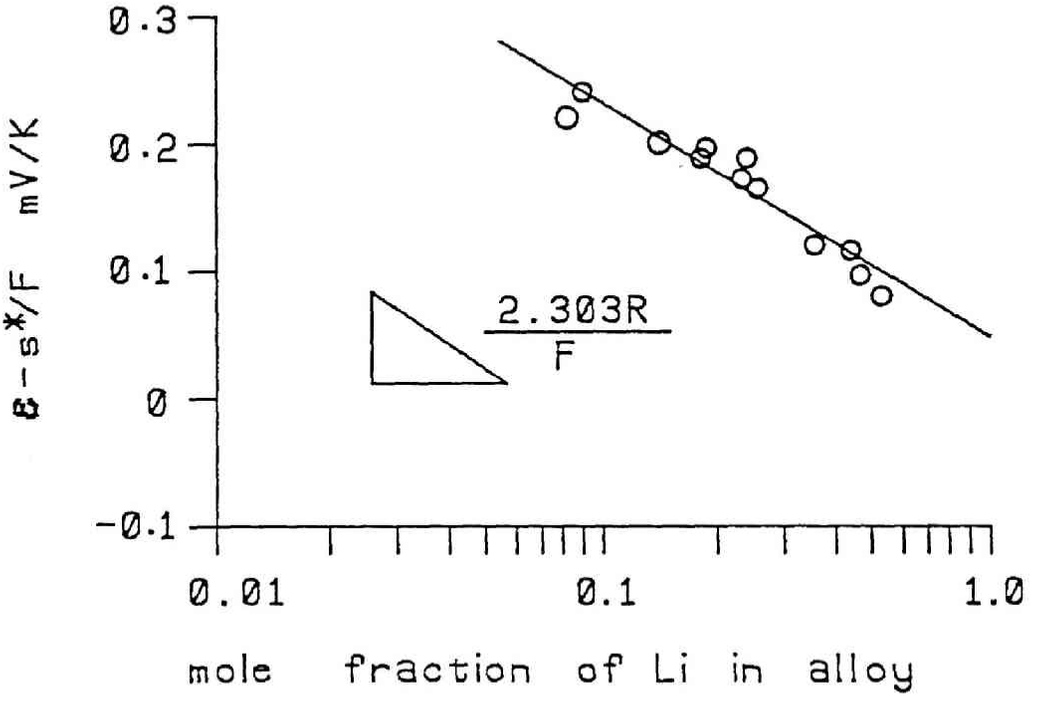

Fig.I-20 Concentration dependence of $\varepsilon - s^*/F$

errors.

3)Sn-Li electrode system (liquid-solid coexisting phase)

Here the thermoelectric power with liquid-solid coexisting electrode will be discussed. The experimental result is shown in Fig.I-21. Since the lithium concentration of this electrode is about 47%, according to the phase diagram, the alloy is single liquid phase over the temperature of 480℃ and separates into liquid and solid phases under this temperature. So the region "A" corresponds to the liquid-solid coexisting zone and the region "B" corresponds to the single liquid phase.

The shape of the graph is quite different from that obtained in the previous experiment. The most different point is the magnitude of thermoelectric power in liquid-solid coexisting zone. It is extremely large in comparison with the case of other single phase electrode systems.

Another unique point in this result is that the relation between temperature difference and electromotive force is not linear in region "A". That is thermoelectric power in liquid-solid coexisting zone cannot be regarded constant with respect to temperature. Theoretical explanations concerning these phenomena are to be discussed below.

As mentioned above, the important point is the entropy change of the electrode region under the transfer of unit charge. So first, it will be discussed how this entropy change is effected by the phase state of an electrode.

As shown in Fig.I-22 the entropy change in the electrode

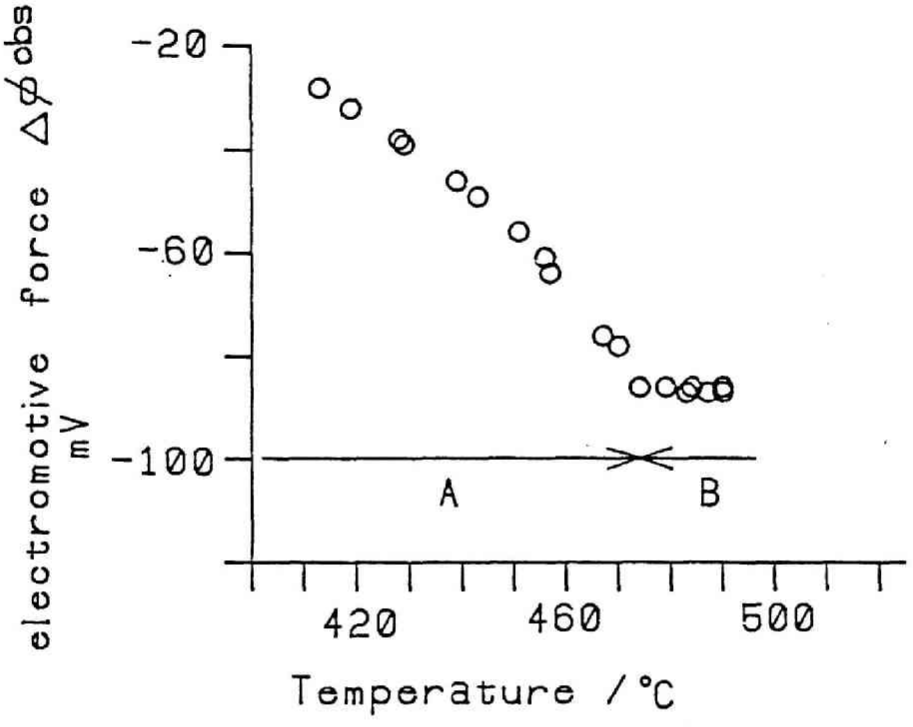

Fig.I-21
Electromotive force
(Li conc. 47.7%)

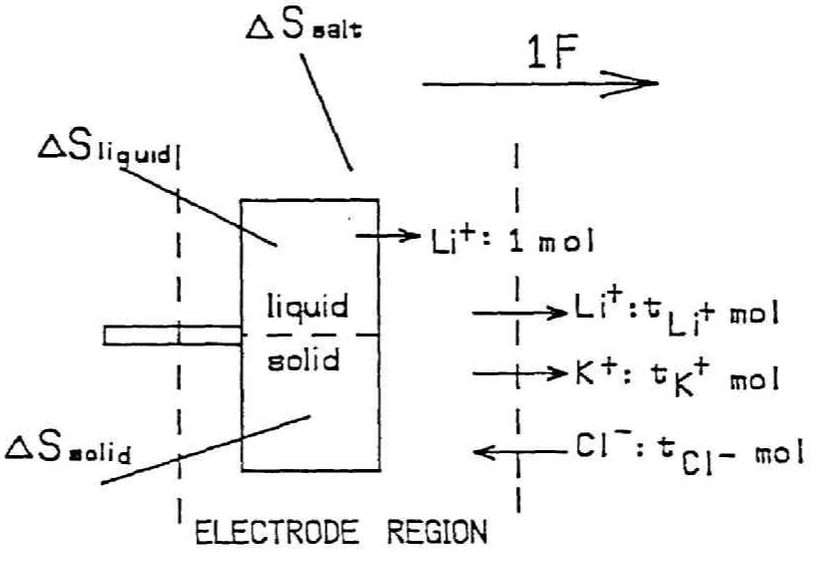

Fig.I-22 Mass and entropy balance in electrode region

region can be divided into three terms as;

$$\Delta s = \Delta s_{salt} + \Delta s_{liquid} + \Delta s_{solid} \qquad (I\text{-}29)$$

The first one is the entropy change of the salt phase, and the second one is that in the liquid alloy phase and the third one is that in the solid alloy phase. Since the first term is not affected by composition or phase state of the electrode metal, we can treat it as constant.

In order to evaluate other two terms, mass transfer between 2 phases under the transfer of unit charge has to be taken into consideration.

When unit amount of lithium dissolves into a salt phase with the transfer of unit charge, as long as two phases coexist and the temperature is constant, the composition of each phase can not be changed.

That is, the effect of lithium dissolution into the salt on the composition of liquid phase must be canceled by the mass transfer between two coexisting phases. This mass transfer of each component in each electrode phase must be quantitatively discussed next.

As shown in Fig.I-23, p mole of Sn-Li solid alloy is supposed to dissolve into liquid phase when 1 mole of lithium dissolves into the salt phase under the transfer of unit charge. Then the molar changes of lithium and tin in liquid phase under the same condition are expressed as;

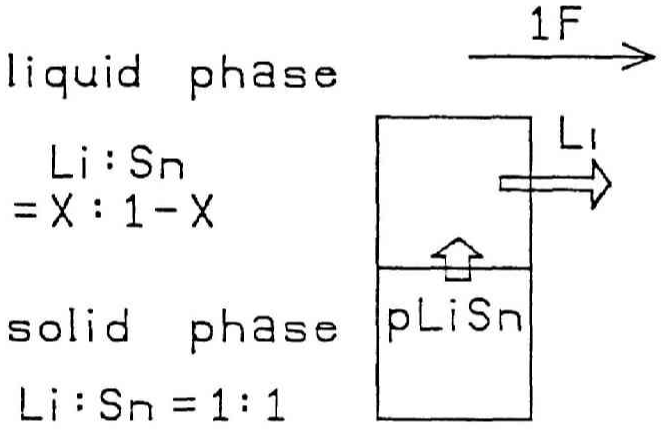

Fig.I-23 Mass balance between two phases

$$\Delta n_{Li} = p-1$$

and $$\Delta n_{Sn} = p \qquad \text{mol}$$

As mentioned above, the composition change in liquid phase can not occur, therefore the ratio $\Delta n_{Li}/\Delta n_{Sn}$ must be equal to the original ratio $X_{Li}/(1-X_{Li})$ and following relations are obtained.

$$\Delta n_{Li}/\Delta n_{Sn} = (p-1)/p$$
$$= X_{Li}/(1-X_{Li})$$
$$\therefore\ p = -(1-X_{Li})/(2X_{Li}-1) \qquad \text{(I-30)}$$

, where X_{Li} stands for mole fraction of lithium in liquid phase before the transfer of unit charge.

Since the mass balance between 2 electrode phases is understood, evaluation of the entropy change of each phase is carried out by using the relation obtained above. The entropy changes of liquid and solid phases are expressed as eqns.(I-31) and (I-32), respectively.

$$\Delta S_{liquid} = p(S_{Li(liquid)}+S_{Sn(liquid)})-S_{Li(liquid)}$$
$$= -\{(1-X)/(2X-1)\}S_{Sn(liquid)}-\{X/(2X-1)\}S_{Li(liquid)} \qquad \text{(I-31)}$$

$$\Delta S_{solid} = -p(S_{Li(solid)}+S_{Sn(solid)})$$
$$= \{(1-X)/(2X-1)\}(S_{Li(solid)}+S_{Sn(solid)}) \qquad \text{(I-32)}$$

On the other hand, the thermoelectric power of liquid-solid

coexisting electrodes is expressed as;

$$\varepsilon_T = -(\bar{\bar{S}} + \Delta S_{salt} + \Delta S_{liquid} + \Delta S_{solid})/F \quad (I-33)$$

,and that of single liquid alloy is expressed as;

$$\varepsilon_T = -(\bar{\bar{S}} + \Delta S_{salt} + \Delta S_{liquid})/F \quad (I-34)$$

,where $\Delta S_{liquid} = -S_{Li(liquid)}$.

So the thermoelectric power difference between them is expressed as the next eqn.(I-35).

$$\begin{aligned}\Delta \varepsilon_T &= [-S_{Li(liquid)} - \Delta S_{liquid} - \Delta S_{solid}]/F \\ &= [(1-X)/(2X-1)\{(S_{Li(liquid)} + S_{Sn(liquid)}) \\ &\quad -(S_{Li(solid)} + S_{Sn(solid)})\}]/F \\ &= \{(1-X)/(2X-1)\}(S_{LiSn(in\ liquid)} - S_{LiSn(in\ solid)})/F\end{aligned} \quad (I-35)$$

The denominator of the coefficient in eqn.(I-35) is zero at the point of 50Li%, which explains the experimental result that the magnitude of thermoelectric power is extremely large when lithium is near 50%.

It also indicates that the sign of thermoelectric power in coexisting phase will change at the same concentration.

In order to verify this, the result of experiment is presented in Fig.I-24, where the lithium concentration of the electrode was 56.6%. In region(B) the thermoelectric power has a large value with an opposite sign of the previous case just as

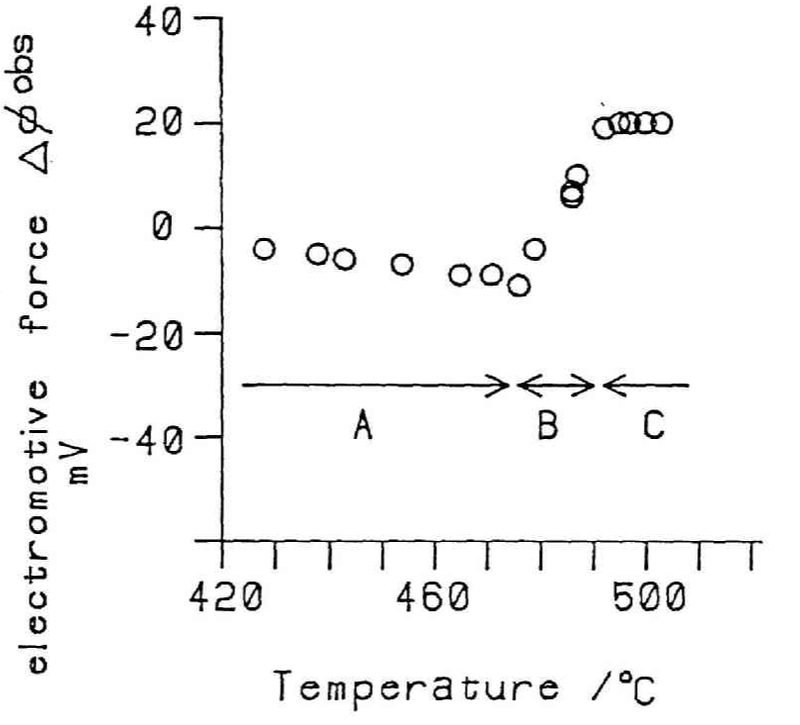

A: solid - solid phase
B: liquid - solid phase
C: single liquid phase

Fig.I-24 Electromotive force (Li conc. 56.6%)

indicated by eqn.(I-35).

On the other hand, thermoelectric power of liquid-solid coexisting electrode was not constant with respect to temperature of a system. But this phenomenon is quite reasonable, because the composition of liquid phase changes as a function of temperature of the system, which means ,--- in liquid-solid coexisting zone, any electrode with different composition must present the same thermoelectric power at the same temperature. It accords to the experimental result shown in Fig.I-25, which also presents that the magnitude of thermoelectric power decreases as the lithium concentration of the alloy get far from 50%.

4)Sn-Li alloy electrode (solid-solid coexisting phase)

The last part of this section is a discussion about solid-solid coexisting electrode. Thermoelectric power of region(A) in Fig.I-24 corresponds to the solid-solid coexisting zone. Its magnitude is not so large and good linearity has been obtained between temperature difference and electromotive force.

In this zone, tin-lithium electrode is composed of 2 solid phases; LiSn and Li_2Sn, so, the single electrode reaction of this electrode is expressed as:

$$LiSn + Li^+ + e^- = Li_2Sn \qquad (I-36)$$

Therefore entropy change of the electrode material caused by the unit charge transfer must be expressed as eqn.(I-37) by using

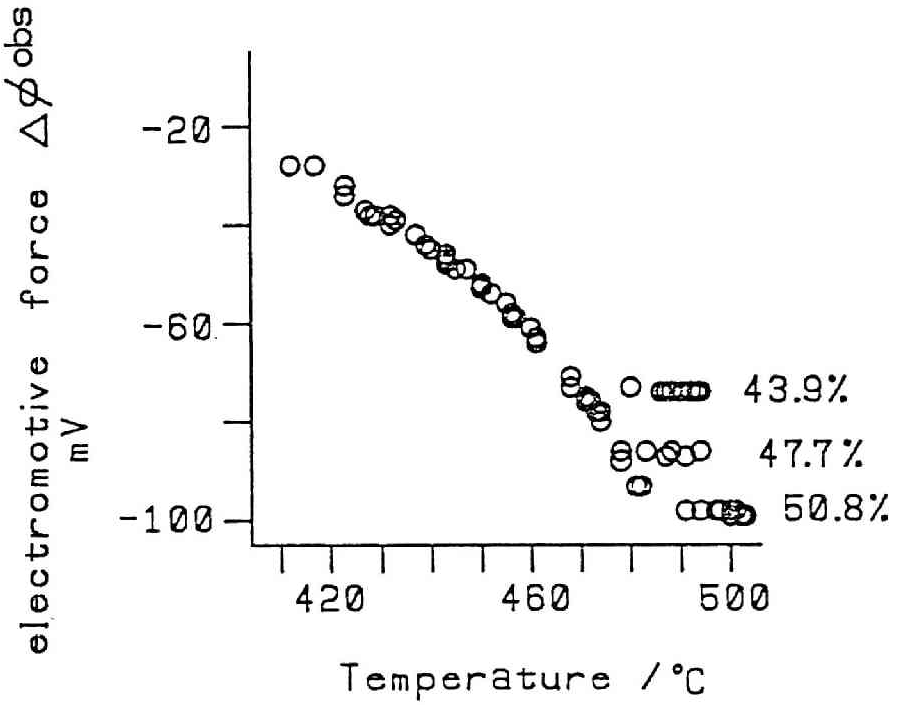

Fig. I-25 Concentration dependence of electromotive force (Sn-Li alloy in liquid-solid phase)

partial molar entropy of lithium in both phases.

$$\Delta S_{metal} = S_{Li<Li_2Sn>} - S_{Li<LiSn>} \qquad (I-37)$$

If this equation is valid, every term in eqn.(I-38) receives no effect from the composition change of the alloy.

$$\varepsilon = -(\bar{\bar{S}} + \Delta S_{salt} + \Delta S_{metal})/F \qquad (I-38)$$

It means thermoelectric power is expected to be independent of the composition of alloy under the temperature of eutectic point. The result is shown in Table.I-2, which accords with this expectation.

Before closing this section, one exceptional data is to be discussed, which is shown in Fig.I-26. Mole fraction of lithium in alloy electrode was 52%.

One of the most conspicuous point of this result is that the width of solid liquid coexisting zone is extremely narrow as compared with previous results. As for this phenomenon, it is estimated that the alloy composition is just that of the solid solution region, which is hatched in Fig.I-27.

At this composition, temperature range of liquid solid coexisting zone is extremely small, which corresponds to the narrow region(B) in Fig.I-26.

Besides, in FigI-26 thermoelectric power in region(c) is smaller than that in region(A). This indicates that the partial molar entropy of Li in solid alloy is much larger than that in liquid alloy at the same composition.

As for this matter, if the whole entropy of the alloy

electrode is expressed as a function of composition just as shown in Fig.I-28, magnitude of the partial molar entropy (slope of the curve line) at the point of P gets larger than that in solid phase, which accords to the experimental result.

Table.I-2 Thermoelectric power (Li-Sn alloy in solid-solid phase)

Li mol%	Thermoelectric power mV/K
54.3	0.13±0.03
56.6	0.13±0.03
57.2	0.13±0.01

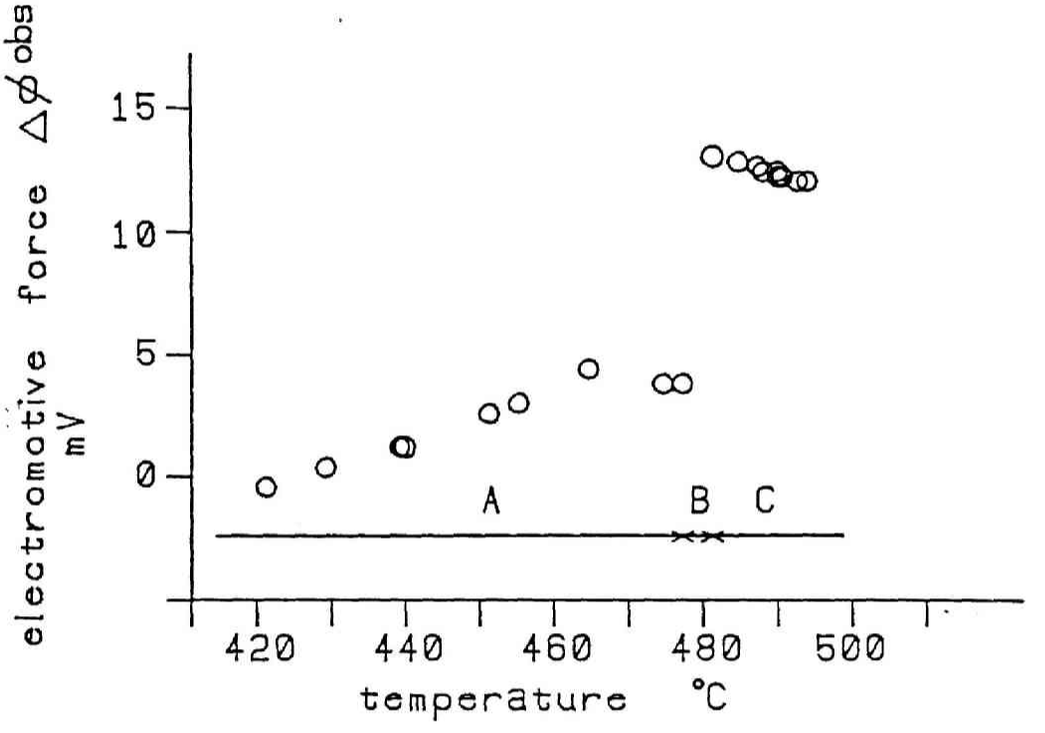

Fig. I-26 Electromotive force
(Li conc. 52%)

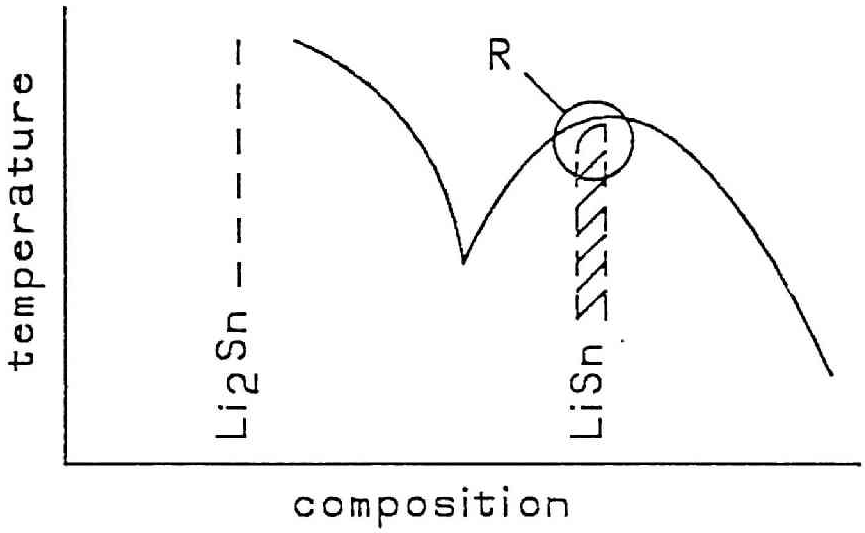

Fig.I-27 Phase diagram

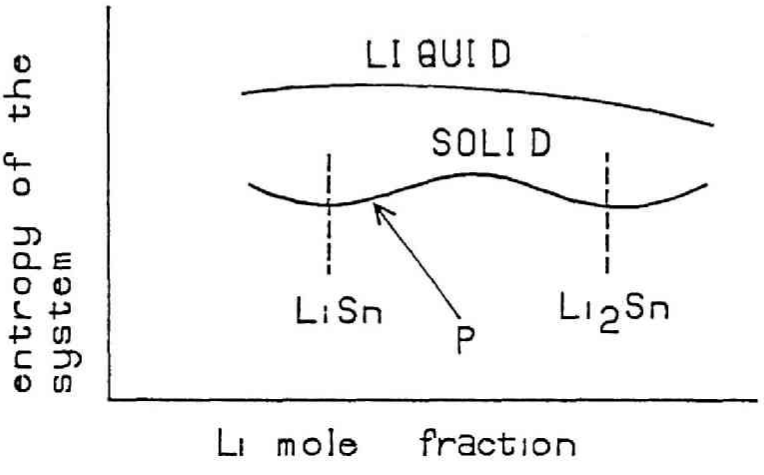

Fig.I-28 Composition dependence of entropy in Li-Sn alloy

2-3 Evaluation of transported entropy

It has been discussed in previous sections how the concentration of electrode reactants and/or the composition of electrode itself effects on thermoelectric power, and the results have been thermodynamically explained by evaluating the first term on the right of next equation, ie. entropy change of electrode region under the transfer of unit charge.

$$d\phi^{obs}/dT = (\Delta s + \bar{\bar{S}})/F \qquad (I\text{-}39)$$

In this section, the second term $\bar{\bar{m}}$; S is to be discussed and its magnitude is to be estimated.

As mentioned above, this term is called transported entropy and defined as the the entropy that flows out from the electrode region into the electrolyte under the transfer of unit charge.

In molten salt systems, when the solute concentration is not too high, since almost all charge is transported by solvent ions (Li^+, K^+, Cl^- in systems mentioned above) through the electrolyte, this transported entropy is considered to be almost independent from solute ions.

This means once the magnitude of transported entropy can be determined in LiCl-KCl molten salt system, thermoelectric power can be calculated with eqn.(I-39) by using Δs obtained from other experiments.

As seen from eqn.(I-39) the value of Δs is necessary to determine transported entropy from thermoelectric power. In case of Li(T)/LiCl-KCl/Li(T+dT) system, this entropy change can be

expressed as;

$$\Delta s = -s_{Li} + s_{Li^+} - t_{Li^+}s_{Li^+} - t_{K^+}s_{K^+} + t_{Cl^-}s_{Cl^-}$$
$$= -s_{Li} - (t_{Li^+} - 1)s_{LiCl} - t_{K^+}s_{KCl} \qquad (I\text{-}40)$$

In this case, since Li^+ ion is a constituent of solvent and is an electrode reactant at the same time, the equation is relatively simple, but in case of a system which includes solute ions like Ag^+, it can be more complicated as shown below.

$$\Delta s = -s_{Ag} - (t_{Ag^+}-1)s_{Ag^+} - t_{Li^+}s_{Li^+} - t_{K^+}s_{K^+} + t_{Cl^-}s_{Cl^-} \qquad (I\text{-}41)$$

This equation can be rewritten as;

$$\Delta s = (s_{Ag^+} + s_{Cl^-} - s_{Ag} - s_{1/2Cl_2})$$
$$- t_{Ag^+}s_{AgCl} - t_{Li^+}s_{LiCl} - t_{K^+}s_{KCl} + s_{1/2Cl_2} \qquad (I\text{-}42)$$

Sum of the first four terms on the right of eqn.(I-42) is the temperature coefficient of decomposition voltage of AgCl in LiCl-KCl and Takahashi[9] experimentally measured this kind of coefficients with respect to AgCl, $NiCl_2$, $ZnCl_2$, $PbCl_2$, etc in LiCl-KCl systems.

On the other hand, when t_{Ag^+} is negligibly small compared to t_{Li^+} or t_{K^+}, the term; $t_{Ag^+}s_{AgCl}$ can be regarded as zero.

Since s_{Li} and s_{Cl2} were already reported[10], if we can evaluate the transport numbers; t_{Li^+} , t_{K^+} and partial molar entropy of LiCl and KCl at eutectic composition, the value of Δs

can be calculated from eqns.(I-40) and (I-42) by use of thermoelectric power measured in previous sections. That means, by substracting this value from thermoelectric power, transported entropy in LiCl-KCl system can be determined. As for $NiCl_2$, $ZnCl_2$ and $PbCl_2$, the procedure is the same.

First transport numbers of Li^+ and K^+ must be determined. Instead of measuring t_{Li+}, t_{K+} in LiCl-KCl system experimentally, these were estimated here.

By using t_{Li+} in pure LiCl and t_{K+} in pure KCl[11], these numbers in LiCl-KCl have been calculated according as the molar ratio of each component in LiCl-KCl. Estimated values are as follows.

$$t_{Li+} : t_{K+} : t_{Cl-} = 0.438:0.258:0.304 \qquad \text{(I-43)}$$

Next, partial molar entropy of LiCl and KCl is to be estimated here.

First, suppose partial molar entropy of LiCl and KCl are expressed as follows.

$$s_{LiCl} = s^{\circ}_{LiCl} - R\cdot \ln X_{LiCl} \qquad \text{(I-44)}$$

$$s_{KCl} = s^{\circ}_{KCl} - R\cdot \ln X_{KCl} \qquad \text{(I-45)}$$

According to J.Lumsden[12], the deviation of s_{KCl} from eqn.(I-45) is approximately 1% of its value.

As for s°_{LiCl} and s°_{KCl}, the summation of fusion entropy and molar entropy of solid LiCl and KCl at 700K was used.

(Difference between these values and the extraporated value from molar entropies of liquid region in higher temperature is small and negligible.)

By use of these values, partial molar entropies of LiCl and KCl are estimated as follows.

$$s_{LiCl}/F = 1.356 \times 10^{-3} \text{ V/K}$$

$$s_{KCl}/F = 1.667 \times 10^{-3} \text{ V/K}$$

Molar entropy of lithium metal and Cl_2 gas had been obtained as follows[10].

$$s^{\circ}_{Li}/F = 0.619 \times 10^{-3} \text{ V/K}$$

$$s^{\circ}_{(1/2)Cl_2}/F = 1.311 \times 10^{-3} \text{ V/K}$$

As a conclusion, transported entropy calculated by use of eqns.(I-40) and (I-42) are shown in TableI-3 and Fig.I-29. Though obtained values of transported entropy measured in various systems are not rigorously coincident with each other, since the difference of thermoelectric power among various systems are about 0.7mV/K, the fact that the transported entropy obtained here agree with each other within $\pm$0.1mV indicates that the transported entropy does not depend on solute ion too much.

But this small disagreement of obtained data is considered to be caused by the effect of solute ions in a system, because in case of nickel, whose chloride has high melting point, obtained

Table.I-3 Transported entropy estimated from different electrode systems

	$\bar{\bar{S}}/F$ mV/K
Li	0.227
Ag	0.366 ± 0.015
Ni	0.204 ± 0.03
Zn	0.304 ± 0.033
Pb	0.364 ± 0.01

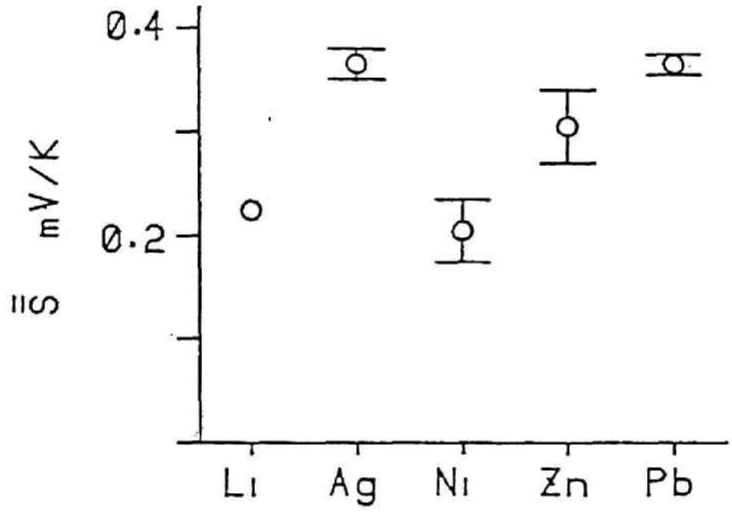

Fig.I-29 Transported entropy

transported entropy is rather small and reversely in case of Zn,Pb,Ag, they are large.

On the other hand, the transported entropy can be divided into many terms as shown below.

$$\bar{\bar{S}} = \bar{\bar{S}}_e + t_{M^+}\cdot\bar{\bar{S}}_{M^+} + t_{Li^+}\cdot\bar{\bar{S}}_{Li^+} + t_{K^+}\cdot\bar{\bar{S}}_{K^+} + t_{X^-}\cdot\bar{\bar{S}}_{X^-} \qquad (I-46)$$

In general, transported entropy of electron in metal is much smaller than that in melt. Besides when the concentration of solute ion is small, the relation $t_{M^+} \ll t_{S^+}$ is available and the transported entropy has been simplified as follows.

$$\bar{\bar{S}} = t_{Li^+}\cdot\bar{\bar{S}}_{Li^+} + t_{K^+}\cdot\bar{\bar{S}}_{K^+} + t_{X^-}\cdot\bar{\bar{S}}_{X^-} \qquad (I-47)$$

In this way, transported entropy can be expressed as that of ionic species and their transport number, so if solute ion effects on the transported entropy of any solvent ion in eqn.(I-47), $\bar{\bar{S}}$ may receive influence from solute ions.

As a conclusion, in order to avoid the effect of solute ion, the data by Li/Li^+ electrode system is considered to be most reliable, which is 0.227mV/K

2-4 Conclusion

1) The thermodynamical expression of thermoelectric power derived in Chapter 1 has been experimentally confirmed in molten LiCl-KCl systems. The equation explains how the concentration and valence number of electrode reactants effect on the thermoelectric power.

2) Thermoelectric power of lithium-tin electrode has been measured and analyzed accurately. The thermoelectric power shows different behaviors summarized below, according as the phase state of the electrode.

i)In single liquid phase: A good linearity exists between temperature difference and electromotive force. The magnitude of thermoelectric power depends on lithium concentration of the electrode.

ii)liquid-solid coexisting phase: Thermoelectric power is extremely large in comparison with other systems and its value is not constant with respect to temperature. Its sign changes at the point of 50 Li%.

iii)solid-solid coexisting phase: A good linearity exists between temperature difference and electromotive force. It is constant between 52 and 60%.

These behaviors have been thermodynamically explained.

3) Transported entropy in LiCl-KCl system at 425℃ has been estimated to be 0.227mV/K.

CHAPTER 3 The effect of mass flow on thermoelectric power

As mentioned in the introduction of this thesis, thermoelectric power can be one of the driving forces of mass transfer phenomena, but these phenomena may also occur due to emf caused by a pressure gradient in a system.

Some theoretical descriptions of the emf in a nonisothermal and static system were presented by Agar[13], Chanu[14] and Ito[15], and that in an isothermal and convective system was presented by Haase[16]. But so far, no one has dealt with the nonisothermal and convective system.

This chapter first presents thermodynamic description of emf in a nonisothermal and convective system, and then presents experimental data obtained by a model experiment using an aqueous system in order to verify the derived theoretical equation and to evaluate the degree of contribution of the pressure gradient in a system to the value of emf.

3-1. Thermodynamic description of thermoelectric power in a convective system

In nonisobaric systems, the gradient of chemical potential $\nabla \mu_{Ti}$ expressed as eqn.(I-7) can be divided into two terms, one of which depends on concentration and the other on pressure.

$$\nabla \mu_{Ti} = \nabla \mu_i - \frac{\delta \mu_i}{\delta T} \cdot \nabla T \qquad \text{(I-48)}$$

$$= \frac{\delta \mu_i}{\delta C_i} \cdot \nabla C_i + \frac{\delta \mu_i}{\delta P} \cdot \nabla P \qquad \text{(I-49)}$$

Since concentration gradient can be neglected in a convective system, the first term of eqn.(I-49) is zero and eqns.(I-4),(I-5) and (I-6) can be simplified as follows.
(It is noted that the condition $\nabla C_i = 0$ is also valid when the initial thermoelectric power is measured.)

$$J_q = -Y_{qq} \nabla \ln T - Y_{qP} \nabla P - Y_{qQ} \nabla \phi^{obs} \qquad \text{(I-50)}$$

$$J_i = -Y_{iq} \nabla \ln T - Y_{iP} \nabla P - Y_{iQ} \nabla \phi^{obs} \qquad \text{(I-51)}$$

$$I = -Y_{Qq} \nabla \ln T - Y_{QP} \nabla P - Y_{QQ} \nabla \phi^{obs} \qquad \text{(I-52)}$$

Two following equations were used in the transformation above.

$$\nabla \phi = \nabla \phi^{obs} \qquad \text{(I-53)}$$

$$Y_{XP} = \Sigma Y_{Xi} \cdot \frac{\delta \mu_{Ti}}{\delta P} \qquad (X=q,i,Q) \qquad \text{(I-54)}$$

Equation (I-54) is only a definition of a new coefficient Y_{XP}. Equation (I-53) is valid since the chemical potential in a solid phase does not depend on pressure too much. It means that the quantity:

$$\nabla \mu_{Ti} = \frac{\delta \mu_i}{\delta P} \nabla P \quad (i=n+1 \sim k) \qquad \text{(I-55)}$$

is negligibly small compared with the other quantities considered.

Taking into account the condition I=0 during emf measurement,

the next equation is obtained from eqn.(I-52).

$$\nabla \phi^{obs} = - \frac{Y_{QP}}{Y_{QQ}} \nabla P - \frac{Y_{Qq}}{Y_{QQ}} \nabla \ln T \qquad (I-56)$$

This is the expression of emf in a loop as a function of both the temperature gradient and pressure gradient.

3-2 Thermoelectric power measurement in a convective system

In order to confirm the appropriateness of eqn.(I-56) and to clarify the physical meaning of each coefficient appearing in it, following two experiments have been conducted.

The first one was carried out in a nonisothermal and isobaric system and the second one in an isothermal and nonisobaric system. From these two experiments, the scale of emf caused by pressure difference was compared with that of emf caused by temperature difference.

3-2-1 Experimental

(I)Emf in a nonisothermal aqueous $AgNO_3$ solution system.

Experimental apparatus is shown in Fig.I-30, which consists of electrodes, chromel-alumel thermocouple coated with teflon, two flasks filled with $AgNO_3$ solution and the bridge to connect these flasks. By using a heater and a water-bath, temperature of each flask can be controlled independently.

The electrode is a coiled silver wire (99.99%, 200mm length, 1.2mm diameter)

After setting a certain temperature difference between two flasks by the heater and the water-bath, electric potential difference between two electrodes was measured with the digital multimeter (Takeda Riken TR6840). This procedure was repeated with respect to several concentrations.

A series of measurements on one concentration was completed

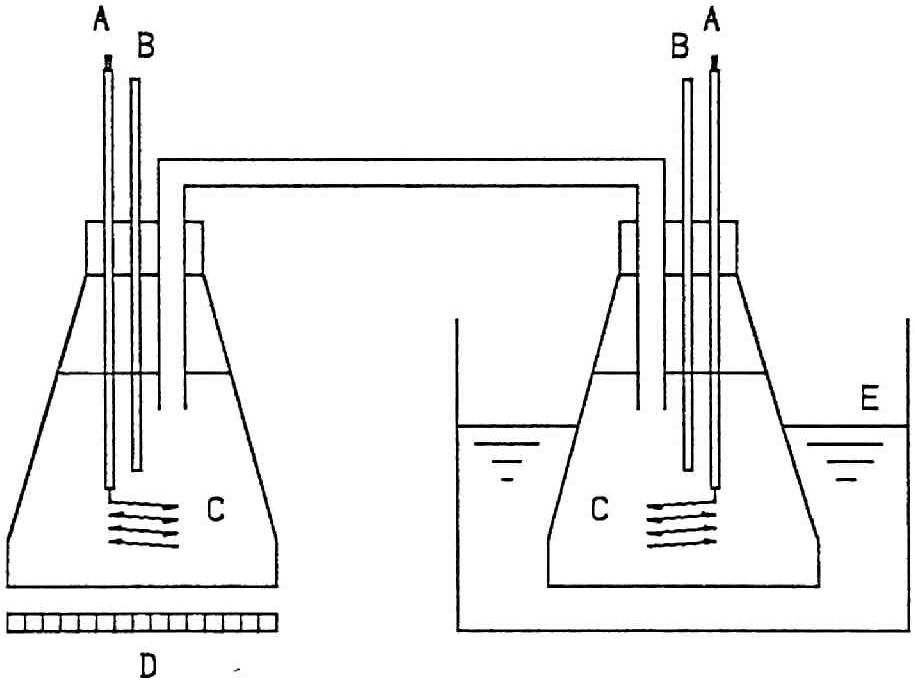

A: Ag electrode
B: thermocouple
C: $AgNO_3$ solution
D: heater
E: water-bath

Fig.I-30 Experimental apparatus

within an hour and it had been confirmed in the other experiment that ΔC_i did not appear in this apparatus within such a short time. Since the value of the Soret coefficient measured by Snowdon and Turner[17] was not negligibly small, this experimental result showed that the system was far from Soret equilibrium.

The temperature of colder flask stayed between 0～5℃.

(II)EMF in a nonisobaric aqueous $AgNO_3$ solution system (a system with volume flow)

Experimental apparatus is shown in Fig.I-31. In part "C", the tube is filled with ceramic beads and pyrex glass capillaries and by this some pressure difference is obtained when solution flows through this part. By controlling a power of pump or velocity of volume flow, pressure difference can be changed between 0～300mmHg.

The pressure near the electrode is measured with a manometer "B", and by reversing the stream of solution, pressure gradient in a system can also be reversed.

The electrode is a silver wire(99.99%, 12mm length, 1.2mm diameter), and just before being inserted into the apparatus, its surface was plated with silver in order to remove oxide layer and to obtain a stable Ag/Ag^+ potential.

After setting a certain pressure difference between two electrode regions by controlling the pump, electric potential difference between two electrodes was measured with a digital multimeter (Takeda Riken TR6840). This procedure was repeated

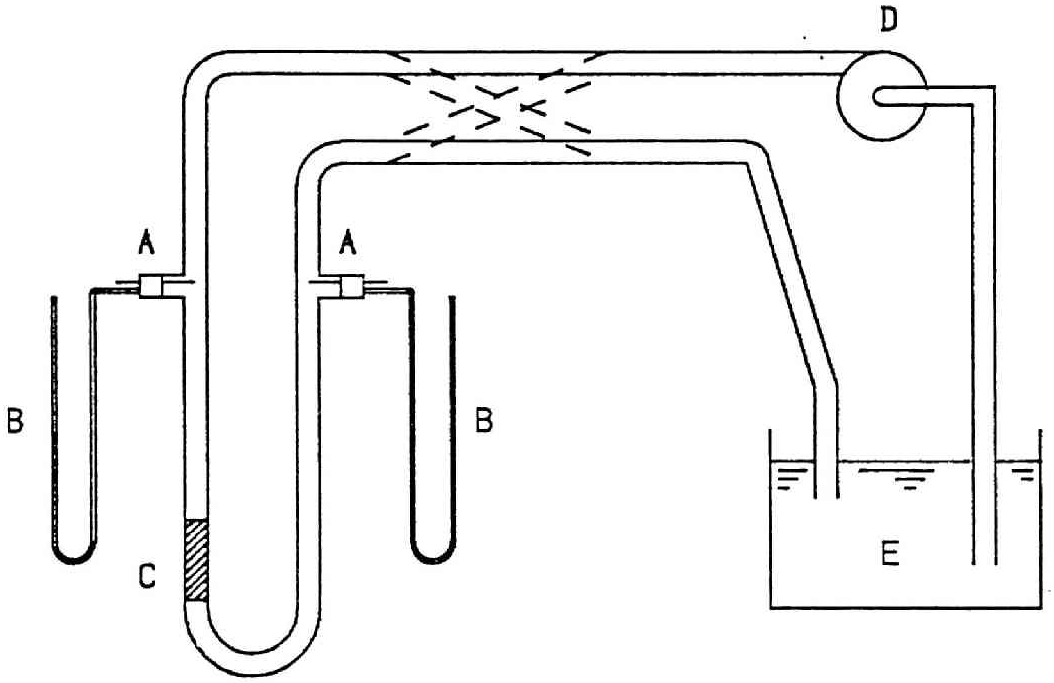

A: Ag electrode
B: manometer
C: ceramic beads and Pyrex glass capillaries
D: pump
E: $AgNO_3$ solutions

Fig.I-31 Experimental apparatus

with respect to several concentrations.

It is noted that the temperature gradient does not exist in this apparatus.

3-2-2 Results and discussion

(I) EMF in a nonisothermal system

Fig.I-32 shows the relation between temperature difference and measured emf when $AgNO_3$ concentration is 0.1M. Linear relation can be observed clearly. Electromotive force on the vertical axis is the value measured on reference to low temperature electrode. This means that the electric potential of high temperature electrode is always more negative than that of low temperature one.

Though similar linear relations were obtained when concentration was changed, the slope, electric potential difference per unit temperature difference, was different. The concentration dependence of this slope is shown in Fig.I-33 and this concentration dependence can be well explained by eqn.(I-20) derived before.

(II) EMF in a nonisobaric system

Fig.I-34 shows the relation between pressure difference and measured emf when $AgNO_3$ concentration is 0.099 M. The linear relation can be observed clearly, just as the case of thermoelectric power experiment described above. Electromotive force on the vertical axis is the value measured on reference to low-pressure electrode. This means that the electric potential

of high pressure electrode is always more positive than that of low pressure one.

Though similar linear relations were obtained when concentration was changed, the slope, electric potential difference per unit pressure difference, was different. The concentration dependence of this slope is shown in Fig.I-35.

In Fig.I-35 the slope is nearly equal to -1, which means that emf caused by the pressure gradient is inversely proportional to the $AgNO_3$ concentration. This relation can be explained as follows.

From eqn.(I-56), electric potential difference caused by unit pressure difference in an isothermal system is:

$$\frac{\Delta \phi^{obs}}{\Delta P} = - \frac{Y_{QP}}{Y_{QQ}} \qquad (I-57)$$

On the other hand, fluxes of heat, mass and charge are expressed as follows by using eqns.(I-50)～(I-52) and the condition $\nabla \ln T=0$.

$$J_q = -Y_{qP}\nabla P - Y_{qQ}\nabla \phi^{obs} \qquad (I-58)$$

$$J_i = -Y_{iP}\nabla P - Y_{iQ}\nabla \phi^{obs} \qquad (I-59)$$

$$I = -Y_{QP}\nabla P - Y_{QQ}\nabla \phi^{obs} \qquad (I-60)$$

Taking into account of eqn.(I-60), it is clearly understood that the coefficient Y_{QQ} in eqn.(I-57) corresponds to electric conductivity and Y_{QP} stands for the "streaming conductivity", that is, current caused by unit pressure gradient.

Since the aqueous $AgNO_3$ solution system does not include

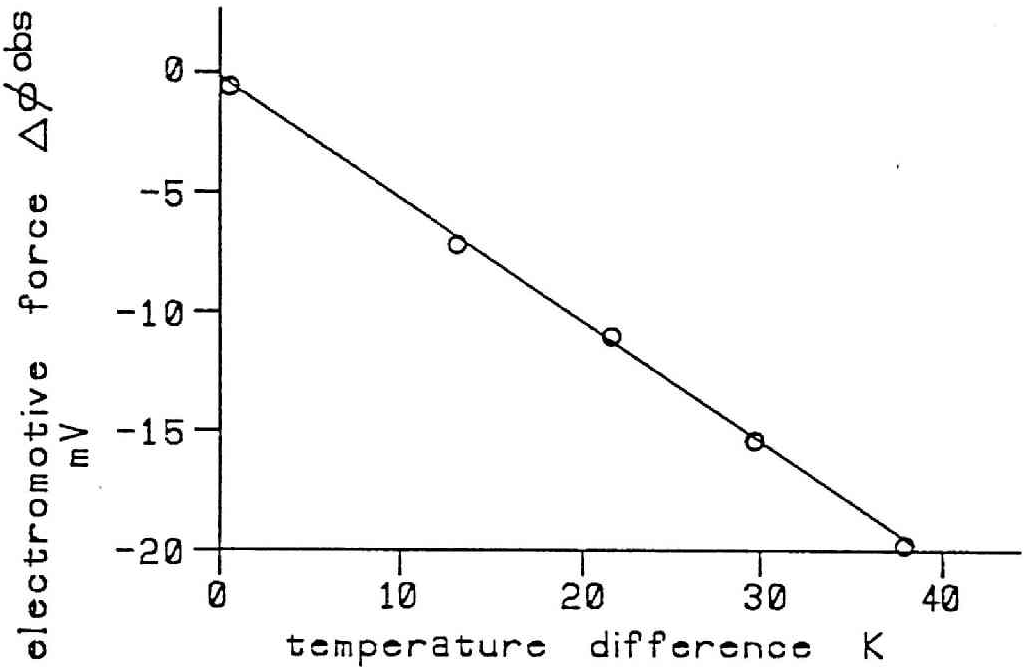

Fig.I-32 Relation between temperature difference and electromotive force

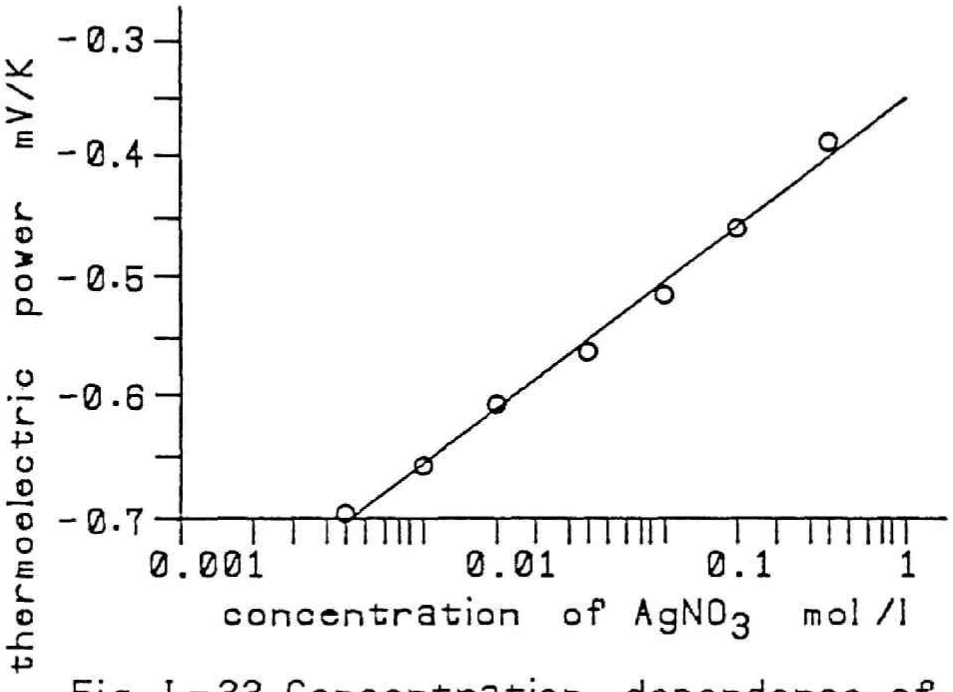

Fig.I-33 Concentration dependence of thermoelectric power

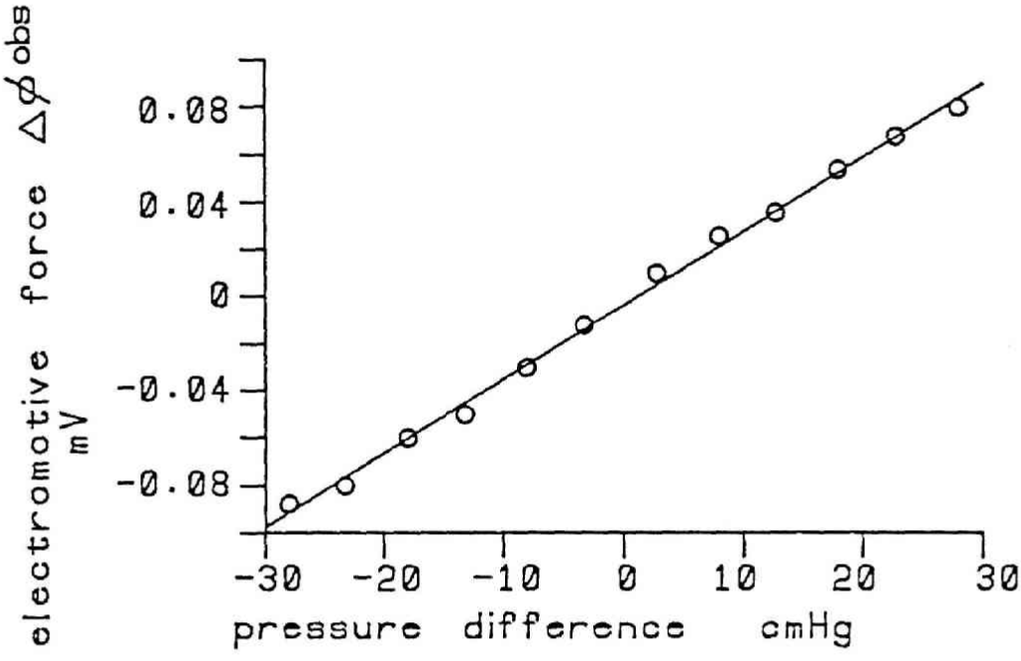

Fig.I-34 Relation between pressure difference and electromotive force

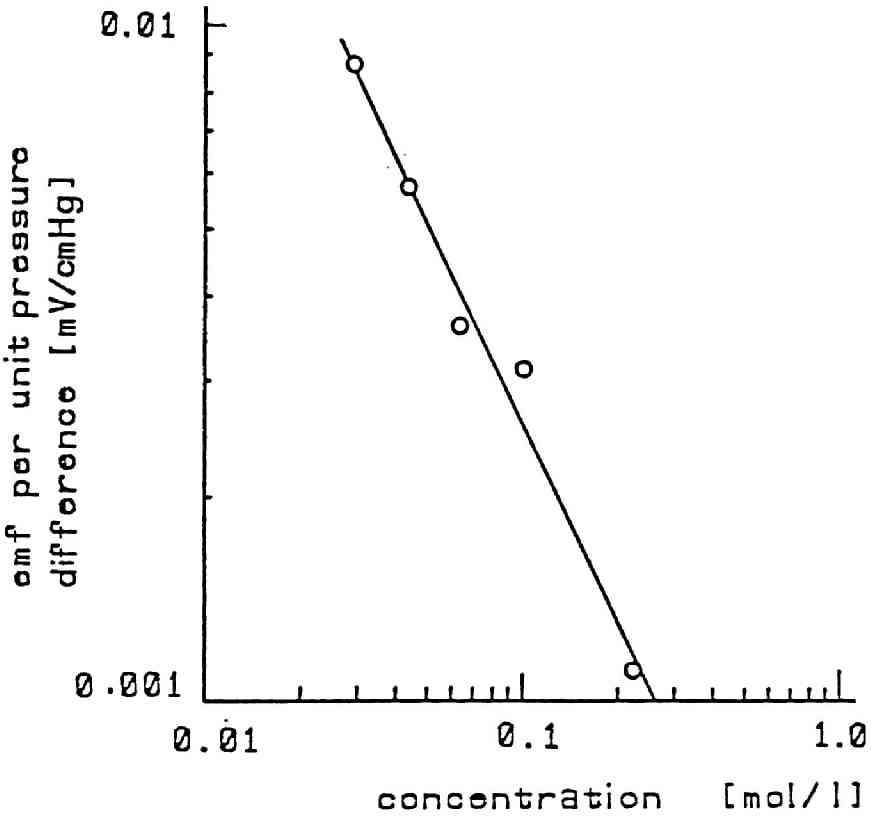

Fig.I-35 Concentration dependence of emf per unit pressure difference in nonisobaric system

other electrolyte, conductivity of the solution is proportional to the concentration of $AgNO_3$[18]. If the streaming conductivity Y_{QP} does not depend on the concentration of the solution very much, the emf given by eqn.(I-57) must be inversely proportional to the $AgNO_3$ concentration.

In fact, linear relations can be observed in Fig.I-34 and Fig.I-35 as has been expected from the discussions above.

3-3 The effect of heat flow through the interface between electrode and electrolyte

In an actual heat transfer loop, there exists a large heat flux through the interface between construction material and heat transfer material, and the experimental apparatus described in previous sections may not simulate this condition.

To examine if this large heat flux affects the value of thermoelectric power, the heat flux dependence of thermoelectric power was investigated experimentally by using a silver electrode with a rod-type heater built in (cf.Fig.I-36)

And no such dependence could be observed. This means that the experimental results and discussions in previous sections are available in order to describe the thermoelectric power in an actual heat transfer loop, where a large heat flux exists through the interface of heat transfer material and constructive material.

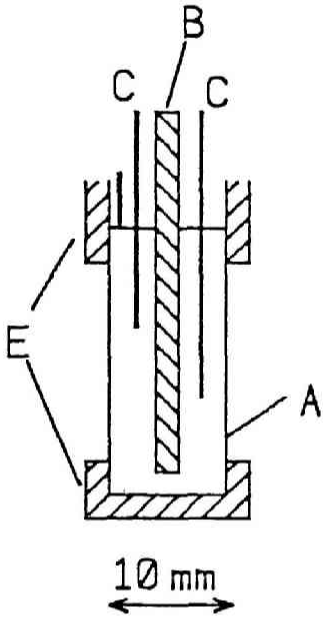

A: Ag block (electrode)
B: rod type heater
C: thermocouple
D: Ag wire (lead)
E: coating material
(silicone rubber)

Fig.I-36

Ag electrode with a heater

3-4 Conclusion

1) Theoretical expression of emf appearing in a heat transfer loop was derived with the aid of irreversible thermodynamics and its appropriateness was confirmed by this series of experiments.

2) Emf caused by a pressure gradient in a system is very small. Besides, this emf is inversely proportional to the electrical conductance of a system. So, especially in a molten salt circulating loop it is considered to be negligibly small compared with that caused by a temperature gradient, since molten salt usually shows high electrical conductivity.

3) A heat flux through the interface between the construction material and the fluid does not affect the thermoelectric power. This means that the thermoelectric power appearing in an actual heat transfer loop can be estimated or analyzed by use of the experimental results and discussions presented in this study.

REFERENCES

[1] T.Førland and S.K.Ratkje, Electrochim.Acta 25, 157(1980)

[2] L.Onsager, Phys.Rev., 37, 405; 38, 2265 (1931)

[3] P.Curie, Journal de physique, 3rd series, 3, 393(1894); "Oeuvres de Pierre Curie," 118, Gauthier-Villars, Paris (1908)

[4] Y.Ito, S.Horikawa, J.Oishi and Y.Ogata, Electrochim.Acta 30, 799(1985)

[5] American Institute of Physics Handbook 2nd ed., 4-7 McGraw-Hill(1963)

[6] "Fundamentals of Molten-Salt Thermal Technology" edited by MSTT, The Society of Molten-Salt Thermal Technology(1980)

[7] M.Matsunaga, Y.Ito and S.Yoshizawa, Journal of Power Sources, 1,159(1976/77)

[8] M.Hansen and K.Anderko, "Constitution of Binary Alloys" McGraw-Hill (1958)

[9] M.Takahashi, J.electrochem.Soc.Jpn, 25,432(1957), 25,481 (1957), 28,313(1960), 28,660(1960)

[10] I.Barin and O.Knache, Editors, "Thermochemical Properties of Inorganic Substances" Springer-Verlag, Berlin(1973)

[11] Janz, Molten Salt Handbook, p344, Academic Press(1967)

[12] J.Lumsden, "Thermodynamics of Molten Salt Mixtures", p49 Academic Press(1966)

[13] J.N. Agar, Thermogalvanic Cells (Advances in Electrochemistry and Electrochemical Engineering, Vol. 3, Interscience, London(1962))

[14] J.Chanu, Electrchim.Acta 22, 1025(1977)

[15] Y.Ito, H.Kaiya, S.Yoshizawa, S.K. Ratkje and T.F.Fφrland, J.electrochem.Soc. 131, 2504(1984)

[16] R.Haase, Z.physik.Chem. Neue Folge 103, 225(1976)

[17] P.N.Snowdon and J.C.R.Turner, Trans.Faraday Soc. 56, 1409(1960)

[18] Landolt-Bornstein Tabellen, II Band, 7 Teil, Electrische Eigenschaften II. Springer (1960)

PART 2. PELTIER HEAT

Chapter 4. The relation between Peltier heat and thermoelectric power

Before the relation between single electrode Peltier heat and thermoelectric power is discussed, entropy balance in an electrode region will be briefly explained here.

When unit charge passes reversibly through the electrolytic cell as shown in Fig. Ⅱ-1(A), entropy change in the anode region is expressed as follows:

$$\Delta s = \Sigma s_i \Delta \nu_i \qquad (Ⅱ-1)$$

,where s_i represents partial molar entropy of component i; $(\delta S/\delta \nu_i)_{T,P}$, and ν_i represents its stoichiometric coefficient in the equation of the electrode reaction.

In order to maintain the electrode region at constant temperature during the electrolysis, appropriate amount of heat Π_a has to be supplied to that region as shown in Fig. Ⅱ-1(B). This heat Π_a is called the single electrode Peltier heat, and the quantity, Π_a divided by temperature T, is called Peltier entropy and symbolized as S'(Q)[1]. When cathodic reaction is the reverse reaction of anodic one, Peltier heat at the cathode is expressed as;

$$\Pi_c = -\Pi_a = -T \cdot S'(Q) \qquad (Ⅱ-2)$$

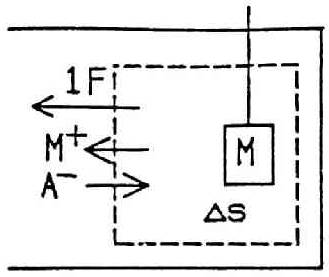

$$\Delta s = \sum_i s_i \nu_i$$

$$s_i = \left(\frac{\partial S}{\partial n_i}\right)_{T,P}$$

(A) Entropy change

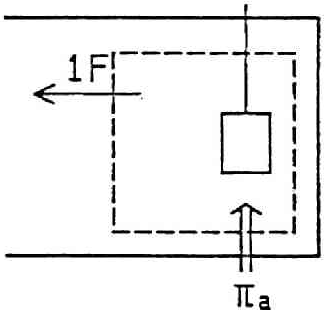

$$\pi_a = T \cdot S'(\theta)$$

(B) Peltier heat

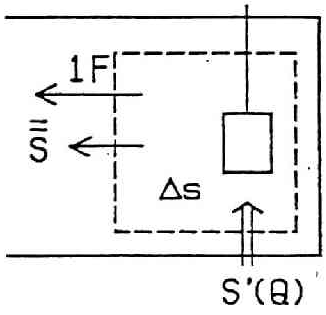

$$\Delta s = S'(\theta) - \bar{\bar{S}}$$

$$\bar{\bar{S}} = t_+ \bar{\bar{S}}_+ - t_- \bar{\bar{S}}_-$$

(C) Entropy balance

Fig.II-1 Entropy change in anode region under the transfer of unit charge

There also exists another entropy that is transported from the electrode region into an electrolyte with the transfer of mass during the electrolysis with unit charge, which is called transported entropy and symbolized as $\overset{=}{S}$.

As shown in Fig. Ⅱ-1(C), entropy change of the electrode region is expressed as the summation of what is transported from the environment and what is transported through the electrolyte. So the entropy change in the electrode region is expressed as follows;

$$\Delta s = S'(Q) - \overset{=}{S} \qquad (Ⅱ-3)$$

Though in a rigorous sense, the transported entropy must include the entropy transported through the lead wire with the transfer of electron, in most cases its value is very small in comparison with those through the electrolyte[2,3,4]. So it is neglected in this study.

Using these quantities mentioned above, the relation between thermoelectric power and the single electrode Peltier heat will be discussed in the followings.

Fig. Ⅱ-2 shows the situation where unit charge passes through the system that consists of two reversible electrodes of the same kind. As mentioned above, the heat $T \cdot S'(Q)$ is absorbed into the anode region from the heat reservoir and the same amount of heat is removed from the cathode region. In this case, no work is necessary to transfer unit charge trough the system because two electrodes are identical and reversible, which means $dW=0$ in

Fig. Ⅱ-2.

Next the case will be discussed where the temperature difference exists between two electrode regions. If it is assumed that Peltier entropy does not depend on temperature so much, similar relation is obtained as shown in Fig. Ⅱ-3. (The appropriateness of this assumption has been confirmed by experimental results where a good linearity was obtained between temperature difference and electromotive force.)

It should be noted in Fig. Ⅱ-3 that the entropy S'(Q) is carried from the reservoir of temperature T_1+dT to that of temperature T_1. This means that the work the whole system does on the environment is expressed as $S'(Q)\cdot dT$. Besides, since this work is done during the unit charge transfer, electric potential difference between two electrodes is expressed as:

$$-F\cdot d\phi^{obs} = S'(Q)\cdot dT \qquad (Ⅱ-4)$$

,where S'(Q) can be rewritten as follows by using eqns.(Ⅱ-1) and (Ⅱ-3).

$$S'(Q) = \sum s_i \nu_i + \bar{S} \qquad (Ⅱ-5)$$

Equation(Ⅱ-4) indicates that Peltier entropy can be obtained from the data on thermoelectric power($d\phi^{obs}/dT$).

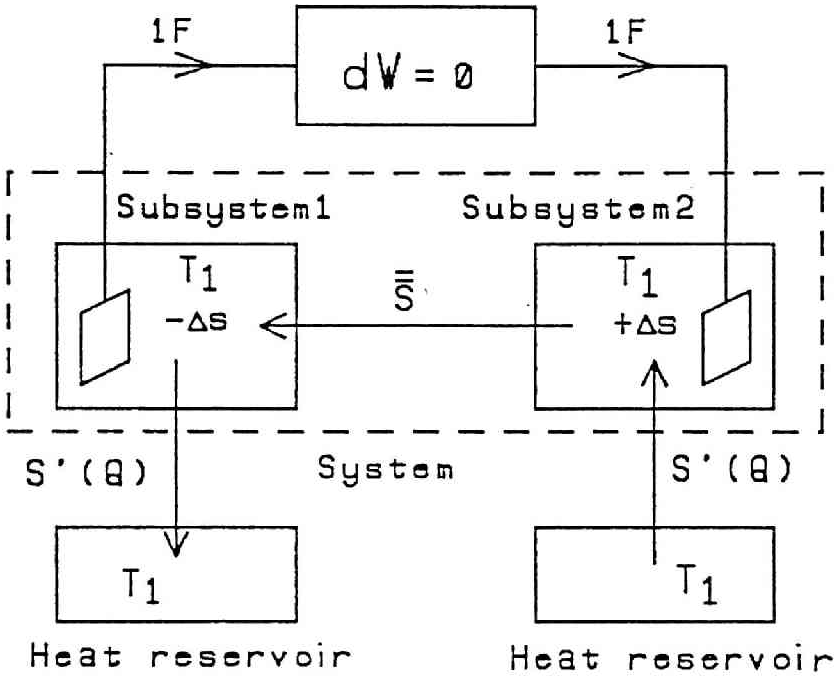

Fig.II-2 Entropy balance in an isothermal system

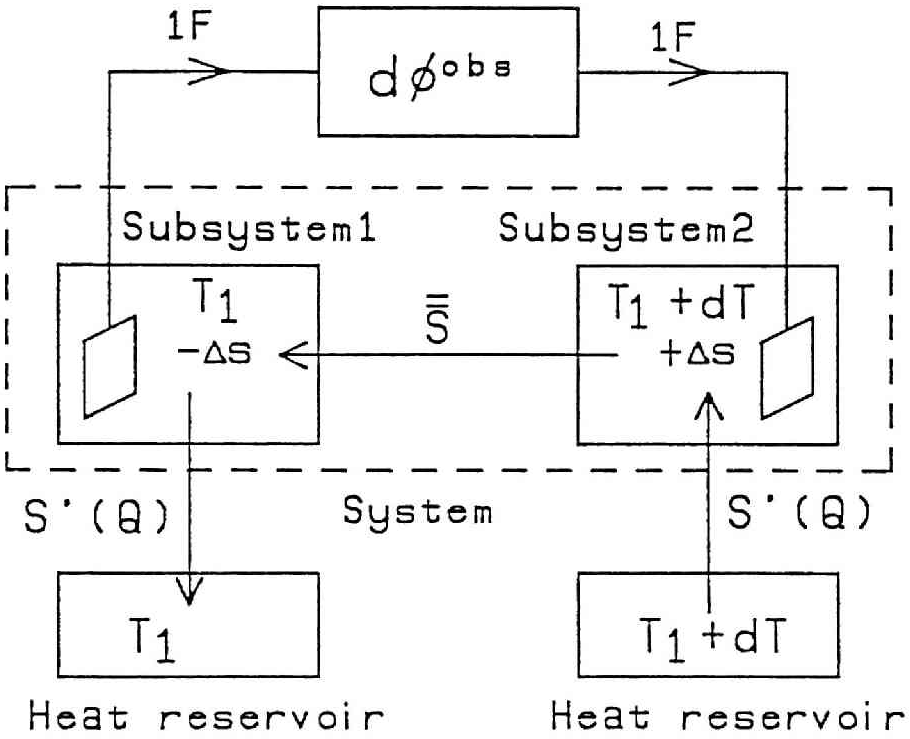

Fig. II -3 Entropy balance in a nonisothermal system

CHAPTER 5. Experimental study on Peltier entropy of hydrogen electrode in NaOH and H_2SO_4 aqueous systems

Single electrode Peltier heat of hydrogen electrodes have been measured by two different methods, one is thermoelectric power measurement and the other is calorimetric one.

The electrolyte of hydrogen electrodes used in this experiment was 0.05～1.0N H_2SO_4 and 0.05～5N NaOH aqueous solutions.

In this chapter, experimental data on thermoelectric power of a hydrogen electrode in various H^+ ion concentrations are to be presented first, where the single electrode Peltier heats are calculated based on these data. Then the study on direct measurement of the single electrode Peltier heat is to be presented, where newly designed electrolytic calorimeter was used.

The values obtained by these two methods are in fairly good agreement, though the value obtained by the thermoelectric power measurement is considered to be more reliable.

5-1 Evaluation of Peltier entropy from thermoelectric power measurement

5-1-1 Experimental

Experimental apparatus to measure the thermoelectric power of a hydrogen electrode is shown in Fig. Ⅱ-4. Two hydrogen electrodes

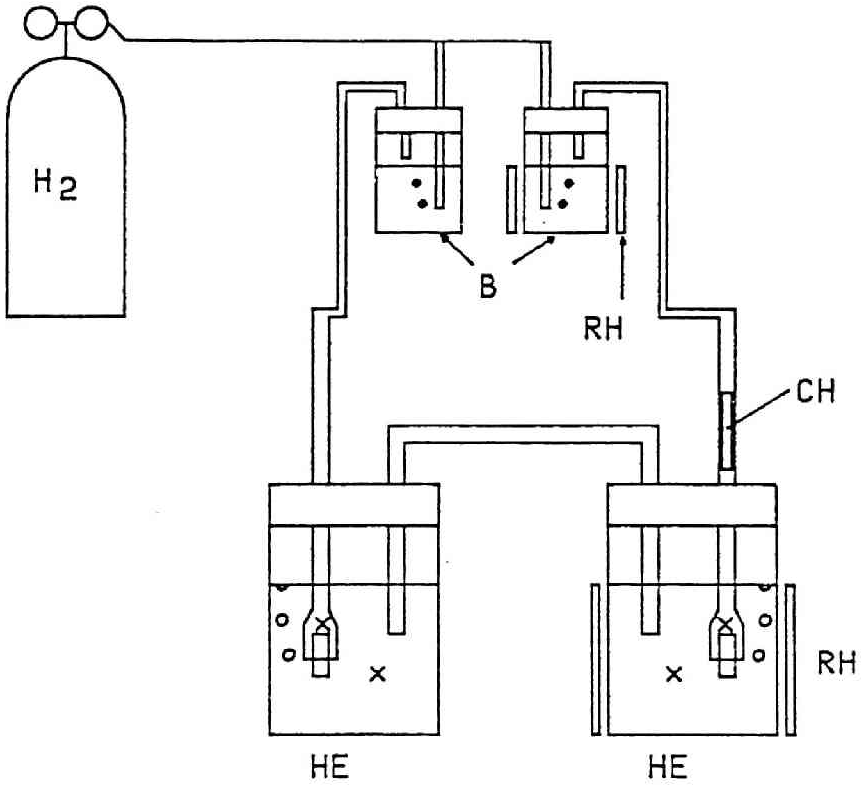

x: thermocouple
HE: hydrogen electrode
RH: ribbon heater
CH: cartridge heater
B: buffer

Fig.Ⅱ-4 Experimental apparatus

of the same kind were connected by a bridge. Platinum plate (10 x 20 x 0.1 mm) coated with platinum black was used as an electrode.

In order to set a temperature difference between two hydrogen electrodes, two kinds of heaters were used, one is a ribbon heater to heat solution and the other is a cartridge heater to heat hydrogen gas. These two heaters were controlled by a microcomputer unit (Casio FP1100 + A/D converter) and temperature difference between gas and solution was maintained within 0.1K.

After setting a certain temperature difference between two electrodes, electric potential difference was measured by the same computer unit with a high impedance amplifier. The maximum temperature difference between two electrodes was 40K and the temperature of the colder electrode stayed at 25℃.

As an electrolyte of a hydrogen electrode, solution of 0.05, 0.1, 0.5 and 1.0 N H_2SO_4, and 0.05, 0.1, 0.5, 1.0 and 5.0 N NaOH were used. Before conducting thermoelectric power experiment, it had been confirmed by use of a Ag/AgCl electrode that each hydrogen electrode gave stable and theoretically reasonable potential in these solutions.

5-1-2 Results and discussion

Fig. Ⅱ-5 shows the relation between temperature difference and emf. Since this emf is the value measured on reference to a low temperature side, the electric potential of a high temperature electrode is more positive than that of a low one. This means that the reaction: $H^+ + e^- \rightarrow 1/2H_2$ is endothermic.

1N H_2SO_4 was used as an electrolyte of the electrode in the

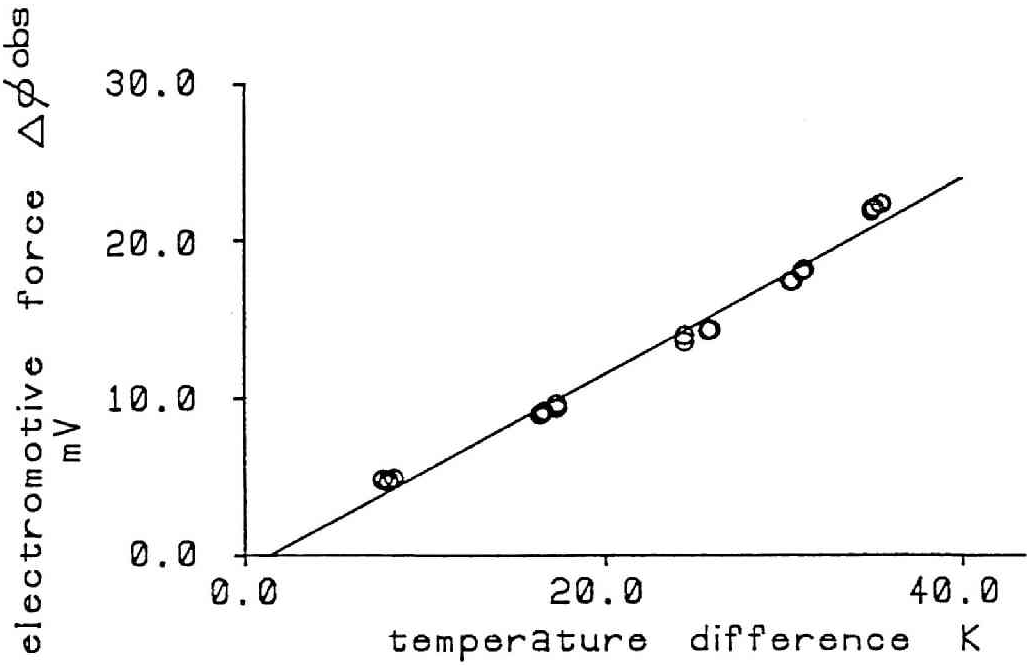

Fig. II-5 Relation between temperature difference and electromotive force (1N H_2SO_4 system)

experiment of Fig. Ⅱ-5 and similar results were obtained with respect to other H^+ ion concentrations. Relations between thermoelectric power ε_T and concentration of H^+ ion are shown in Fig. Ⅱ-6 and Fig. Ⅱ-7. These two results show that measured thermoelectric power ε_T is in good accordance with the theoretical equation;

$$\varepsilon_T = \text{const} + (2.303R/F)\cdot\log[H^+] \qquad (Ⅱ-6)$$

just as the case of molten salt systems presented in Chapter2.

On the other hand, there are a lot of works on Peltier effect[5][6] and according to Ito et al[7][8], Peltier heat Π_c, which is the heat absorbed from the external heat reservoir by the reversible transfer of unit charge, is expressed as follows in case of hydrogen electrodes by using the initial thermoelectric power ε_T.

$$\Pi_c = FT\cdot(\varepsilon_T - \varepsilon') \qquad (Ⅱ-7)$$

,where F represents Faraday constant and ε' represents thermoelectric power of the thermocouple consisting of electrode material and lead material. But since in this experiment the same platinum has been used where the temperature gradient exists, ε' should be equal to zero.

According to Fig. Ⅱ-6 and Fig. Ⅱ-7, the values of measured thermoelectric power are expressed as follows:

$$\varepsilon_T = A + B\cdot\log[H^+] \qquad (Ⅱ-8)$$

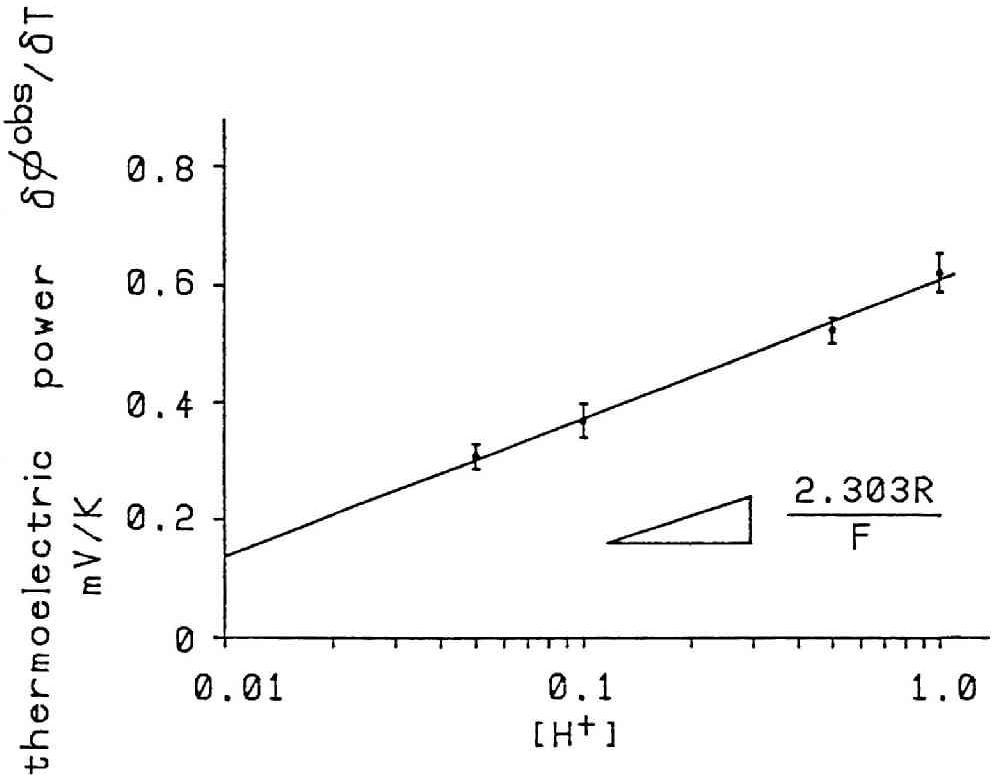

Fig. II-6 Concentration dependence of thermoelectric power (1N H_2SO_4 system)

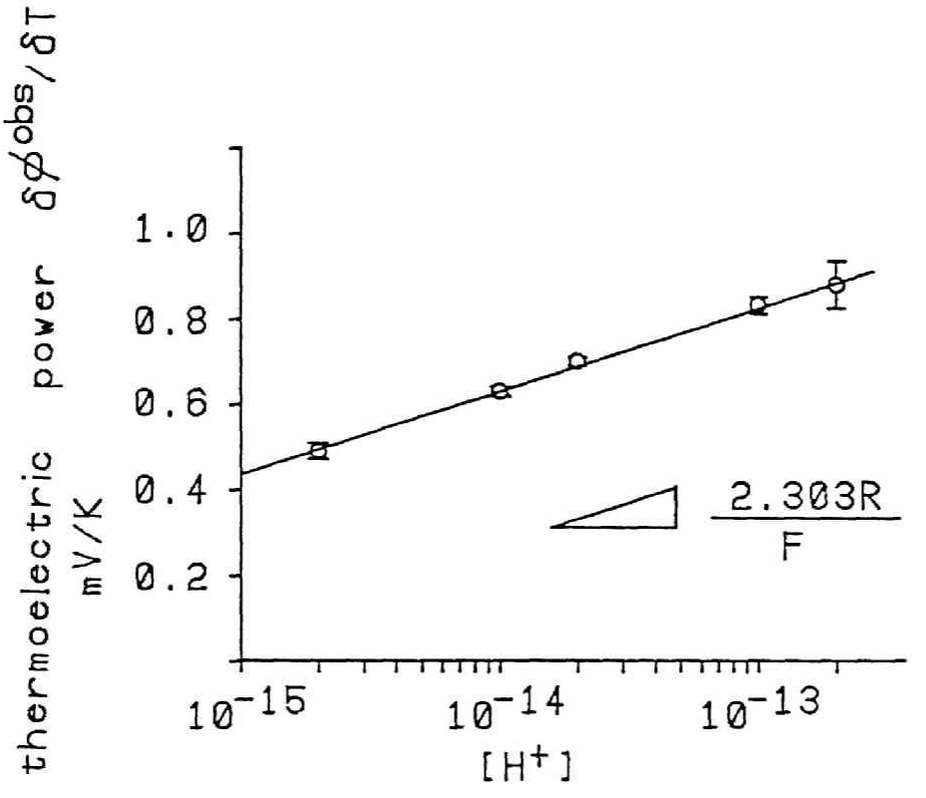

Fig. II-7 Concentration dependence of thermoelectric power (1N NaOH system)

,where in a H_2SO_4 system:

$$A = 0.610 \pm 0.048 \ [\times 10^{-3} \ V/K]$$

and $$B = 0.236 \pm 0.057 \ [\times 10^{-3} \ V/K]$$

,and in a NaOH system:

$$A = 3.38 \pm 0.21 \ [\times 10^{-3} \ V/K]$$

and $$B = 0.196 \pm 0.015 \ [\times 10^{-3} \ V/K]$$

, respectively.

Peltier heat of hydrogen evolution calculated from these values and eqn.(Ⅱ-7) are,

$$\Pi_e = 17600 + 6800 \cdot \log[H^+] \ [J/F] \ (25℃)$$

and $$\Pi_e = 18100 + 5600 \cdot \log[OH^-] \ [J/F]$$

in a H_2SO_4 system and in a NaOH system, respectively.

These results show that there is a big difference between the values of thermoelectric power in a H_2SO_4 system and those in a NaOH system when both H^+ ion concentrations are extraporated to the same value. For example when the concentration of H^+ ion is unity, ε_T is 0.610 mV/K in a H_2SO_4 system and ε_T is 3.38 mV/K in a NaOH system.

These results can be explained quantitatively by using Eastman entropy that Agar uses in his work[9].

According to Agar, thermodynamical expression of thermoelectric power in a H_2SO_4 system is expressed as :

$$\varepsilon_T = -(1/F)[(\bar{\bar{S}}_e - s\langle(1/2)H_2\rangle + s^o\langle H^+\rangle) + t\langle H^+\rangle\hat{S}\langle H^+\rangle - (t\langle SO_4^{2-}\rangle/2)\hat{S}\langle SO_4^{2-}\rangle - R\ln[H^+]] \qquad (Ⅱ-9)$$

,and that in a NaOH system as :

$$\varepsilon_T = -(1/F)[(\bar{\bar{S}}_e - s\langle(1/2)H_2\rangle + s\langle H_2O\rangle - s^\circ\langle OH^-\rangle) + t\langle Na^+\rangle\hat{S}\langle Na^+\rangle - t\langle OH^-\rangle\hat{S}\langle OH^-\rangle + R\ln[OH^-]] \qquad (\text{II}-10)$$

,where $\bar{\bar{S}}_e$ denotes transported entropy of electron in Pt, and $s\langle i\rangle$, $\hat{S}\langle i\rangle$ and $t\langle i\rangle$ denote partial molar entropy, Eastman entropy and transport number of component i, respectively.

In order to compare eqns.(II-9) and (II-10), $s^\circ\langle OH^-\rangle$ and $s^\circ\langle H_2O\rangle$ in eqn.(II-10) are to be rewritten with $s^\circ\langle H^+\rangle$.

As a dissociation of water is in equilibrium, eqn.(II-11) is valid among chemical potentials of each species.

$$\mu\langle H_2O\rangle = \mu\langle H^+\rangle + \mu\langle OH^-\rangle \qquad (\text{II}-11)$$

When concentration dependence of chemical potential is taken into consideration with respect to each ion, eqn.(II-11) is transformed as follows:

$$\begin{aligned}\mu\langle H_2O\rangle &= \mu^\circ\langle H^+\rangle + RT\ln[H^+] + \mu^\circ\langle OH^-\rangle + RT\ln[OH^-] \\ &= \mu^\circ\langle H^+\rangle + \mu^\circ\langle OH^-\rangle + RT\ln[H^+][OH^-] \\ &= \mu^\circ\langle H^+\rangle + \mu^\circ\langle OH^-\rangle + RT\ln Kw \qquad (\text{II}-12)\end{aligned}$$

,where Kw is the ionic product of water.

When concentration of H^+ or OH^- ion is large so that excess chemical potential is not negligible, μ° can be considered as the sum of standard chemical potential and excess chemical potential.

Since the partial molar entropy of component i is expressed

as:

$$s_i = -(\delta \mu_i / \delta T)_{P,n_i} \qquad (\text{II}-13)$$

,by differentiating eqn.(II-12) by temperature T:

$$\frac{\delta \mu \langle H_2O \rangle}{\delta T} = \frac{\delta \mu^\circ \langle H^+ \rangle}{\delta T} + \frac{\delta \mu^\circ \langle OH^- \rangle}{\delta T} - R \ln Kw - RT \frac{\delta \ln Kw}{\delta T}$$

$$s\langle H_2O \rangle = s^\circ \langle OH^- \rangle + s^\circ \langle H^+ \rangle - R \ln Kw - RT(\delta \ln Kw / \delta T) \qquad (\text{II}-14)$$

is obtained.

Since the ionic product of water is reported[10] as :

$$\log Kw = -14.166 \quad \text{at } 20℃$$

$$\text{and} \quad \log Kw = -13.833 \quad \text{at } 30℃$$

,the value of $(\delta \ln Kw / \delta T)$ is estimated to be approximately 0.0767. By using this value in eqn.(II-14), the following relation is obtained.

$$s\langle H_2O \rangle = s^\circ \langle OH- \rangle + s^\circ \langle H^+ \rangle - R \ln Kw - 0.0764RT$$

$$s^\circ \langle H^+ \rangle - R \ln [H^+] - 0.0767RT = s\langle H_2O \rangle - s^\circ \langle OH^- \rangle + R \ln [OH^-] \qquad (\text{II}-15)$$

By substituting eqn.(II-15) into eqn.(II-10), the thermoelectric power is expressed as follows:

$$\varepsilon_T = -(1/F)[(\bar{\bar{S}}_e - s\langle (1/2)H_2 \rangle + s^\circ \langle H^+ \rangle) - 0.0767RT + t\langle Na^+ \rangle \hat{S}\langle Na^+ \rangle - t\langle OH^- \rangle \hat{S}\langle OH^- \rangle - R \ln [H^+]] \qquad (\text{II}-16)$$

By comparing this equation with eqn.(II-9), it is expected

that the thermoelectric power measured in a NaOH system is larger than that in a H_2SO_4 system by:

$$\Delta \varepsilon_T = (1/F)(0.0767RT-(t\langle Na^+\rangle \hat{S}\langle Na^+\rangle - t\langle OH^-\rangle \hat{S}\langle OH^-\rangle) + t\langle H^+\rangle \hat{S}\langle H^+\rangle - (t\langle SO_4^{2-}\rangle/2)\hat{S}\langle SO_4^{2-}\rangle) \qquad (\text{II}-17)$$

The value of $\Delta \varepsilon_T$ can be calculated from the following data[9]

F	: 96500	[C/mol]
R	: 8.314	[J/K mol]
T	: 298	[K]
$t\langle Na^+\rangle$	: 0.202	
$t\langle OH^-\rangle$	: 0.798	
$t\langle H^+\rangle$	: 0.82	
$t\langle SO_4^{2-}\rangle$	: 0.18	
$\hat{S}\langle Na^+\rangle$	: 12.01	[J/mol·K]
$\hat{S}\langle OH^-\rangle$	: 56.53	[J/mol·K]
$\hat{S}\langle H^+\rangle$	: 42.68	[J/mol·K]
$\hat{S}\langle SO_4^{2-}\rangle$	: 26.78	[J/mol·K]

,where last four values represent Eastman entropy of each ion at infinite dilution where the $\hat{S}\langle Cl^-\rangle$ is used as a standard.

$\Delta \varepsilon_T$ calculated from these values is 2.75 mV/K which is in good accord with the experimental value 3.38-0.610=2.77mV/K.

Though the term $s°\langle H^+\rangle$ in eqns.(II-9) and (II-16) must include the excess partial molar entropy, which depends on concentration, the sum of all other terms but $R\ln[H^+]$ in both equations has been observed as constant as seen from eqn.(II-6).

The reason for this is considered to be that the excess partial molar entropy is canceled by the concentration dependence of the Eastman entropy.

5-2. Direct calorimetric measurement of Peltier entropy

5-2-1 Experimental

Figure. Ⅱ-8 shows an experimental apparatus to measure Peltier heat. The function of this apparatus is as follows: a part of the heat evolved in the reaction vessel P flows into the heat sink Q through the heat conducting tube and this heat flow is measured by the heat transducer M. The amount of heat evolved in the reaction vessel can be estimated from the value of the output signal from this heat transducer. As an output signal, a changing ratio of the heat flow just after heat evolution, or a changing ratio of temperature in the reaction vessel, was used.

The reaction vessel, the heat conducting tube and the heat sink are all made of copper and this apparatus was set in a constant temperature room. The inside of the reaction vessel is double coated with nickel and gold.

The heat transducer is made of piled 22 chromel-constantan thermocouples which are fixed to copper blocks surrounding the heat conducting tube. The electromotive force from these thermocouples are analyzed by a microcomputer (NEC PC-8801) after being amplified (YEW 3131) and degitalized.

By using the calibration heater H in the reaction vessel, a calibration line between the heat evolved in the vessel and the output signal from the heat transducer was obtained as Fig. Ⅱ-9, which was used to estimate Peltier heat from the measured output signal.

The counter electrode A is made of Platinum plate (20x20mm)

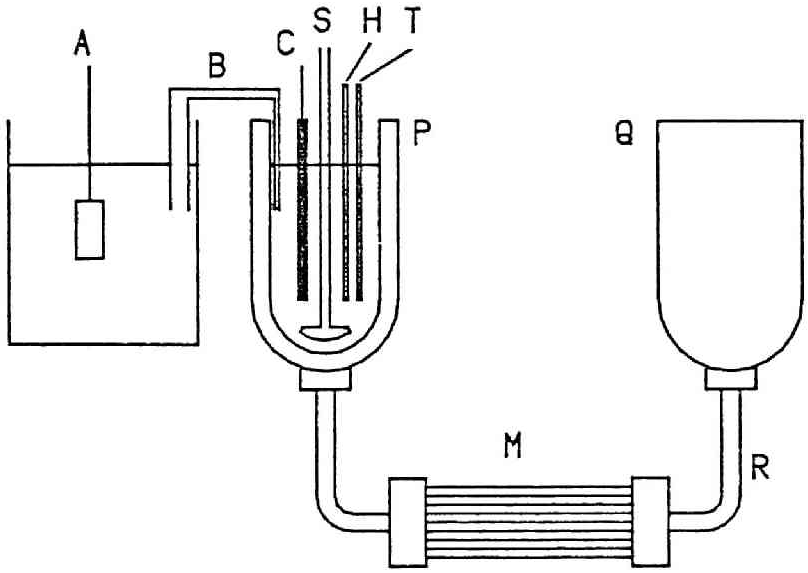

A: counter electrode
B: bridge
C: working electrode (pt-Pt)
S: stirrer
H: heater
T: thermocouple
P: reaction vessel
Q: heat sink
R: heat conducting tube
M: heat transducer

Fig.II-8 Experimental apparatus

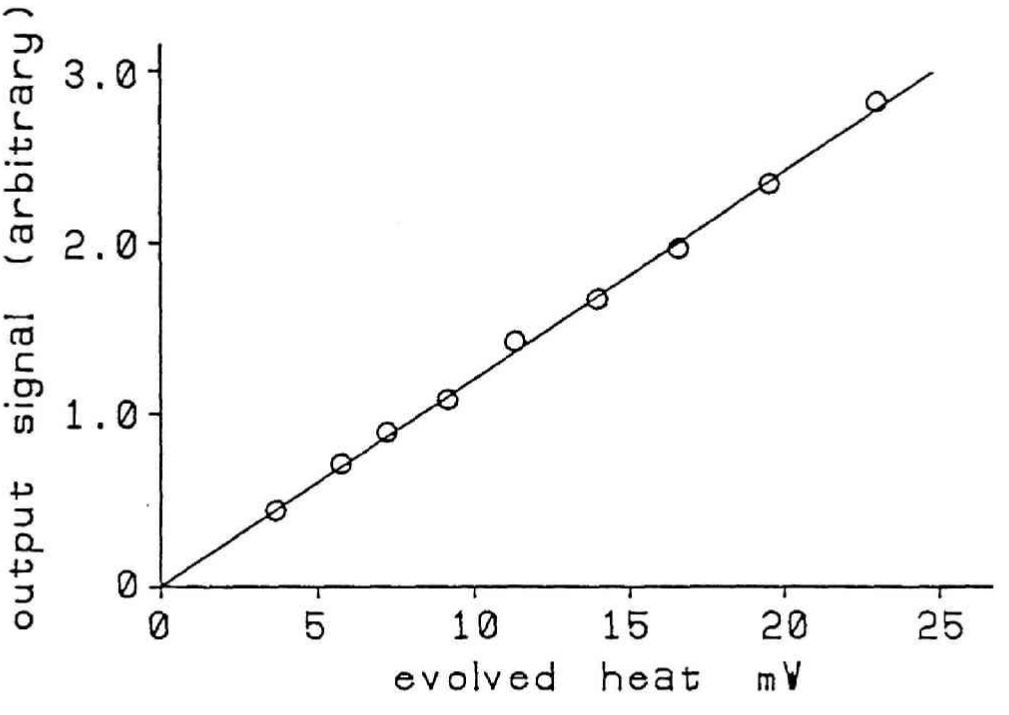

Fig. II-9 Calibration line

and the working electrode C is a cylindrical(30*dia5mm) platinum mesh coated with platinum black. The measurement of Peltier heat was carried out with respect to 1N H_2SO_4 and 1N NaOH solution systems.

As can be seen from its appearance, this apparatus had originally been designed as a differential calorimeter, however, in this work it was not used as such.

Before the experimental results are presented, heat balance of an electrode region is to be discussed.

According to Ito et al [7] the heat W_c to be absorbed in a cathodic region during the constant electrolysis is expressed as follows:

$$W_c = \Pi_c \cdot i/F - \eta \cdot i + \lambda (dT/dx)_{x=1} \qquad (\text{II}-18)$$

,where Π_c, i, η, and λ denote Peltier heat, electrolytic current, overpotential and thermal conductivity respectively, and $(dT/dx)_{x=1}$ represents temperature gradient at the interface between cathodic region and electrolyte region.

However, in this experiment, there exists temperature gradient in a cathodic region as shown schematically in Fig. II-10, and the extra heat of $C \cdot \Delta T$ evolves there with a transfer of unit charge. So, an additional term $C \cdot \Delta T$ should be necessary in eqn.(II-18).

Here, C represents heat content of matters that are transferred with unit charge, and ΔT is the temperature difference across cathodic region, which is assumed to be

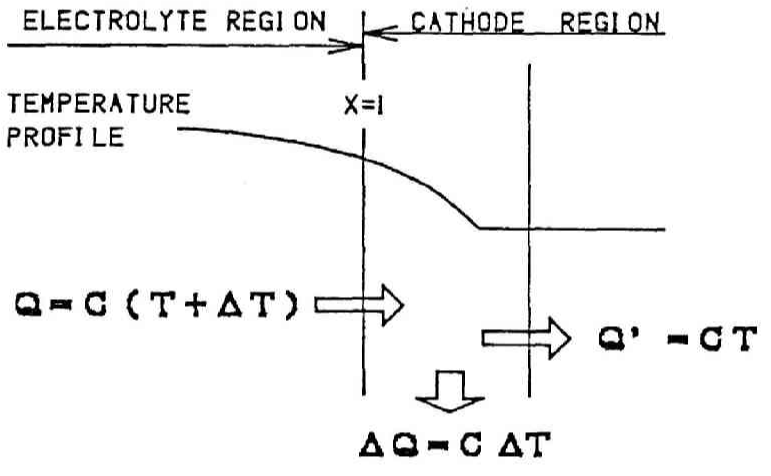

Fig.II-10 Illustration of heat flow in an electrode region

proportional to $(\delta T/\delta x)_{x=1}$. The extra heat $C\cdot\Delta T$ is thus rewritten as $C(dT/dx)_{x=1}\cdot\beta$ with a proportional constant β.

Hence, more appropriate expression of the single electrode heat balance can be obtained as:

$$W_c = \Pi_c \cdot i/F - \eta_o \cdot i + \lambda (dT/dx)_{x=1} + C(dT/dx)_{x=1}\cdot\beta\cdot i \quad (\text{II}-19)$$

On the other hand it was also derived by Ito[7] that $(dT/dx)_{x=1}$ is proportional to the square of electrolytic current i when most of the temperature gradient in a system is caused by Joule heat. Besides overpotential η_o can be regarded to be proportional to current i as shown later. (cf. Fig.II-13,14)

Thus, eqn.(II-19) can be transformed into the following equation by dividing by i.

$$W_c/i = \Pi_c/F + A\cdot i + B\cdot i^2 \quad (\text{II}-20)$$

Since an amount of heat absorption W_c can be measured by a calorimetric method with respect to various current i, the Peltier heat Π_c can be determined by plotting W_c/i against i and fitting them to a square function.

5-2-2 Results and discussion

Fig.II-11 shows the relation between $-W_c/i$ and i in a 1N H_2SO_4 solution system, and Fig.II-12 shows that in a 1N NaOH solution system. The value of Peltier heat derived from these results are presented below with those calculated from

thermoelectric power.

Πc [J/F] measured by a calorimetric method

1N H_2SO_4	1N NaOH
12700	15200

Πc [J/F] calculated from thermoelectric power

1N H_2SO_4	1N NaOH	
17600	18100	(at 25℃)

These fairly good coincidences give us also a sufficient support for the appropriateness of our experimental procedures and theoretical considerations mentioned above.

However, since the Joule heat evolved in a system is relatively large compared with Peltier heat, it is inevitable for calorimetric data to include some deviation, i.e. from an experimental viewpoint, determination of Peltier heat should be carried out by use of the thermoelectric power except in some special cases.

The appropriateness of the assumption that the overpotential η_o is proportional to electrolytic current has been confirmed from other experiments.(cf Fig. Ⅱ-13, Fig. Ⅱ-14)

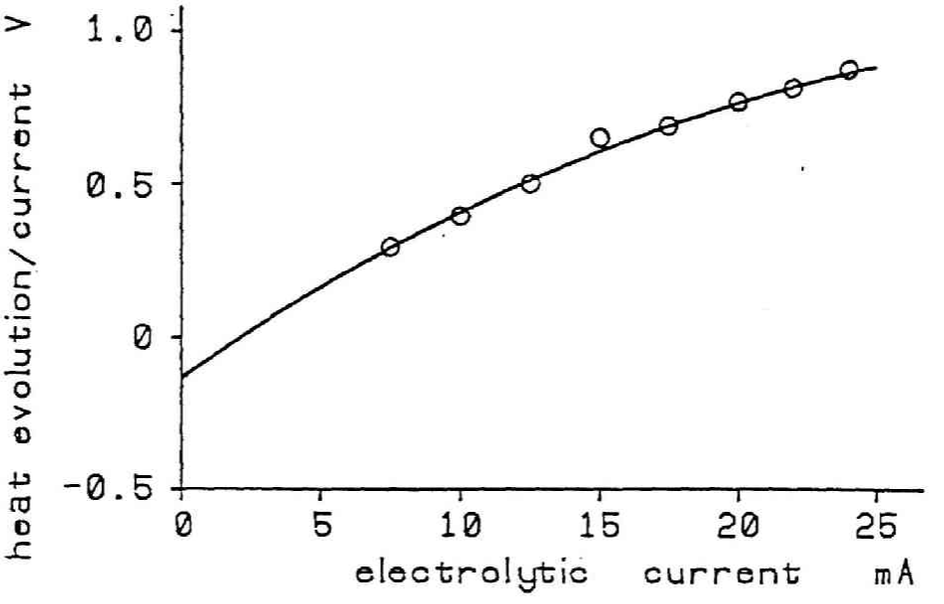

Fig.II-11
Experimental result (1N H_2SO_4 system)

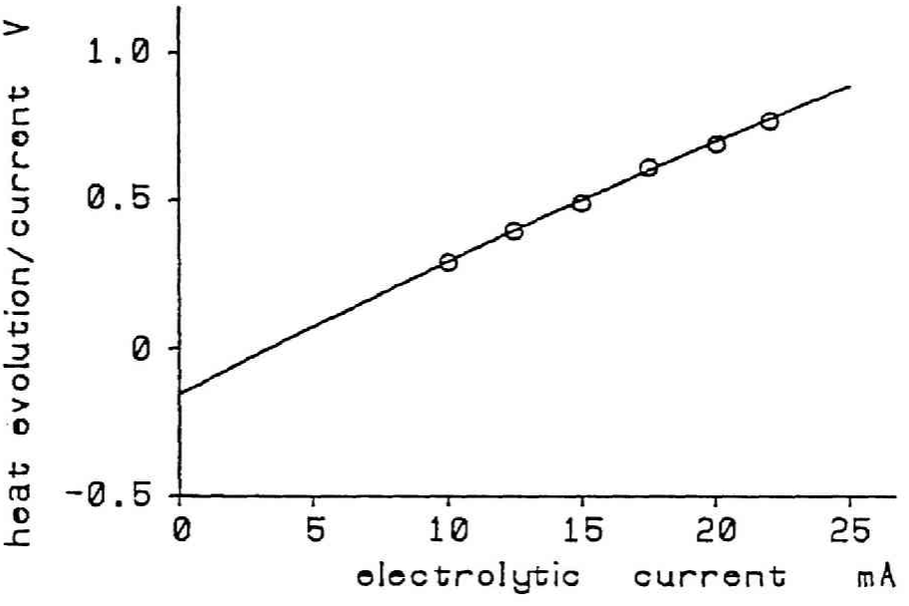

Fig.II－12
Experimental result (1N NaOH system)

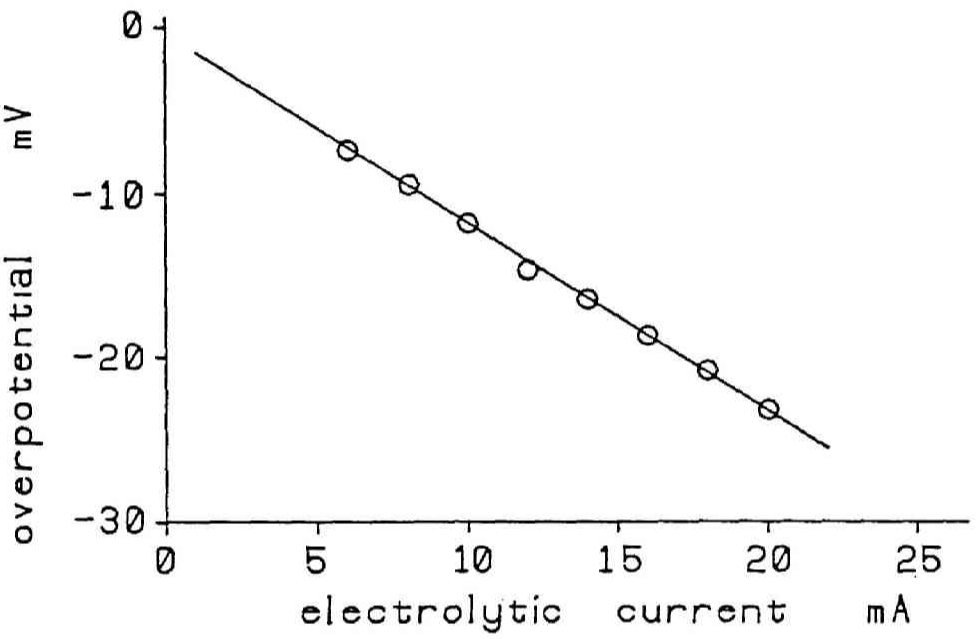

Fig.II-13 Overpotential of hydrogen electrode ($1NH_2SO_4$ system)

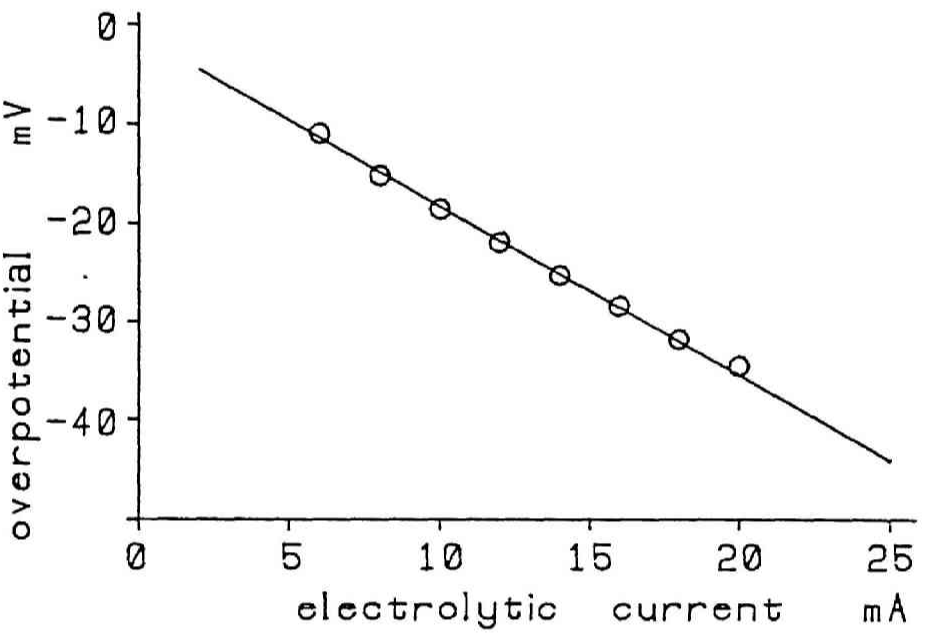

Fig. II-14 Overpotential of hydrogen electrode (1N NaOH system)

5-3 Conclusion

Experimental results on thermoelectric power or Peltier entropy of hydrogen electrode in NaOH and H_2SO_4 systems are summarized as follows.

1) The thermoelectric power of a hydrogen electrode was measured accurately with respect to various H^+ ion concentrations. H^+ ion concentration dependence of the thermoelectric power accords with the theoretical equation derived in Chapter 1.

2) The value of thermoelectric power depends on the kinds of species in a solution. This phenomenon can be explained quantitatively by using Eastman entropy.

3) Single electrode Peltier heat of cathodic hydrogen evolution has been determined to be 17600 [J/F] in 1N H_2SO_4 and 18100 [J/F] in 1N NaOH, respectively at 25℃.

CHAPTER 6. Experimental study on Peltier entropy of Hydrogen electrode in NaOH solutions at high concentrations

In this chapter, single electrode heats of H_2 gas evolution in NaOH solutions were experimentally investigated and theoretically analyzed with respect to various concentrations up to 10N.

Especially the data on NaOH aqueous systems at high concentration are important from the engineering viewpoint because such solutions are to be used in water electrolyzers and brine electrolyzers, etc.

As shown in Chapter 5, since the more reliable data can be obtained by thermoelectric power measurement than by direct calorimetric measurement, in this work the former method was adopted to determine the single electrode heat of hydrogen gas electrode.

6-1 Evaluation of Peltier entropy from thermoelectric power measurement

Thermoelectric power of H_2 gas electrode in NaOH solution was measured with respect to several concentrations of NaOH.

Fig. Ⅱ-15 shows an experimental apparatus to deal with the solution of high concentrations (up to 10N). The outline of the apparatus is basically the same as that of the previous one shown in Chapter5, except that a couple of points have been improved as

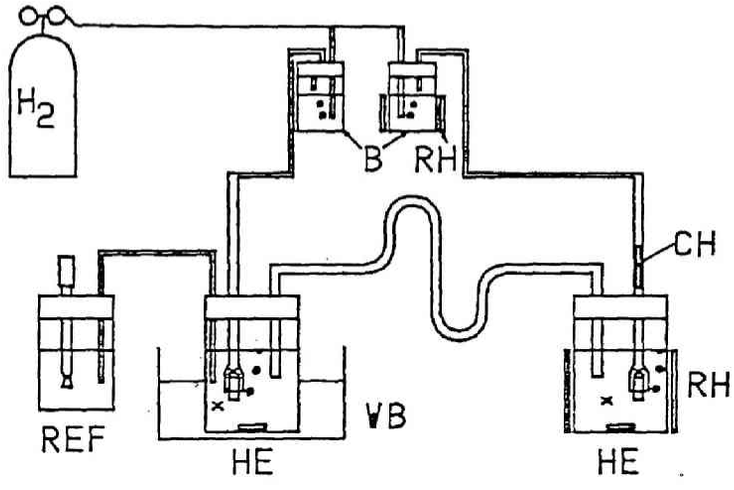

X : thermocouple
HE: hydrogen electrode
RH: ribbon heater
CH: cartridge heater
B : buffer
VB: water bath
REF: reference electrode

Fig. II - 15 Experimental apparatus

follows.

The shape of a bridge has been changed as shown in Fig. Ⅱ-15 to prevent the mixing of the solutions between the high temperature side and the low temperature side. A Ag/AgCl reference electrode was put into the apparatus to monitor the electric potential of H_2 gas electrode in the low temperature side, and it has been confirmed that the potential of H_2 gas electrode in NaOH solutions is theoretically reasonable during the measurement even in high concentration range.

Furthermore, the extra pure H_2 gas (6N) delivered by Kyoto Teisan Co.Ltd., was used in this experiment in order to reduce the effect of impurity.

The procedure of measurement is the same as that in the previous one.

The relation between the temperature difference and emf is shown in Fig. Ⅱ-16 and the concentration dependence of thermoelectric power is shown in Fig. Ⅱ-17. As seen from this figure, the theoretical equation derived in Chapterl is no longer available in high concentration range (5N～10N) and theoretical discussions concerning this phenomenon are to be presented in next chapter.

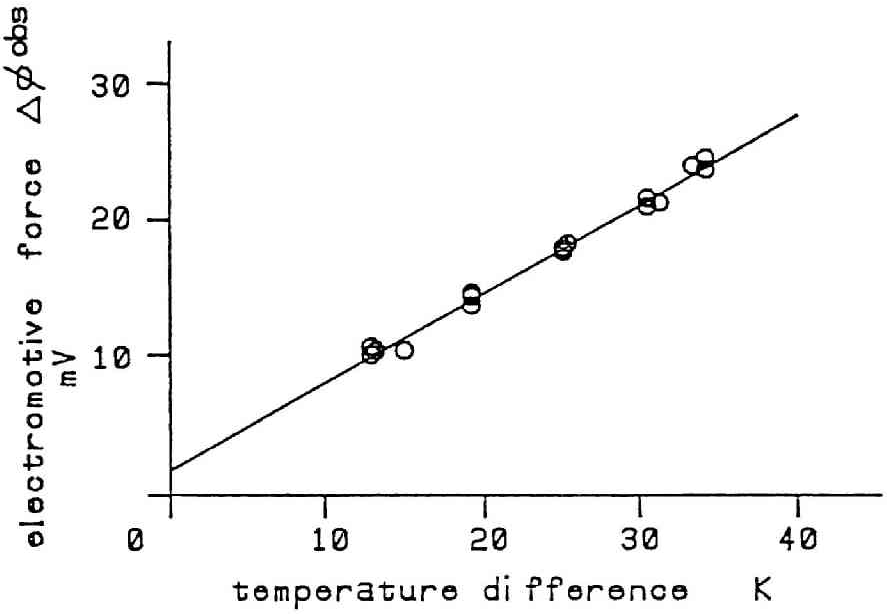

Fig. II-16 Relation between temperature difference and electromotive force

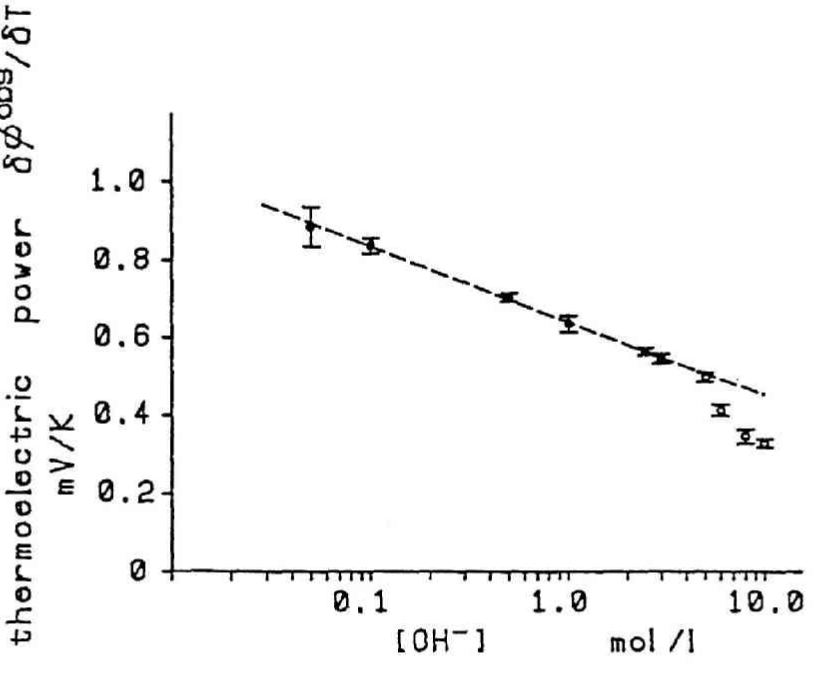

Fig.II-17 Concentration dependence of thermoelectric power

6-2 Discussion

Here, the results obtained in highly concentrated NaOH solutions (up to 10N) are to be discussed. In this range, the thermoelectric power shows a different dependence on OH^- ion concentration and eqn.(Ⅱ-6) no longer applies. Some theoretical explanations are to be presented about this deviation.

According to Agar[9], thermoelectric power in NaOH solutions is expressed as follows;

$$\varepsilon_T = -(1/F)[(\bar{\bar{S}}_e - s\langle(1/2)H_2\rangle + s\langle H_2O\rangle - s^\circ\langle OH^-\rangle) + t\langle Na^+\rangle\hat{S}\langle Na^+\rangle - t\langle OH^-\rangle\hat{S}\langle OH^-\rangle + R\cdot\ln[OH^-]] \quad (Ⅱ-21)$$

,where $\bar{\bar{S}}_e$ denotes transported entropy of electron, and $\hat{S}\langle i\rangle$, $s\langle i\rangle$ and $t\langle i\rangle$ denote Eastman entropy, partial molar entropy and transport number of component i, respectively. When concentration of OH^- ion is large so that excess partial molar entropy is not negligible, $s^\circ\langle OH^-\rangle$ can be considered as the sum of standard partial molar entropy and excess one.

It is quite understandable that the thermoelectric power is not proportional to the logarithm of $[OH^-]$ in high concentration ranges, because the partial molar entropy of H_2O and the excess partial molar entropy of OH^- can not be regarded as constant in such solutions.

If the concentration dependence of other terms are neglected, eqn.(Ⅱ-21) can be rewritten as;

$$\varepsilon_T = \text{const.} - (1/F)\cdot(s\langle H_2O\rangle - s\langle OH^-\rangle) \quad (Ⅱ-22)$$

By differentiating eqn.(Ⅱ-22),

$$d\varepsilon_T = -(1/F)\cdot(ds\langle H_2O\rangle - ds\langle OH^-\rangle) \qquad (Ⅱ-23)$$

is obtained.

On the other hand, there exists the following relation among the partial molar entropies of each component in the system.

$$X\langle H_2O\rangle\cdot ds\langle H_2O\rangle + X\langle Na^+\rangle\cdot ds\langle Na^+\rangle + X\langle OH^-\rangle\cdot ds\langle OH^-\rangle = 0 \qquad (Ⅱ-24)$$

,where $X\langle i\rangle$ denotes the mole fraction of component i.

Here, if the average partial molar entropy of NaOH defined as;

$$ds\langle\pm\rangle = (ds\langle Na^+\rangle + ds\langle OH^-\rangle)/2 \qquad (Ⅱ-25)$$

is introduced in eqn.(Ⅱ-24), the following equation is obtained.

$$X\langle H_2O\rangle\cdot ds\langle H_2O\rangle + 2X\langle NaOH\rangle\cdot ds\langle\pm\rangle = 0$$

$$ds\langle H_2O\rangle = -(2X\langle NaOH\rangle/X\langle H_2O\rangle)\cdot ds\langle\pm\rangle \qquad (Ⅱ-26)$$

When $ds\langle OH^-\rangle$ in eqn.(Ⅱ-23) is substituted by $ds\langle\pm\rangle$, eqn.(Ⅱ-23) is transformed as follows by using eqn.(Ⅱ-26).

$$d\varepsilon_T = (1/F)\cdot(2X\langle NaOH\rangle/X\langle H_2O\rangle + 1)\cdot ds\langle\pm\rangle \qquad (Ⅱ-27)$$

Though this substitution is not rigorous, $d\langle OH^-\rangle$ is

considered to be approximately equal to $ds_{\pm}$. This comes from the fact that both Na^+ ion and OH^- ion have the same amount of charge, and the effect that the unit Na^+ ion gives to the whole entropy of the system is regarded as nearly equal to that the unit OH^- ion gives.

At least in a dilute solution, this approximate relation can be theoretically proved with the theory of Debye and Huckel[11].

Equation(Ⅱ-27) means that the thermoelectric power ε_T at some concentration N_1 can be calculated by means of integrating the right hand to the value of $s_{\pm}$ at the concentration of N_1 from some standard value. Here the values at 2N were taken as standard, because the experimental data under that concentration are in good accordance with our theoretical equation and what we are most interested in is the phenomenon in higher concentration range.

By use of thermodynamical data on the activity coefficient of NaOH[12] and the following relation,

$$s^{*} = - R \cdot \ln \gamma - RT \cdot (d \ln \gamma / dT) \qquad (Ⅱ-28)$$

the excess partial molar entropy can be calculated as shown in Table Ⅱ-1, therefore the partial molar entropy of NaOH can be obtained.

By integrating eqn.(Ⅱ-27) with the data in Table Ⅱ-1, the thermoelectric powers at various concentrations are obtained and shown in Fig.Ⅱ-18 as a solid line.

But this curve line does not accord with the experimental

Table.II-1 Activity coefficient of NaOH

	2.0	4.0	6.0	8.0	10.0 [mol/l]
30℃	0.712	0.911	1.32	2.06	3.31
50℃	0.693	0.872	1.21	1.78	2.67
s°/F [mV/K]	.0589	.0651	.0896	0.128	0.177

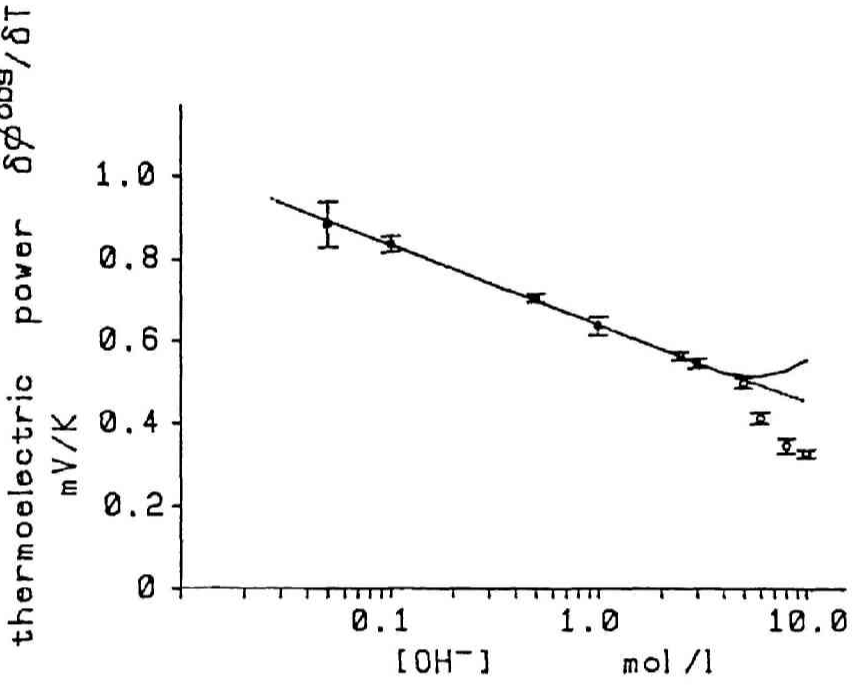

Fig.II - 18 Concentration dependence of thermoelectric power

data, and deviation of the experimental data from ideal curve line became larger.

This fact indicates that the deviation is considered to be caused by the concentration dependence of the terms that contain Eastman entropy rather than that of partial molar entropy of H_2O or OH^-. The relation between the concentration of OH^- ions and the deviation of experimental data from ideal curve is shown in Fig. II-19, which is considered to present the concentration dependence of the terms that contain Eastman entropy;

$$t\langle Na^+\rangle\hat{S}\langle Na^+\rangle - t\langle OH^-\rangle\hat{S}\langle OH^-\rangle.$$

On the other hand, the value of single electrode Peltier heat of H_2 gas evolution in 8N and 10N NaOH solutions are estimated as 1.03×10^4J/F and 9.79×10^3J/F respectively, from the experimental data obtained here.

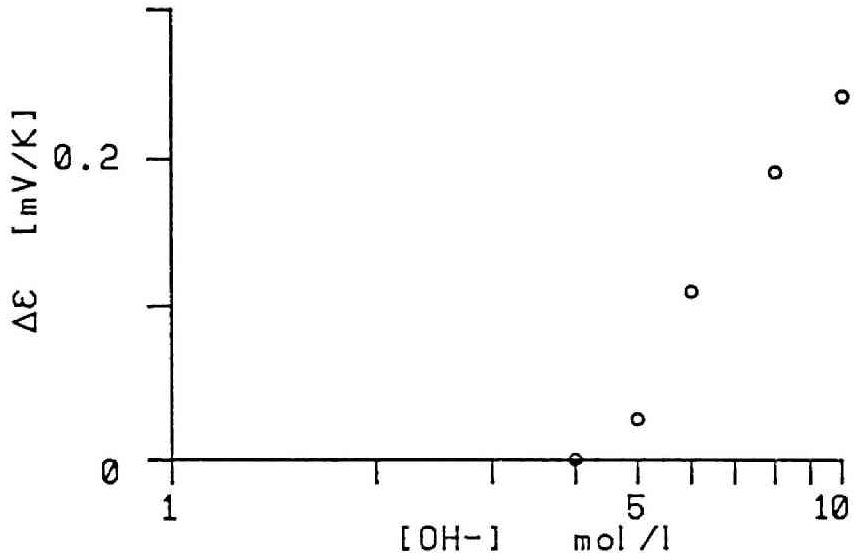

Fig. II-19 The difference between observed thermoelectric power and theoretical one

6-3 Conclusion

The results obtained in this chapter are summarizes as follows;

1)Thermoelectric power of H_2 gas electrode in NaOH solutions has been measured accurately in NaOH solutions in a wide concentration range. Using this result, single electrode Peltier heats of H_2 gas evolution in 8N and 10N NaOH solutions are calculated as 1.03×10^{4} J/F and 9.79×10^{3} J/F, respectively.

2)The concentration dependence of thermoelectric power in high concentration range (5N ~ 10N) is different from that in more dilute range. The theoretical equation of thermoelectric power derived in Chapter 1 is no longer available in high concentration range.

3)The cause of 2) is considered to be the concentration dependence of Eastman entropy (or transport number) rather than that of partial molar entropy.

CHAPTER 7 The estimation of single electrode Peltier heat in a couple of electrochemical reactors

As mentioned in previous chapters, single electrode Peltier heat can be calculated from measured thermoelectric power by use of eqn.(Ⅱ-7).

In this chapter, it is to be demonstrated how the single electrode. Peltier heats of a working electrode and a counter one in an electrochemical reactor are calculated respectively with the data of measured thermoelectric power.

Here, by using the single electrode Peltier heat of electrodeposition of lithium metal in molten LiCl-KCl systems (LiCl electrolytic cell) and that of hydrogen gas evolution from high concentration NaOH solutions (water electrolyzers), the heat balance of these reactors is to be discussed. The condition will also be discussed under which the evaluation of the single electrode Peltier heat is very important.

Though in case of a water electrolyzer there exists a considerable amount of heat absorption at the gas evolution electrode due to vaporization of electrolyte, this sort of heat absorption is not to be discussed here because it is not directly related to the electric current.

First, according to the experimental results in Chapter 2-1, thermoelectric power of Li/Li(I) electrode system is $0.0947 \pm 0.001 mV/K$, therfore the single electrode Peltier entropy of the following reaction;

$$Li^{+} + e^{-} \rightarrow Li \qquad (\text{II}-29)$$

is $0.0947 \times 10^{-3} \times 96500 = 9.138$J/F·K(endothermic).

On the other hand, the reaction at the counter electrode of LiCl electrolyzer is the evolution of Cl_2 gas when LiCl-KCl is used as an electrolyte. This Peltier entropy of Cl_2 gas evolution at the counter electrode can be obtained by substracting that of the other electrode from the entropy change of the total reaction;

$$\Delta S = s_{Li} + s_{\langle 1/2 \rangle Cl2} - s_{LiCl}$$

,where s_{LiCl} represents the partial molar entropy of LiCl in LiCl-KCl eutectic composition, whose value is 130.8J/F·K as shown in Chapter 2-3. The molar entropy of lithium metal s_{Li} and that of Cl_2 gas $s_{\langle 1/2 \rangle Cl2}$ are 59.7J/F·K and 126.5J/F·K, respectively accoring to the published data[13].

Therfore, since the total entropy change ΔS described above is calculated as 55.4J/F·K(endothermic), the single electrode Peltier heat of Cl_2 gas evolution is obatined as follows.

$$55.4-9.1=46.3\text{J/F·K (endothermic)}.$$

Suppose the reactor is operated at 700K, the heat to be supplied into the electrode regions are calculated as follows and illustrated in Fig. II-20.

cathode (Li) : 6.4×10^3 J/F

anode (Cl_2) : 3.2×10^4 J/F

This means that more than 80% of the total heat for the electrolytic reaction must be supplied to the anode region in this case.

Since Peltier heat is proportinal to the current and Joule heat is proportional to the square of current, the ratio of Peltier heat to the total heat change in an electrolyzer is not necessarily large when the current is relatively large. Therefore, under such a condition, the evaluation of Peltier heat is not so important.

But in molten salt systems, since their electrical conductivity is large(eg, 1.572S/cm in case of LiCl-KCl at 723K [14]), the ratio of Peltier heat to Joule heat is not so small under the condition of low current.

For example, when the current density is $10A/dm^2$, Joule heat evolved in a $1cm^3$ cube is estimated as $6.4 \times 10^{-3}J/s$ and Peltier heat from a $1cm^2$ square anode is estimated as $3.32 \times 10^{-2}J/s$. This means that Peltier heat is about 5 times larger than Joule heat, besides when the current gets 10 times smaller, the latter gets 50 times larger than the former and can not be negligible.

Next the case of water electrolyzers is to be discussed.

In case of H_2 gas evolution in 8N and 10N NaOH solutions, they are estimated as $1.03X10^4J/F$ and $9.79X10^3J/F$ at 40℃, respectively from the data of thermoelectric power measurement.

This means if water electrolysis is carried out in these

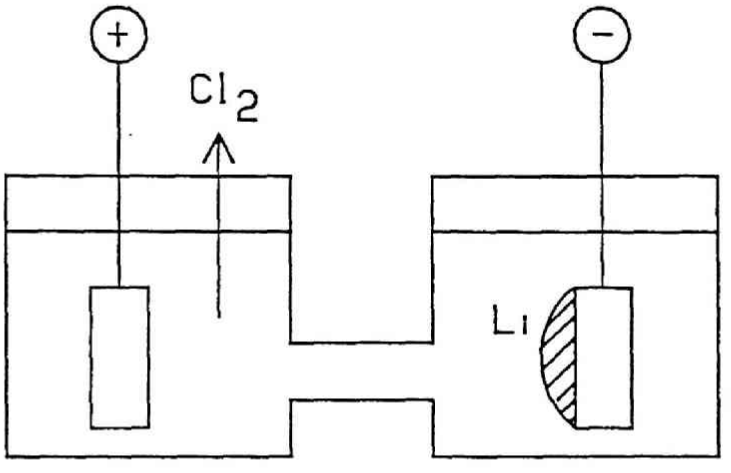

3.2×10^4 6.4×10^3

[J/F]

Fig. II-20
Peltier heat of each electrode in a LiCl electrolyzer

NaOH solutions, the single electrode Peltier heat of anode is also endothermic as shown in Fig. Ⅱ-21, which is calculated in the same way mentioned above on basis that the entropy change of total reaction shown below is 80.8J/F·K[11].

$$\Delta s = s\langle H_2\rangle + (1/2)\cdot s\langle O_2\rangle - s\langle H_2O\rangle \qquad (Ⅱ-30)$$

Though $s\langle H_2O\rangle$ stands for the partial molar entropy of water in NaOH solutions, molar entropy of pure water was used in the calculation instead. This substitution is quite acceptable because the difference between partial molar entropy of water in NaOH solutions and that in pure water is negligibly small (within 1%), which has been confirmed by estimating the activity coefficient of water, ie. excess partial molar entropy of water, with the data on the vapor pressure of NaOH solutions[15].

As a conclusion, the evaluation of single electrode heat is important when the electrolysis current or overpotential is low, electric conductivity is large, and the single electrode Peltier heat of the anode is very different from that of the cathode.

From such a viewpoint, the energy analysis of LiCl electrolyzers should be carrid out with an accurate evaluation on the single electrode Peltier heat of each electrode.

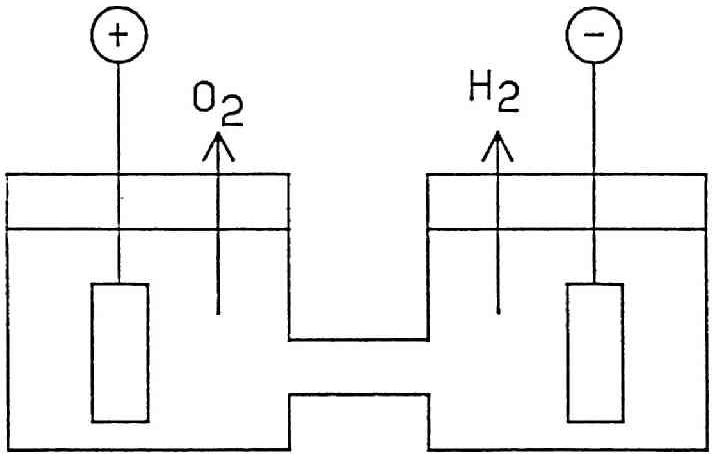

8N	$1.50X10^4$	$1.03X10^4$
10N	$1.55X10^4$	$9.79X10^3$

[J/F]

Fig.II-21
Peltier heat of each electrode in a water electrolyzer

REFERENCES

[1] Y.Ito, S.Horikawa, J.Oishi and Y.Ogata, Electrochim.Acta 30, 799(1985)

[2] Christian,J.W.,J.-P.Jan, W.B.Pearson, and I.M.Templeton, Proc.Roy.Soc.(London),A245,213(1958)

[3] Temkin,M.I., and A.V.Khoroshin,Zhur.Fiz.Khim.,26,500 (1952)

[4] Handbook of Chemistry and Physics, 42nd ed., Chemical Rubber Publishing Co,Cleveland(1960)

[5] Lange and Hesse,Z.Electrochem.38,428(1932). 39,374 (1933).

[6] R.Haase,Trans.Faraday Soc.49,1 (1953)

[7] Y.Ito,F.R.Foulkes and S.Yoshizawa, J.electrochem.Soc. 129,1936(1982)

[8] Y.Ito, H.Kaiya, S.Yoshizawa, S.K.Ratkje and T.Fϕrland, J.electrochem.Soc. 131,2504(1984).

[9] J.N. Agar, Thermogalvanic Cells (Advances in Electrochemistry and Electrochemical Engineering, Vol. 3, Interscience, London(1962))

[10] H.S.Harned and R.A.Robinson, Trans.Faraday Soc.36, 973(1940)

[11] J.O'M.Bockris and A.K.N.Reddy,"Modern Electrochemistry vol.1", Plenum(1977).

[12] H.S.Harned and B.B.Owen, "The Physical Chemistry of Electrolytic Solutions", P.716, Reinhold(1958)

[13] I.Barin and O.Knache, Editors, "Thermochemical Properties of Inorganic Substances", Springer-Verlag, Berlin (1973)

[14] A.J.Bard, Ed., "Encyclopedia of Electrochemistry of the Elements", Vol.X, Marcel Dekker(1976)

[15] J.H.Perry, "Chem. Engineers' Handbook", McGraw Hill Co.Inc. (1950)

GENERAL CONCLUSION

This thesis has described the theoretical and experimental studies on thermoelectric power in various systems from an engineering viewpoint.

The major points of obtained results in this work can be summarized as follows.

(1)It has been confirmed that mass transfer phenomena by thermoelectric power can occur in molten salt systems under some condition.

(2)The relation between thermoelectric power and single electrode Peltier entropy has been confirmed by using a newly designed single electrode calorimeter in aqueous systems.

(3)Thermodynamical descriptions of thermoelectric power in both nonconvective and convective systems have beed derived by use of irreversible thermodynamics, and the appropriateness of these descriptions have been experimentally confirmed in both molten salt systems and aqueous systems.

(4)The effects of composition and phase change of electrode material on thermoelectric power have been investigated by using lithium-tin alloy electrodes. The thermoelectric power shows different behaviors according as the phase state of the electrode and these behaviors have been theoreticaly

explained by considering mass and entropy balance in the electrode region.

(5)Thermoelectric powers of various electrode systems in molten LiCl-KCl have been measured and by using these data, transported entropy in a LiCl-KCl system has been estimated.

(6)The single elctrode Peltier heat of hydrogen evolution in high concentration NaOH solutions and that of lithium metal electrodeposition in molten LiCl-KCl have been estimated from the thermoelectric power measurement with these electrode systems. As for the former, theoretical consideration of its concentration dependence has also been carried out.

The author believes that the work in this thesis will certainly contribute to the study on mass transfer phenomena of nonisothermal systems and to the energy analysis of electrochemical reactors.

Especially the work in Chapter 2-2. (The effect of composition and phase change of .....) is expected to directly contribute to the heat analysis of the energy storage battery whose electrode is made of tin-lithium alloy.

Besides, the obtained Peltier heat in Chapter 7 (The estimation of single electrode ......) can also be directly applied to the energy analysis of water electrolyzers where high concentration NaOH solution is used as an electrolyte.

A part of this study has been or will be published in scientific journals or proceedings of international conferences as follows:

(1) Y.Ito, M.Kamata, S.Horikawa and J.Oishi, "Mass Transfer and Its Electromotive Force in a Nonisothermal Molten Salt Systems", DENKIKAGAKU Vol.53, pp375～380 (1985)
(INTRODUCTION)

(2) M.Kamata, Y.Ito and J.Oishi, "Electromotive Force in a Nonisothermal and Convective System", Electrochimica Acta, Vol.31 pp521～525 (1986)
(Chapter1 and Chapter3)

(3) M.Kamata, Y.Ito and J.Oishi, "Single Electrode Peltier Heat of a Hydrogen Electrode in H_2SO_4 and NaOH solutions", Electrochimica Acta, Vol.32 pp1377～1381 (1987)
(Chapter5)

(4) M.Kamata, Y.Ito and J.Oishi, "Single Electrode Peltier Heat of a Hydrogen Electrode in NaOH Solutions at High Concentration", Electrochimica Acta, in printing.
(Chapter4 and Chapter6)

(5) Y.Ito, M.Kamata, M.Inoue and J.Oishi "Thermoelectric Power in a Molten Salt System", Proceedings of the 1st Chinese-Japanese Bilateral Symposium on Molten Salt Chemistry and Technology, pp74～78 (1986)
(Chapter2-1)

(6) M.Kamata, Y.Ito, M.Inoue and J.Oishi "Thermoelectric Power in LiCl-KCl Eutectic Systems", Proceedings of the Symposium on High Temperature Materials Chemistry IV (1987)
(Chapter2-2)

NOMENCLATURE

C_i	concentration of component i,		mol m^{-3}
C	heat content		J kg^{-1}
F	Faraday constant,	96500	C mol^{-1}
I	current density,		A m^{-2}
i	electrolysis current,		A
J_i	mass flux of component i,		mol $m^{-2}s^{-1}$
J_q	thermal flux,		J $m^{-2}s^{-1}$
Kw	ionic product of water		-
n	valence number,		-
P	pressure,		Pa
R	gas constant	8.314	J $mol^{-1}K^{-1}$
S'(Q)	Peltier entropy,		J $K^{-1}mol^{-1}$
s_i	(partial) molar entropy of component i,		J $K^{-1}mol^{-1}$
s^*	excess partial molar entropy of component i,		J $K^{-1}mol^{-1}$
$\bar{\bar{S}}$	transported entropy,		J $K^{-1}mol^{-1}$
$\bar{\bar{S}}_i$	transported entropy of component i,		J $K^{-1}mol^{-1}$
$\hat{S}_i$	Eastman entropy of component i,		J $K^{-1}mol^{-1}$
T	temperature,		K
t	transport number of component i,		-
W_c	evolved heat in cathode region		J s^{-1}
X_i	mole fraction of component i,		-
Y_{qq}	Onsager coefficient,		J $m^{-1}s^{-1}$

Y_{qi}	Onsager coefficient,	mol $m^{-1}s^{-1}$
Y_{qQ}	Onsager coefficient,	J $V^{-1}m^{-1}s^{-1}$
Y_{iq}	Onsager coefficient,	mol $m^{-1}s^{-1}$
Y_{ii}	Onsager coefficient,	mol^2 $J^{-1}m^{-1}s^{-1}$
Y_{iQ}	Onsager coefficient,	mol $V^{-1}m^{-1}s^{-1}$
Y_{Qq}	Onsager coefficient,	C $m^{-1}s^{-1}$
Y_{Qi}	Onsager coefficient,	mol $V^{-1}m^{-1}s^{-1}$
Y_{QQ}	Onsager coefficient,	C $V^{-1}m^{-1}s^{-1}$
Y_{qP}	Onsager coefficient,	J $Pa^{-1}m^{-1}s^{-1}$
Y_{iP}	Onsager coefficient,	mol $Pa^{-1}m^{-1}s^{-1}$
Y_{QP}	Onsager coefficient,	C $Pa^{-1}m^{-1}s^{-1}$
Z_i	complete coupling coefficient between mass flux of component i(i=n+1,n+2,...k) and current density,	mol C^{-1}

Greek letters

γ	activity coefficient,	-
ε_T	thermoelectric power,	V K^{-1}
ε'	thermoelectric power between electrode and lead metal,	V K^{-1}
θ	entropy production per unit volume per unit time,	J $K^{-1}s^{-1}m^{-3}$
λ	thermal conductivity,	J m $s^{-1}K^{-1}$
μ_i	chemical potential of component i,	J mol^{-1}
ν	stoichiometric coefficient,	-

ϕ	electric potential,	V
Π	Peltier heat,	J F^{-1}